Fall 5-11-2019

DETERMINING THE PATHOLOGICAL EFFECTS OF PRENATAL ALCOHOL EXPOSURE ON PERIPHERAL NEUROPATHY VIA SPINAL AND PERIPHERAL IMMUNE MECHANISMS

Joshua J. Sanchez
University of New Mexico - Main Campus

Follow this and additional works at: https://digitalrepository.unm.edu/biom_etds

Part of the Medicine and Health Sciences Commons, and the Neuroscience and Neurobiology Commons

Recommended Citation

Sanchez, Joshua J.. "DETERMINING THE PATHOLOGICAL EFFECTS OF PRENATAL ALCOHOL EXPOSURE ON PERIPHERAL NEUROPATHY VIA SPINAL AND PERIPHERAL IMMUNE MECHANISMS." (2019). https://digitalrepository.unm.edu/biom_etds/189

This Dissertation is brought to you for free and open access by the Electronic Theses and Dissertations at UNM Digital Repository. It has been accepted for inclusion in Biomedical Sciences ETDs by an authorized administrator of UNM Digital Repository. For more information, please contact amywinter@unm.edu.

Joshua J. Sanchez

Candidate

Biomedical Sciences Graduate Program: Neuroscience

Department

This dissertation is approved, and it is acceptable in quality and form for publication:

Approved by the Dissertation Committee:

Erin D. Milligan, Ph.D, Chairperson

Kevin Caldwell, Ph.D.

Jason Weick, Ph. D.

Lauren Jantzie, Ph. D.

DETERMINING THE PATHOLOGICAL EFFECTS OF PRENATAL ALCOHOL EXPOSURE ON PERIPHERAL NEUROPATHY VIA SPINAL AND PERIPHERAL IMMUNE MECHANISMS

by

JOSHUA J. SANCHEZ

B.S., Psychology, University of New Mexico, 2012

DISSERTATION
Submitted in Partial Fulfillment of the
Requirements for the Degree of

**Doctor of Philosophy
Biomedical Sciences**

The University of New Mexico
Albuquerque, New Mexico

May 2019

DEDICATION

To my Mom, Grandma, and Grandpa

All of whom have shown me what hard work truly means.

Thank you for always supporting me in everything that I do and always

encouraging me to do my best.

ACKNOWLEDGEMENTS

DETERMINING THE PATHOLOGICAL EFFECTS OF PRENATAL ALCOHOL EXPOSURE ON PERIPHERAL NEUROPATHY VIA SPINAL AND PERIPHERAL IMMUNE MECHANISMS

By

Joshua J. Sanchez
B.S. Psychology, University of New Mexico, 2012
Ph.D., Biomedical Sciences, University of New Mexico, 2019

ABSTRACT

Previous studies have suggested that children with Fetal Alcohol Spectrum Disorder (FASD) display hypersensitivity to light touch. In support of this notion, we have demonstrated that applying a chronic constriction injury (CCI) to the sciatic nerve of rats that have prenatal alcohol exposure (PAE) results in heightened sensitivity to light touch, clinically termed allodynia. These observations coincided with heightened glial activation and enhanced peripheral immune reactivity. Considering allodynia is known to be mediated by both peripheral immune responses and spinal glial activation, it is reasonable to speculate that allodynia following PAE may be mediated through an alteration of immune reactivity. Thus, I hypothesized that PAE results in immune sensitization leading to enhanced susceptibility to developing allodynia.

To address the possibility that PAE creates susceptibility to developing neuropathy, a minor CCI was applied to rats that have been prenatally exposed to saccharin (Sac) or alcohol (PAE). Induction of allodynia occurs only in PAE rats with a minor injury. Interestingly, data acquired by immunohistochemistry (IHC) and subsequent microscopy analyses show that spinal astrocyte activation was altered compared to Sac rats. Furthermore, pharmacological blockade of

spinal cytokines leading to reduced allodynia also demonstrate an alteration in the proinflammatory cytokine profile at the spinal cord and the sciatic nerve. Strikingly, PAE resulted in downregulation of normal IL-10 responses within the spinal cord and dorsal root ganglia (DRG) as shown by IHC. Additionally, satellite glial cells were activated in the DRG compared to controls which coincided with heightened expression of the proinflammatory cytokine IL-1β. Spinal cord IHC analysis of glutamate transporters demonstrated that PAE alone is sufficient to upregulate both glutamate transporter 1 (GLT-1) and the astrocyte specific transporter glutamate aspartate transporter (GLAST) followed by a downregulation after minor CCI. These data suggest that an increase in synaptic and peri-synaptic glutamate develops following minor injury that is regulated predominantly by glia. Interestingly, no significant change was seen in the neuronal specific transporter EAAC1 or in NMDA receptor subunits.

Collectively, the work described and presented in this dissertation demonstrates that PAE primes peripheral and spinal neuroimmune responses which lead to allodynia following minor CCI. Additionally, my data demonstrate that PAE may alter glutamate transporters in the spinal cord which may lead to continued heightened glial activation and increased cytokine actions following injury. Furthermore, our studies support the possibility that glial cells are sensitized as a consequence of PAE, which in turn influence neuronal activity. Taken together, the results from this work demonstrate that PAE leads to life-long susceptibility to developing allodynia.

TABLE OF CONTENTS

List of Figures

<u>Chapter 4</u>

Chapter 1
Introduction

Fetal alcohol spectrum disorder (FASD) is caused by exposure to alcohol during gestation and results in a continuum of disabilities ranging from mild to severe that includes cognitive (i.e. intellectual ability, learning, and memory) and behavioral (e.g. mood, attention, and impulse control) deficits (Mattson et al., 1998). In 2017, a study showed that globally 10% of women consume alcohol while pregnant (Popova et al., 2017). Additionally, it has been shown that the prevalence of FASD is 2% to 5% within the United States (May et al., 2014). Unfortunately, many of these children with FASD either go undiagnosed or misdiagnosed (Chasnoff et al., 2015).

Early studies began by describing many issues as a result of alcohol exposure during gestation such as physical facial characteristics as well as cognitive disorders. Many of these studies focus on women who consumed large amounts of alcohol during pregnancy. As research on FASD has grown, we have quickly learned that even small amounts of alcohol during pregnancy can result in abnormalities. Many of these abnormalities may not be physical, and more so, some may not be detected until later in life. Over 40 years of research through clinical studies and in animal models of FASD have focused on issues that range from physical alterations to cognitive disorders as well as sensory disorders.

The first studies demonstrating sensory alterations in children with FASD was done by Morse and Cermak (Morse and Cermak, 1994). These studies describe many characteristics of sensory processing disorders (SPD) in FASD children. Interestingly, ensuing studies done by Jirikowic and colleagues support

prior findings and demonstrate issues with sensory processing in young school-aged children with FASD (Jirikowic et al., 2008). In support of this possibility, studies in rhesus monkey demonstrate that prenatal alcohol exposure (PAE) leads to light touch hypersensitivity (Schneider et al., 2005). These reports hint at a potential underlying mechanism of the adverse effects of PAE resulting in neurological dysfunction.

Clinically, touch hypersensitivity, referred to as allodynia, is a well-known neuropathic pain condition in patients with peripheral nerve damage. The neurological mechanisms underlying allodynia are thought to include non-neuronal immune cells that become functionally augmented within the dorsal horn of the spinal cord. Interestingly, recent reports demonstrate neuroimmune dysfunction both within the clinic and in animal models of FASD. These studies uncover that FASD as a result of PAE leads to heightened severity of illness and dysfunctional immune cell production (McGill et al., 2009).

Interestingly, preclinical studies in the brain show exaggerated release of proinflammatory cytokine expression following PAE (Topper et al., 2015). Unfortunately, much of this work has only been demonstrated in brains of neonates. Little is known about how PAE alters immune function within the spinal cord which could potentially explain hypersensitivity seen in children with FASD and in animal models with PAE. Additionally, these reports fail to demonstrate whether the effects of PAE on neuroimmune function are life-long. Furthermore, these studies focus primarily on chronic and high PAE to mimic situations such as binge and heavy drinking. These reports do not characterize the effects of

moderate exposure to alcohol which would reflect a woman having a drink or two during pregnancy. Thus, much still needs to be explored on the life-long effects of moderate PAE. The following sections describe FASD, how moderate PAE has life-long effects on neuroimmune function, and how these alterations may result in a heightened susceptibility to developing allodynia.

Fetal Alcohol Spectrum Disorder (FASD)

The effects of prenatal alcohol exposure was first described in 1973 by Jones and Smith (Jones and Smith, 1973). Here they described Fetal Alcohol Syndrome (FAS) which shows the most severe symptoms such as growth abnormalities, facial dysmorphology, as well as fine motor dysfunction (Jones and Smith, 1973). Although the exact amount of alcohol was not known in this study, it was known that the mothers were alcoholic women who ingested high amounts of alcohol throughout pregnancy. As research on FASD has grown we now know that high amounts of alcohol exposure result in FAS. Along with the above-mentioned symptoms others include visual, auditory, as well as cardiac issues (Riley et al., 2011). Interestingly, many symptoms are not correlated with the amount of alcohol exposure (Bailey et al., 2004). It has been discovered that the types of symptoms and the severity seem to be a combination of the amount of alcohol, the pattern of drinking, consistency of drinking, at what developmental timeframe the mother was drinking, as well as the nutrition of the mother (Sood et al., 2001; Bailey et al., 2004; Alfonso-Loeches and Guerri, 2011). As a result, the term "fetal alcohol spectrum disorder" (FASD) was coined to encompass a

range of severity of symptoms that can be mild to severe. Thus, diagnosed children fall within an umbrella of FASD, that is, FAS, partial FAS (pFAS), static encephalopathy/alcohol exposed, and neurobehavioral disorder/alcohol exposed (Astley et al., 1999).

Since 1973, much has been discovered about FASD children. Outside of the obvious physical characteristics sometimes observed of FASD in infants, some symptoms are not known until later in life. Some of these include cognitive and behavioral problems, learning and memory deficits, as well as issues with executive and motor function (Burd et al., 2012; Popova et al., 2017). Additionally, many of these children have issues with social functioning and substance abuse disorders (Lange et al., 2012; Stevens et al., 2012). Evidently, PAE has significant functional alterations not readily or overtly detected until later in life. Unfortunately, the insidious effects of moderate PAE are not well characterized.

Reports on moderate PAE

To date a limited number of reports have been published that show the effects of a moderate PAE (1 standard drink or 14g of ethanol per day (Valenzuela et al., 2012)) on children with FASD. Furthermore, of the published studies, none find any significant issues with moderate drinking and child behavior, IQ scores, or problems with attention, learning, and cognitive abilities (O'Callaghan et al., 2007; Robinson et al., 2010; Falgreen Eriksen et al., 2012). Additionally, no issues are demonstrated in these children up to 5 years of age (Kelly et al., 2010). In contrast, Murray and colleagues demonstrate that moderate exposure to alcohol

results in conduct problems such as stealing, lying, and aggressive outburst (Larkby et al., 2011; Murray et al., 2016). A separate study demonstrates that low levels of alcohol consumption can influence craniofacial development (Muggli et al., 2017). Many of these reports have significant limitations which prevents researchers from making conclusions. For example, in these reports, many of the women in the study self-reported their alcohol consumption. Additionally, the blood alcohol content of these women during pregnancy was unknown, thereby limiting the ability to determine the exact amount of alcohol consumed. Furthermore, many of these studies could not fully determine whether the cohorts of children were true representations of the population. Thus, larger cohorts and extensive details about the children are needed to make definite conclusions about the effects of moderate PAE. These limitations led Malmuk and colleagues to conclude that there is no safe limit of alcohol that can be consumed while pregnant (Mamluk et al., 2017). Interestingly, despite the limited clinical studies showing significant alterations as a result of moderate PAE, studies using animal models of PAE have furthered our understanding of the insidious effects of alcohol exposure.

Shedding light on the effects of PAE using animal models

Many studies using animal models demonstrate the impact that moderate PAE can have on the central nervous system (CNS). Furthermore, these studies show that these effects can have life-long implications where some can only be uncovered following injury or insult. Previous studies utilizing moderate PAE

expose rodents to alcohol throughout gestation (human equivalent to first and second trimester), or postnatally until about Day 8 after birth (third trimester). It should be noted that a moderate alcohol exposure involves blood alcohol levels of ≤ 0.17grams/deciliter (g/dl) of alcohol daily where the US legal limit is about 0.08g/dl (Valenzuela et al., 2012). Reports that explore the effects of moderate PAE focus on both behavioral outcomes and biochemical changes within the brain.

Interestingly, previous studies demonstrate that moderate exposure to alcohol results in significant alterations to hippocampal dependent memory (Savage et al., 2002). Strikingly, this study demonstrates deficits in rodents that have exposure levels as low as 0.03g/dl. A separate study shows that moderate PAE also effects learning ability in rodents (Savage et al., 2010). Furthermore, other studies demonstrate that moderate PAE is able to alter motor coordination, social behavior, and stress responses (Valenzuela et al., 2012). These studies provide strong evidence for significant and subtle behavioral alterations as a result of moderate PAE.

When brains of rodents exposed to moderate amounts of alcohol are examined, significant cellular phenotype and subcellular alterations are observed. Many of these rodents that demonstrate issues with learning and memory also display alterations in glutamate receptors that are crucial for brain function (Valenzuela et al., 2012). Additionally, changes in neurotransmitters that are necessary for brain plasticity are observed suggesting a potential mechanism as to how PAE can alter brain function (Valenzuela et al., 2012). Interestingly,

studies demonstrate that moderate PAE can alter neurogenesis. One study demonstrates that although alcohol exposure does not affect the number of neurons that are able to survive and differentiate within the dentate gyrus; moderate PAE did affect the neurons ability to increase neurogenesis during enrichment conditions (Choi et al., 2005). Strikingly, disruption in neurogenesis is observed in adult rodents suggesting the life-long effects of moderate PAE (Akers et al., 2014). What many of these studies demonstrate are the significant consequences of moderate alcohol exposure. The data suggest that despite not seeing observable consequences of PAE, that underlying consequences can still be present. It is not until brain function is challenged through various behavioral tasks that the adverse effects of PAE are observed. The implications for this could point to the need for more extensive clinical studies where little effects are observed in children as a result of drinking moderate amount of alcohol during pregnancy.

Does PAE lead to underlying immune alteration

The first description of immune dysfunction in FASD children was done by Johnson and colleagues (Johnson et al., 1981). Here they describe that in the clinic, children with FAS tend to have greater susceptibility to developing infectious diseases. This report additionally demonstrates alterations in the formation and migration of the immune cells responsible for fighting against infection (Johnson et al., 1981). Other studies have shown that children with FASD do in fact have increased risk for middle ear infections (Church and Gerkin,

1988), respiratory infections (Gauthier and Brown, 2017), as well as meningitis and autoimmune neuromuscular diseases (Chiapelli and Taylor, 1995). Many observations suggest that alcohol exposure has significant effects on immune function. Interestingly, previous reports suggest that immune alterations can also be linked to problems in cognition (Marin and Kipnis, 2013), which may be linked to impairments seen in FASD children. These reports provide strong evidence for further exploration of the immune system following PAE.

Interestingly, studies involving PAE animals demonstrate underlying immune alterations that are not initially apparent. For example one study demonstrates reduction in neuronal number and alterations in glia specifically within the dentate gyrus (Uban et al., 2010). This suggests that in addition to neuronal dysfunction, moderate PAE may also alter neuroimmune function. Within the CNS, glial cells (astrocytes and microglia) are primarily responsible for mediating immune reactions and maintaining proper neural function. Microglia are considered the resident immune cells of the CNS where their primary function is to protect the CNS from potential infectious agents following insult or lesion (Kettenmann et al., 2011; Perry and Teeling, 2013). Along with microglia, astrocytes are also crucial for maintaining the CNS. They have numerous functions such as being supportive to neurons, regulating blood flow, playing a role in CNS metabolism, and also maintaining the blood brain barrier (Sofroniew and Vinters, 2010). In addition to this, astrocytes release various immune factors responsible for mounting immune reactions similar to microglia (Sofroniew and Vinters, 2010).

Upon immune activation, glia are able to secrete proinflammatory cytokines such as IL-1β, TNF, as well as anti-inflammatory cytokines such as IL-10. The release of these immune factors results in neuroinflammatory response at the site of injury or insult. In addition to this, glia secrete chemokines which initiate the infiltration of other innate and adaptive immune cells from the periphery (Gao et al., 2010b; Prinz and Priller, 2017). These factors include the chemotactic cytokines such as CCL2, CXCL1, CXCL10, and CX3CL1 (Lindia et al., 2005; Gao et al., 2010b; Liu et al., 2013; Chen et al., 2014). This infiltration of peripheral leukocytes results in increased expression of proinflammatory cytokines. Overall, these events result in a heightened immune response that leads to neuropathology.

Much of the work that has explored the effects of PAE on immune function utilize third trimester binge alcohol exposure. These studies demonstrate that alcohol exposure is able to decrease the viability of microglial cells within the cerebellum (Kane et al., 2011). The blood alcohol levels of 250-325mg/dl may suggest that viability may be decreased due to the toxic levels of alcohol exposure (Kane et al., 2011). A separate study utilizing a similar binge alcohol exposure model demonstrate that within the hippocampus, glial cells have increased activation compared to controls. Additionally, this study show increased expression of proinflammatory cytokines IL-1β and the anti-inflammatory IL-10. Curiously, this study utilizes a binge alcohol exposure during the third trimester but only saw their effects during the withdrawal period of alcohol exposure (Topper et al., 2015). Both of these studies demonstrate the

alcohol exposure does in fact alter glial function. Unfortunately, these studies do not examine how a more moderate exposure may affect glia.

A recent study utilizing a moderate PAE during the first and second trimester explore the effects within the mother and the brains of the offspring. Interestingly, alcohol exposure increased the expression of IL-1β and the chemokines macrophage inflammatory protein (MIP) and fractalkine (CX3CL1) within the maternal sera and amniotic fluid. In addition to this, these immune factors are increased within the offspring. Furthermore, the offspring demonstrate activated microglia (Pascual et al., 2017). A separate study utilizing a moderate PAE during the first and second trimester look at both brain and peripheral immune responses. This study demonstrates that following alcohol exposure the expression levels of CCL2, IL-10, and TNFα were all significantly increased within the cerebral cortex (Terasaki and Schwarz, 2016b). Overall these studies demonstrate alcohol is able to disrupt basal immune expression in PAE offspring. Considering these data show that PAE is able to alter the expression of immune factors, one question that arises is whether alcohol exposure may also affect immune responses following insult or injury.

The effects of PAE on immune responses following challenge

Many studies that explore the effects of PAE on immune factors have only demonstrated effects on basal responses. Most of these studies have not examined whether PAE may alter the function and responses of these immune cells. Teraski and Schwarz explored the effects of administering the immune

activator lipopolysaccharide (LPS) to moderate PAE adult offspring (Terasaki and Schwarz, 2016b). Interestingly, this study found that within the hippocampus, exaggerated expression of the IL-1β was seen. Additionally, the expression level of the microglial activation marker CD11b was also increased compared to control conditions. Peripherally, the levels of IL-1β were also significantly increased specifically within the spleen following LPS challenge (Terasaki and Schwarz, 2016b). These studies demonstrate that following immune challenge, moderate PAE is able to alter both brain and peripheral immune responses.

A separate study examined the effects of moderate PAE on the immune response following a CNS injury. This report exposed rodents to alcohol prenatally and inflicted a CNS injury in adult offspring. Interestingly, this study demonstrates that rodents that are alcohol exposed have a decreased astrocyte and TNF response following injury compared to control conditions (DeVito and Stone, 2001). This in combination with the report from Terasaki and Schwarz would suggest that PAE can have opposite effects on immune responses. These differences may be explained by the exposure paradigms. Additionally, the type of damage could also result in the opposite effects observed. Overall, both studies described above suggest that the effects of PAE may be life-long in that these effects were demonstrated in adult PAE offspring. Additionally, these studies suggest that PAE may alter immune responses such that a secondary challenge such as LPS or a CNS wound is able to reveal dysfunctional immune responses compared to control conditions.

The majority of studies that explore the effects of PAE on immune function focus primarily within the brain and peripherally. These studies neglect the effects of PAE within the spinal cord. Considering that PAE can significantly alter immune responses within the brain it would stand to reason that these effects may also extend to the spinal cord. Considering the spinal cord is responsible for motor and sensory function (Prochazka and Mushahwar, 2001) and the immune system within the spinal cord modulates pathological sensory function (Milligan and Watkins, 2009), it would suggest that PAE may have significant effects on sensory processing within the spinal cord. Furthermore, because the effects of PAE are life-long, it would suggest that PAE may render an individual susceptible to sensory disorders, such as neuropathic pain later in life.

The effects of PAE on spinal neuroimmune function and neuropathic pain

As mentioned previously, PAE affects immune function within the brain and peripherally as well. While speculative, it would suggest that PAE alters neuroimmune function similarly within the spinal cord. Thus, it is possible that disruptions in sensory processing may occur in children that FASD.

The first reports of sensory alteration as a result of FASD was demonstrated by Morse and Cermak (Morse and Cermak, 1994). This study looked at people with FASD that ranged from 2 to 19 years of age. Interestingly, their data show that individuals with FASD are 2 to 6 times more likely to display sensory processing disorders (SPDs) which include clumsiness, inattention, and

hypersensitivity to stimuli (Morse and Cermak, 1994). A separate study utilizes more comprehensive methods to diagnose children with FASD and to determine whether these individuals display sensory impairments (Jirikowic et al., 2008). Interestingly, this study replicated prior findings showing that FASD children display deficits in sensory processing and decreased sensory-motor performance (Jirikowic et al., 2008). Together, these reports claim that children with FASD display touch hypersensitivity as evidenced by clinical studies. Further support for this notion, are shown in animals models of FASD. Studies in rhesus monkeys with PAE demonstrate increased sensitivity to tactile stimuli (Schneider et al., 2008). Coincidentally, touch hypersensitivity, referred to as allodynia, is a well-known pathological pain condition in patients with peripheral nerve damage.

Neuropathic pain occurs through trauma and/or inflammation of peripheral nerves that communicate to pain transmission neurons in the dorsal horn of the spinal cord. Following sciatic nerve damage, the process of Wallerian degeneration commences. Wallerian degeneration is the process that occurs leading to the loss of function in axons and nerve terminals when peripheral nerves undergo trauma or damage (Gaudet et al., 2011). A subsequent inflammatory response occurs within the periphery at the site of tissue injury (Gaudet et al., 2011). More specifically, peripheral leukocytes release proinflammatory cytokines such as IL-1β and TNFα. In addition, chemokines such as CXCL10, CCL2, CX3CL1, CXCL1 are released from surrounding glia. These chemokines work to recruit other leukocytes to the site of injury to further aid in the induction of allodynia (Zhuang et al., 2007; Gao et al., 2010b; Zhang et

al., 2013; Jiang et al., 2016). In addition to this, the anti-inflammatory IL-10 downregulates within the spinal cord following sciatic nerve damage (Wilkerson et al., 2012a). Overall, these changes result in a proinflammatory environment resulting in inflammation at the sciatic nerve.

During the induction of inflammation at the sciatic nerve, inflammatory factors communicate with sensory nociceptors (Milligan and Watkins, 2009). These factors bind their receptors which are located at the post-synaptic terminal of these sensory neurons. IL-1β binds its receptor IL-1 whereas TNFα binds its receptor TNF receptor 1 (Milligan and Watkins, 2009). Once bound, intracellular signals such as ERK and PKC are activated, leading to depolarization which sends pain signals through primary afferents of sensory nociceptors towards the DRG (Okuse, 2007; Milligan and Watkins, 2009). The cell bodies of sensory neurons are located in the DRG. These neurons bifurcate meaning they have two projections sites: one towards the sciatic nerve and the other projects to the spinal cord dorsal horn (Milligan and Watkins, 2009). Thus, these cells communicate with incoming signals from the periphery to the central nervous system namely the spinal cord.

At the DRG site, these cells communicate with satellite glial cells (SGCs) which surround the cell bodies of the primary afferent cells (Costa and Moreira Neto, 2015). SGCs work to maintain the cellular environment similar to astrocytes within the spinal cord (Verderio and Matteoli, 2011; Franke et al., 2012). Under neuropathic conditions, sensory neurons release neurotransmitters in a paracrine fashion into the extracellular space which activate SGCs. In

response to this, SGCs will release proinflammatory cytokines which bind their receptors found on sensory neuron cell bodies (Takeda et al., 2009). Additionally, activation of SGCs results in upregulation of the intermediate filament protein glial fibrillary acidic protein (GFAP) (Takeda et al., 2009; Nascimento et al., 2014). Following activation primary afferent neurons release various factors such as glutamate and substance P which work to communicate with and activate SGCs (Takeda et al., 2009). This results in SGCs to release their own proinflammatory factors such as IL-1β which then communicate back to primary afferent neurons as well as other nearby cell bodies (Takeda et al., 2009). Thus, SGCs and sensory neurons communicate through various inflammatory factors such as IL-1β. This communication has been shown to aid in the induction of allodynia (Takeda et al., 2009).

Following activation of SGCs at the DRG, pain signals travel into the dorsal horn spinal cord (Takeda et al., 2009). After sciatic CCI, DRG projections to the dorsal horn of the spinal cord occur at three distinct levels; the lumbar L4-L6 segments (Lindborg et al., 2018). In addition to this, the spinal cord is organized into laminae starting at the superficial layer of the dorsal horn (Milligan and Watkins, 2009). The pain relevant laminae extend throughout the dorsal horn spinal cord, ending at lamina 6 (Milligan and Watkins, 2009).

When the DRG sensory cells project into the spinal cord, communication about both noxious and non-noxious stimuli occurs through distinct nerve fibers which differ in their myelination (Milligan and Watkins, 2009). Aβ fibers are heavily myelinated and respond to stimuli that are non-noxious such as vibration

and light touch (Milligan and Watkins, 2009). Additionally, Aδ fibers are lightly myelinated whereas C fibers are unmyelinated and respond to pain signals (Milligan and Watkins, 2009). More specifically, these two fibers communicate to pain projection neurons which are located in the spinal cord lamina I, IV and V of the dorsal horn (Milligan and Watkins, 2009). These pain projection neurons then cross over from the ipsilateral side of the spinal cord to the contralateral side where they then ascend into pain relevant regions of the brain such as the brainstem and thalamus and ultimately into the somatosensory cortex where pain is perceived (Hucho and Levine, 2007).

Interestingly, many changes occur within the spinal cord resulting in light touch to be coded as painful. As mentioned previously, pain signals travel into the spinal cord through Aδ and C nerve fibers. These fibers communicate with pain projection neurons but also communicate with a specific type of neuron called wide dynamic range (WDR) neurons (D'mello and Dickenson, 2008). These neurons are found within lamina 5 of the dorsal horn spinal cord (D'mello and Dickenson, 2008). Additionally, these neurons are able to receive input from all nerve fibers that project into the spinal cord meaning they respond to many incoming stimuli. Thus, these neurons respond to both incoming touch stimuli as well as painful stimuli. More specifically, during pathological conditions when persistent stimulation occurs from Aδ and C fibers, WDRs undergo synaptic plasticity referred to as "wind up" (D'mello and Dickenson, 2008). This plasticity results in alteration of WDR where information that was previously coded as non-painful from Aβ fibers is now considered painful. This ultimately results in

allodynia (D'mello and Dickenson, 2008; Milligan and Watkins, 2009). Although neurons play an important part in the induction of allodynia, the communication to non-neuronal glial cells also plays a crucial role.

Within the dorsal horn spinal cord, synapses between sensory neurons and pain projection neurons are surrounded by glial cells such as astrocytes and microglia (Milligan and Watkins, 2009). These cells respond to a large number of factors including other excitatory neurotransmitters such as glutamate (Milligan and Watkins, 2009). Following nerve damage, the excitatory pain neurotransmitter glutamate is released in the synaptic terminal within the dorsal horn of the spinal cord. Synaptic glutamate concentration is influenced not only by the degree of presynaptic release, but also by glutamate clearance through glutamate transporters which are found on neurons and glial cells (Danbolt, 2001). Five glutamate transporters have been identified, with GLAST found on astrocytes, GLT-1 found on neurons and glia, and EAAC1 found solely on neurons. Two others, EAAT4 and EAAT5 are found within the brain (Furuta et al., 1997). In spinal cord laminae I-II where pain projection neurons exist, only GLT-1 and EAAT3 are expressed at the highest levels, while GLAST is expressed throughout the dorsal horn (Furuta et al., 1997; Sweitzer et al., 2002). Normally, glutamate transporters (GLT-1, GLAST, and EAAC1) clear glutamate from the perisynaptic cleft (Danbolt, 2001). However, during peripheral nerve injury, an initial two-fold upregulation of glutamate transporters occurs followed by a two-fold downregulation (Sung et al., 2003). More specifically, previous reports have demonstrated that the expression of GLAST, GLT-1, and EAAC1 peaks at Day 4

post-CCI injury followed by their down regulation by Day 7 (Sung et al., 2003). This ultimately results in glutamate accumulation which contributes to induction of allodynia through the process known as central sensitization.

Following sciatic nerve injury, glutamate-responsive glial cells (astrocytes and microglia) within the dorsal horn release cytokines IL-1β and TNFα (Milligan and Watkins, 2009) which bind to and activate their receptors on pain projection neurons as well as on nearby glial cells. Under these pathological conditions, astrocytes and neurons release the chemotactic cytokines such as CCL2, CX3CL1, CXCL10, and CXCL1 that binds their receptor and work to recruit peripheral leukocytes which release proinflammatory cytokines into the synapse further augmenting glial function and aiding in the induction of allodynia (Zhuang et al., 2007; Gao et al., 2010b; Zhang et al., 2013; Jiang et al., 2016). An example of this occurs when CCL2 bind its receptor CCR2 found on endothelial cells. This binding increases the expression of the ligand ICAM-1 typically found on the surface of endothelial cells (Marlin and Springer, 1987; Ostermann et al., 2002). This allows peripheral leukocytes such as T-cells and macrophages to infiltrate the spinal cord through the binding of ICAM-1 to the β-2 integrin leukocyte function-associated antigen 1 (LFA-1) expressed on leukocytes (Marlin and Springer, 1987; Ostermann et al., 2002). Over time, persistent release of excitatory neurotransmitters from leukocytes as well as surrounding glia results in constant depolarization of pain projection neurons. Normally, only the glutamate receptors AMPA and Kainate depolarize following the binding of the excess glutamate within the synaptic cleft. NMDA receptors do not depolarize because

magnesium prevents ions from infiltrating the receptor (Grace et al., 2014). During pathological conditions, constant release of glutamate into the synapse leads to NMDAR plasticity, where phosphorylation of various NMDA receptor subunits such as NR2b occurs, leading to release of the magnesium block allowing NMDA receptors to be depolarized (Latremoliere and Woolf, 2009). This ultimately, leads to over-excited pain projection neurons which relay amplified signals to the brain (Schäfers et al., 2003).

Does PAE alter immune function leading to enhanced neuropathic pain?

Considering how immune signaling play a large role in the induction of allodynia, and PAE alters immune function, it would stand to reason that PAE may have significant effects on neuropathic pain. Thus, to explore this, an animal model of neuropathic pain using sciatic CCI was applied to adult (4 month) rats with moderate PAE. Using this study design, we wondered whether CCI results in exaggerated sensitivity to light touch, whether altered immune responses are observed as an effect of PAE, and whether the effects of PAE are long-lasting into adulthood. The initial study determined baseline (BL) responses of both prenatal saccharin (Sac) and PAE rats using von Frey behavioral test. At this point either a sham or standard (4-suture) CCI to both prenatal saccharin and PAE rats was performed. Following surgery, responses to touch stimuli were determined at Day 3 and 10 post-surgery (**Fig. 1**). As expected, sham conditions display normal sensitivity at baseline and at Day 3 and 10 in that responses fall

at about 10 grams of stimulus intensity. In contrast, Sac rats with CCI develop

robust allodynia in that these animals respond at stimulus intensity of less than

one gram. Strikingly, PAE rats develop potentiated allodynia at both Days 3 and

10 in that significant differences were seen compared to Sac rats (**Fig. 1a**).

Curiously, contralateral allodynia is also seen following a standard CCI in Sac

Figure 1

a)
4 Month PAE Rats
Ipsilateral

b)
4 Month PAE Rats
Contralateral

Noor and Sanchez *et al., BBI,* 2017

Figure 1. Prenatal alcohol exposure (PAE) potentiates allodynia in adult rats following CCI. Absolute threshold behavioral responses for (a) ipsilateral and (b) contralateral hindpaws are shown. At baseline (BL), responses to low threshold mechanical stimuli were similar in all groups (ipsilateral, $F_{1,36} = 1.877$, $P = 0.179$; contralateral, $F_{1,36} = 1.228$, $P = 0.275$), regardless of PAE or Sac treatment. Statistics show a main effect of alcohol exposure from data collected from the ipsilateral hindpaw ($F_{1,36}=12.009$, $P = 0.001$) but not in the contralateral hindpaw ($F_{1,36} = 4.169$, $P = 0.049$). There was a main effect of CCI surgery (ipsilateral, $F_{1,36} = 311.943$, $P < 0.001$; contralateral, $F_{1,36} = 54.554$, $P < 0.001$). In addition, an interaction between alcohol exposure and CCI surgery only in the ipsilateral hindpaw (ipsilateral, $F_{1,36} = 5.246$, $P = 0.028$; contralateral, $F_{1,36} = 1.383$, $P = 0.247$) is observed. Comparison of treatment groups post-surgery demonstrate a larger increase in sensitivity following CCI in PAE animals compared to their Sac-CCI counterparts where a main effect of alcohol exposure in the ipsilateral hindpaw (ipsilateral, $F_{1,36} = 12.938$, $P = 0.001$; contralateral, $F_{1,36} = 4.003$, $P = 0.053$] is observed. In addition, a main effect of CCI surgery [ipsilateral, $F1,36 = 347.595$, $P < 0.001$; contralateral, $F_{1,36} = 58.406$, $P < 0.001$] and an interaction of alcohol exposure and CCI surgery in the ipsilateral paw [ipsilateral, $F_{1,36} = 8.312$, $P = 0.007$; contralateral, $F_{1,36} = 1.928$, $P = 0.174$] was revealed. N = 10 rats in each group.

rats at Days 3 and 10. Exaggerated allodynia is also observed in PAE allodynia only at Day 3 but not 10 (**Fig. 1b**). Interestingly, PAE alone was not sufficient to elicit an effect on sensitivity in that no differences were seen between Sac and PAE rats with sham surgery (**Fig. 1**). Additionally, it is not until CCI is applied that the effects of PAE are seen in that exaggerated sensitivity to light touch is demonstrated (**Fig. 1**). Furthermore, although not demonstrated in young juveniles (3 to 8 week rats), the effects of PAE are seen in 4 month rats suggesting that the effects of PAE are long-lasting.

To determine whether PAE has significant effects on glial cell activation, spinal cord from behaviorally verified rats at Day 10 (**Fig. 1**) were collected. More specifically, rats underwent saline/paraformaldehyde perfusion followed by spinal cord processing and mounting for IHC. At this point, IHC was run on spinal cords and images were collected using fluorescence microscopy. Immunoreactivity (IR) was determined for both GFAP expression to determine astrocyte activation and for Ionized binding calcium adaptor protein 1 (Iba1) to determine microglial activation. IR was specifically quantified within the entire dorsal horn spinal cord (**Fig. 2a,c**). As previously mentioned the dorsal horn spinal cord is the region of the spinal cord where the majority of pain processing occurs. GFAP data demonstrate that Sac and PAE rats with sham surgery as well as Sac rats with CCI display similar levels of astrocyte activation. Interestingly, it is not until CCI is applied to PAE rats that significant increases in astrocyte activation were seen (**Fig. 2b**). Microglial data demonstrated no significant differences between either sham groups whether they are Sac or PAE rats in the ipsilateral or contralateral

hindpaw. Additionally, although not significant slight increases in microglial activation were seen in Sac rats with CCI. Similarly, although not significant, PAE rats with CCI demonstrated the highest microglial activation. Curiously, significant differences are seen in PAE rats with CCI despite not showing

Figure 2

Noor and Sanchez *et al., BBI,* 2017

Figure 2. PAE results in heightened glial activation following CCI. Image analysis of acquired IR images for (**a**) GFAP and (**b**) Iba1 that include the representative images in lower panels. White dotted line represents the dorsal horn spinal cord. Arrows indicate superficial lamina. PAE-CCI treated spinal cords display heightened GFAP expression compared to sham (ipsilateral: $F_{1,14} = 0.04474$, $p = 0.0030$; contralateral: $F_{1,14} = 0.04399$, $p = 0.0039$). While Iba-1 IR is significantly increased in PAE rats with CCI compared to PAE sham rats (ipsilateral: $F_{1,12} = 2.639$; $p = 0.0011$; contralateral, $F_{1,12} = 2.639$, $p = 0.0161$) and Sac CCI (ipsilateral: $F_{1,12} = 19.52$; $p = 0.0173$; contralateral, $F_{1,12} = 11.01$, $p = 0.2708$) in the ipsilateral hindpaw N = 4-5 rats per group.

significant increases in sensitivity at Day 10 when tissues were collected (**Fig. 1 and 2d**). Astrocyte data show differences only in PAE rats with CCI despite prior

reports demonstrating upregulation of astrocyte activation in healthy animals with CCI (Wilkerson et al., 2012a). Additionally, despite potentiated allodynia in PAE rats with CCI, clear differences are not seen in microglial cells despite data demonstrating that microglia mediate induction of allodynia (Wilkerson et al., 2012a). These datademonstrate that the observed potentiated allodynia may be mediated by the increased expression of glial activation.

To further our studies, we wanted to determine whether the effects of a standard CCI are enduring past Day 10. It is possible that the effects of PAE on sensitivity might be temporary and may return to levels comparable to Sac rats. Thus, separate cohorts of Sac and PAE rats were used and BL responses were determined prior to applying either sham or CCI surgery. Behavioral sensitivity was determined up until Day 28 post-surgery. As shown previously (**Fig. 1**), rats displayed normal sensitivity at BL and following sham surgery until at least Day 28 (**Fig. 3**). Sac rats with a standard CCI developed robust allodynia following surgery as expected. Interestingly, PAE rats with CCI developed potentiated allodynia which endures until Day 28 (**Fig. 3**). These data demonstrated the chronicity of CCI on PAE rats. In addition, results replicated previous findings (**Fig. 1**) and show that potentiated allodynia persists long-term (**Fig. 3**).

At Day 28, behavioral testing commenced, and rats underwent saline perfusion in order to collect tissue for analysis of various immune factors in pain relevant regions (Noor et al., 2017). Flow cytometry was used within the lumbar spinal cord to determine the expression of microglial and macrophage cells. As shown through IHC, no significant differences were demonstrated in both

23

microglia or peripheral immune macrophages following CCI in Sac rats or in sham groups. As expected, significant increases were seen in both microglia and macrophages in PAE rats with standard CCI. Interestingly, splenic cells from PAE CCI rats that were stimulated demonstrated heightened expression of the chemokine CCL2 suggesting that peripheral leukocytes may be playing a role in potentiated allodynia (**Fig. 1 and 3**).

Figure 3

a)
4 Month PAE Rats
Ipsilateral

b)
4 Month PAE Rats
Contalateral

Noor and Sanchez *et al., BBI,* 2017

Figure 3. Potentiated allodynia is enduring in PAE rats. At baseline (BL), (a) ipsilateral and (b) contralateral threshold responses are similar between all groups (ipsilateral, $F_{1,16}$ = 1.209, P = 0.288; contralateral, $F_{1,16}$ = 0.036, P = 0.852). Following CCI surgery, both PAE and Sac control rats displayed significantly increased hindpaw sensitivity on Days 3, 10,15, 18, 23, and 28 post-surgery where there was a main effect of alcohol exposure (ipsilateral, $F_{1,16}$ = 84.616, P < 0.001; contralateral, $F_{1,16}$ = 138.980, P < 0.001), CCI surgery (ipsilateral, $F_{1,16}$ = 787.072, P < 0.001; contralateral, $F_{1,16}$ = 1180.917, P < 0.0010), and an interaction between alcohol exposure and CCI surgery (ipsilateral, $F_{1,16}$ = 82.506, P < 0.001; contralateral, $F_{1,16}$ = 103.264, P < 0.001). Compared to Sac animals, PAE rats displayed the greatest degree of hindpaw sensitivity following CCI surgery where a main effect of alcohol exposure (ipsilateral, $F_{1,16}$ = 93.167, P < 0.001; contralateral, $F_{1,16}$ = 149.318, P < 0.001), CCI surgery (ipsilateral, $F_{1,16}$ = 857.901, P < 0.001; contralateral, $F_{1,16}$ = 1258.469, P < 0.001) is observed, and an interaction between alcohol exposure and CCI surgery (ipsilateral, $F_{1,16}$ = 92.780, P < 0.001; contralateral, $F_{1,16}$ = 110.212, P < 0.001).

Additionally, the β2 integrin LFA-1 was significantly upregulated in PAE rats without CCI and was further increased following CCI. These data demonstrate that in addition to glial cells playing a role in potentiated allodynia, peripheral leukocytes may also contribute. Analysis of the SCN looked at the expression of IL-1β, TNF, and CXCL1. Interestingly, sham groups did not demonstrate any significant increases in any of these factors. It is not until CCI is applied that significant increases in CXCL1 are seen in Sac rats. In contrast, PAE rats with CCI demonstrated significant increases compared to Sac rats with CCI in all three immune factors. Furthermore, the expression of IL-10 was analyzed within both the DRG and SCN. Interestingly within the SCN, IL-10 responses increased in Sac rats with CCI but were blunted in PAE rats with injury. DRG data demonstrated that whereas healthy Sac rats with sham surgery display basal levels of IL-10, PAE sham rats do not demonstrate similar expression. Furthermore, following CCI, Sac rats have upregulation of IL-10 whereas PAE rats do not. The data suggest that potentiated allodynia may be induced as a result of heightened proinflammatory immune responses in combination with blunted anti-inflammatory responses.

The above data show that the effects of PAE are both peripheral and central and are not localized to one specific CNS region. Many of the immune alterations that were demonstrated were seen within the lumbar spinal, the sciatic nerve and in the DRG. Other prior reports that have been mentioned also demonstrated alterations within the brain (Drew and Kane, 2014; Topper et al., 2015).

Curiously, no effects of PAE are shown at BL or following sham surgery despite seeing some alterations in LFA-1 expression and in IL-10 responses within the DRG. Thus, the data suggest that the effects of PAE are not apparent until after a secondary insult is applied such as CCI. Furthermore, immune responses within the spinal cord and peripherally seem to be primed, meaning they become more reactive, where insult results in exaggerated responses which may explain potentiated allodynia following CCI.

The deleterious effects of PAE were demonstrated to be life-long by applying a standard CCI. Heightened sensitivity as well as immune responses were shown. Additionally, results suggest that PAE results in immune priming where a secondary insult is sufficient to result in these exaggerated responses. This was seen peripherally with CCL2, IL-1β, LFA-1, and in TNF. Interestingly, glia also demonstrated heightened reactivity following CCI. This data makes it difficult to determine what specific factors may be mediating potentiated allodynia. Despite seeing significant differences following CCI, in some situations clear differences were not observed. This would raise the importance of trying to unmask the effects of PAE in order to better pinpoint what specific alterations PAE is having on the immune response. Noor and colleagues (Noor et al., 2017) demonstrated many factors that could potentially be contributing to exaggerated sensitivity following CCI. Glial responses within the dorsal horn demonstrated heightened responses compared to controls. Additionally, LFA-1 expression was heightened as a result of PAE alone suggesting that peripheral leukocyte migration may be altered and could contribute to potentiated allodynia within the

spinal cord. Furthermore, CCL2 and CXCL1 expression was heightened following CCI further supporting this idea. Overall, this suggests that PAE may result in heightened susceptibility to developing allodynia through alteration of immune responses.

One cannot ignore other factors may result in potentiated allodynia. Previous studies show glial cells within the brain are altered corresponding with what Noor and colleagues demonstrate (Topper et al., 2015). It is possible that PAE alters mechanisms within glial cells resulting in potentiated allodynia. Recall, that during peripheral neuropathy, glutamate transporters are responsible for clearing glutamate from the synapse. These transporters eventually downregulate which ultimately leads to central sensitization (Sung et al., 2003). These studies also look at the effects of inhibiting these transporters to determine the effects on touch sensitivity. When the glutamate transporter GLT-1 and EAAC1 are inhibited, small increases in sensitivity are seen. Strikingly, when GLAST is inhibited in addition to the other glutamate transporters, potentiated allodynia is seen similar to what is seen in PAE rats (Sung et al., 2003). Thus, it is possible that PAE may work through the alteration of glutamate transporters which would potentiate allodynia. Prior reports demonstrate that PAE does decrease both the expression of GLAST and the glutamate uptake (Brolese et al., 2015). This suggests that PAE alters glutamate uptake within the synapse resulting in heightened susceptibility to developing allodynia.

Neuronal communication may play a specific role in potentiated allodynia seen in PAE rats with CCI. Previous studies show that following CCI, NMDA

receptor subunits become phosphorylated (Huang et al., 2018). This leads to NMDA receptors to become activated leading to strong depolarization following the binding of glutamate which leads to allodynia. It is possible that PAE may lead to alterations of the NMDA receptor which could aid in the induction of allodynia. Interestingly, previous studies utilizing animals with moderate PAE show alterations of NMDA receptor subunits in the brain (Brady et al., 2012). More specifically, decreases in NR2B are shown which is a subunit involved in the induction of allodynia (Brady et al., 2012; Huang et al., 2018). It stands to reason that PAE may alter NMDA receptor function in order to heighten the susceptibility of developing allodynia.

Specific Aims

Based on the above detailed background and initial experiments recently published (Noor, et al., 2017), my <u>central hypothesis is: PAE potentiates glial-neuroimmune responses and leukocyte actions underlying the lifelong risk for developing neuropathic pain</u>. This work is conducted to achieve the following specific aims:

<u>**Specific Aim 1:**</u> **Determine whether PAE generates life-long spinal glial and peripheral immune dysregulation resulting in susceptibility to allodynia.**

The sub-hypothesis for this aim is: Applying a minor sciatic nerve injury results in allodynia and glial activation only in PAE rats.

Approach: To do this, 1-year old PAE and Sac controls are used. Behavioral responses are assessed prior to and after either Sham or *minor* CCI. At the Day 10 post-surgery, spinal cords are processed for IHC staining and IR of glial activation markers is assessed. Additionally, pain relevant tissues as well as peripheral blood monocytes are collected from a separate group of 1-year old PAE and Sac rats. These tissues are assessed using flow cytometry and enzyme-linked immunosorbent assay (ELISA) to characterize the immune profile of PAE and Sac rats.

*This data has been published

Specific Aim 2: **Determine whether susceptibility to allodynia from PAE is mediated by spinal and peripheral immune cytokine dysregulation.**

The sub-hypothesis for this aim is**:** PAE alters proinflammatory immune reactivity leading to increased susceptibility to chronic peripheral neuropathic pain.

Approach: Using adult (4 month) PAE and Sac rats, minor or sham surgery is applied. The enduring effects of a minor injury are determined by assessing behavior until Day 28. These rats then receive i.t. injection of an LFA-1 antagonist and spinal cords and DRGs are collected at peak drug efficacy. IHC is used to determine glial activation and expression of LFA-1 in the spinal cord. In addition, expression of IL-1β and IL-10 is assessed in spinal cords and DRGs. A separate group of only PAE rats are assessed following minor CCI until Day 10. At this point, i.t. injection of IL-1 receptor antagonist (IL-1RA) are given and behavior is assessed. Finally, another group of both PAE and Sac rats receive either sham or minor CCI and are assessed until Day 10. At this point, intrathecal (i.t.) injection of an LFA-1 antagonist is administered and behavioral assessment is done until peak drug efficacy. Ipsilateral and contralateral sciatic nerve (SCN), dorsal root ganglia (DRG), and lumbar spinal cord is collected and assessed using qrt-PCR and electrochemiluminescence.

*This data is in review

Specific Aim 3: Determine whether PAE-induced susceptibility to allodynia is due to altered astrocyte glutamate transporter function.

The sub-hypothesis for this aim is: PAE alters basal glutamate transporter function resulting in heightened susceptibility to developing chronic peripheral neuropathic pain.

Approach: Adult (5-7 month) PAE and Sac rats received either sham or minor CCI and are behaviorally assessed up to Day 10 post-sciatic nerve manipulation. At Day10, all rats receive i.t. UCPH101 (GLAST inhibitor) and assessed up to 3 and at 24 hours post-injection. Spinal cords are examined for the glutamate transporters GLT-1, EAAC1, and GLAST using IHC procedures for immunoreactive detection under microscopy followed by image acquisition and analysis. Additionally, qrt-PCR is used to assess gene expression of these transported from spinal tissues collected from a separate group of PAE and Sac rats receiving sham and minor CCI. Furthermore, semi-quantitative protein analysis by western blot is used to determine the expression of the NMDA receptor subunit NR2B as well as phosphorylated NR2B in an effort to detect alterations in the sensitization state of spinal neurons under basal or neuropathic conditions.

*This data is in preparation

Chapter 2 - Prenatal alcohol exposure is a risk factor for adult neuropathic pain via aberrant neuroimmune function

Abstract

Background: Clinical studies show that prenatal alcohol exposure (PAE) results in effects that persist into adulthood. Experimental animal models of moderate PAE demonstrate that young-adults with PAE display potentiated sensitivity to light touch, clinically termed allodynia, following sciatic nerve chronic constriction injury (CCI) that coincides with heightened spinal glial, spinal macrophage, and peripheral immune responses. However, basal touch sensitivity and corresponding glial and leukocyte activation are unaltered. Therefore, the current study explored whether the enduring pathological consequences of moderate PAE on sensory processing are unmasked only following secondary neural insult.

Methods: In middle-aged (1 year) Long Evans rats that underwent either prenatal saccharin exposure (control) or moderate PAE, we modified the well-characterized model of sciatic neuropathy, CCI, to study the effects of PAE on neuro-immune responses in adult offspring. Standard CCI manipulation required 4 chromic gut sutures, while the modified version applied a single suture loosely ligated around one sciatic nerve. Spinal glial immunoreactivity was examined using immunohistochemistry. The characterization and functional responses of leukocyte populations were studied using flow cytometry and cell stimulation assays followed by quantification of the proinflammatory cytokines interleukin-1beta (IL-1β) and tumor necrosis factor-alpha (TNF-α). Data were statistically analyzed by ANOVA and unpaired t-tests.

Results: The current report demonstrates that significant reduction of CCI generates robust allodynia only in PAE rats, while the pathological effects of PAE following the application of a standard CCI are revealed by enhanced allodynia and elevated spinal glial activation. Additionally, minor CCI increases spinal astrocyte activation but not microglia, suggesting astrocytes play a larger role in PAE-induced susceptibility to aberrant sensory processing. Leukocyte populations from PAE are altered under basal conditions (i.e. prior to secondary insult), as the distribution of leukocyte populations in lymphoid organs and other regions are different from those of controls. Lastly, following *in vitro* leukocyte stimulation, only PAE augments the immune response to antigen stimulation as assessed by heightened production of TNF-α and IL-1β.

Conclusions: These studies demonstrate PAE may prime spinal astrocytes and peripheral leukocytes that contribute to enduring susceptibility to adult-onset neuropathic pain that is not apparent until a secondary insult later in life.

Background

The adverse effects of alcohol consumption on the developing central nervous system (CNS) have been recognized for decades and include an overt and distinct pattern of malformations that occur following the highest exposure levels, referred to as fetal alcohol syndrome (Jones and Smith, 1973; Hoyme et al., 2016). However, it is now recognized that a wide range of disabilities are associated with much lower levels of alcohol exposure during fetal development resulting in a spectrum of CNS-related disorders. This spectrum of disorders is referred to as fetal alcohol spectrum disorder (FASD) (Valenzuela et al., 2012; Reid et al., 2015; Hoyme et al., 2016). Associated disabilities that occur across the lifespan as a result of moderate exposure to alcohol during CNS development include not only behavioral and cognitive deficits (Mattson et al., 1998; Alfonso-Loeches and Guerri, 2011; Reid et al., 2015), but also sensory touch abnormalities in individuals with FASD (Franklin et al., 2008). In support of these clinical observations, preclinical experiments in adult rhesus monkeys reveal touch abnormalities such as tactile hypersensitivity are observed in monkeys exposed prenatally to low/moderate levels of alcohol (Schneider et al., 2005).

Tactile hypersensitivity, referred to as light-touch mechanical allodynia frequently observed in chronic pain patients, is caused by spinal cord neuronal alterations that pathologically convert non-painful touch into painful signals (Braz et al., 2014). Anatomically, sensory peripheral nerve terminals project to the spinal cord and communicate to these pain-responsive neurons in the spinal cord

(Grace et al., 2014). Notably, allodynia often occurs following damage to peripheral nerves (Dworkin et al., 2003). Studies using animal models of neuropathic pain, such as a standard localized sciatic nerve damage referred to as chronic constriction injury (CCI), have demonstrated that spinal immune and glial cells (astrocytes and microglia) release proinflammatory cytokines such as interleukin-1β (IL-1β) and tumor necrosis factor-α (TNF-α), which play critical roles in mediating chronic allodynia (Costigan et al., 2009a; Milligan and Watkins, 2009; Calvo et al., 2012; Grace et al., 2014). A number of reports accumulating for several decades show that animal models of chronic peripheral neuropathy develop pathological pain through aberrant neuroimmune mechanisms (i.e. activated glia and proinflammatory cytokines) (Milligan and Watkins, 2009; Grace et al., 2014).

Similarly, animal models of prenatal alcohol exposure (PAE) have advanced our understanding of the pathophysiology caused by mild to moderate levels of alcohol exposure and some support possible aberrant neuroimmune actions underlying CNS-related pathologies that persist into adulthood (Drew and Kane, 2014). For example, experimental rodent PAE models show increased reactive brain microglial and astrocyte responses (Drew and Kane, 2014; Topper et al., 2015), elevated brain proinflammatory cytokine and chemokine production (Tiwari and Chopra, 2011; Topper et al., 2015; Bodnar et al., 2016; Boschen and Klintsova, 2017), decreased microglial survival (Drew and Kane, 2014), and altered brain glial and immune responses following injury (DeVito and Stone, 2001; Arjona et al., 2006; Zhang et al., 2012). Notably, these data support clinical

observations of patients with FASD that also present with aberrant immune responses such as augmented lymphocyte formation (Johnson et al., 1981) and altered cytokine synthesis (Ahluwalia et al., 2000).

More recently, rat offspring with moderate levels of PAE reveal potentiated tactile hypersensitivity (a.k.a. allodynia) following adult-onset peripheral nerve damage that occurs in parallel with augmented spinal glial activation and peripheral immune responses, while no such changes are observed in non-alcohol exposed rodents (Noor et al., 2017). These data suggest PAE-induced aberrations in neuroimmune function may underlie the clinical sensory abnormalities observed in individuals with FASD. Moreover, the most intriguing aspects of the data are that PAE alone is insufficient to alter basal touch sensitivity. Specifically, the adverse effects of PAE on abnormal sensory processing and associated spinal glial and immune function only becomes apparent following a secondary insult, which in these experiments, is the application of a well characterized CCI nerve injury model (Noor et al., 2017). These data suggest that moderate PAE may create susceptibility for developing neuropathic pain that occurs long into adulthood. Therefore, the hypotheses of the current set of studies are twofold: (1) that the damaging effects of PAE on the CNS are unmasked only following an insult or challenge to the peripheral/central nervous system, and (2) the magnitude of the response to the insult is disproportionately greater to the degree of the insult itself. The goal of these studies is to determine that PAE renders one susceptible to neuropathic pain

induced by minor sciatic nerve injury, with PAE-induced neuropathy mediated by exaggerated alterations in spinal glial and immune responses.

Applying a well-characterized rodent model of sciatic neuropathy in adult offspring with PAE provides insight into understanding (1) aberrant immune cell and glial CNS activation as a consequence of PAE, and (2) adverse conditions during CNS development that create adult susceptibility to developing chronic neuropathic pain from minor insults. Reducing injury to the sciatic nerve from the well characterized standard 4-suture to a minor 1-suture CCI addresses two critical questions. First, while the standard sciatic nerve CCI in the rat is well-characterized to involve spinal glial activation and other trafficking leukocytes (Bennett and Xie, 1988; Wilkerson et al., 2012a; Dengler et al., 2014; Grace et al., 2014), no reports exist showing 1-suture CCI generates allodynia. Second, the chronic underlying pathology from PAE on CNS sensory processing is best unmasked following minor injury. Thus, the goals of the current report sought to unmask the effects of PAE on augmented spinal glial (astrocyte and microglial) phenotypes and profiles, and functional responses of peripheral immune cells characterized to traffic to the spinal cord to identify aberrant allodynia and neuroimmune reactivity.

Materials and Methods

Animals and Study Group Strategy

All procedures were approved by the Institutional Animal Care and Use Committee (IACUC) of The University of New Mexico Health Sciences Center,

and closely adhered to guidelines from the International Association for the Study of Pain for the use of animals in research. Long-Evans rat breeders purchased from Harlan Industries (Indianapolis, IN) were maintained in a breeding colony on a 12:12-hour reverse light/dark schedule (lights on from 2100 to 0900 hours), and fed standard rat chow and water, available *ad libitum*. For all experiments, 12-13 month male prenatal alcohol or saccharin exposed (described below) rat offspring derived from 14 litters were used. Offspring were habituated to a standard light/dark cycle (lights on from 0600 hours to 1800 hours) for at least 5 days and kept in these conditions for the duration of the study. A total of 14 female Long-Evans rat dams and 50 male offspring were used in all experiments. Offspring (12-13 months of age) were predominantly pair housed with 5 singled housed due to incompatibility with a cage mate.

Moderate Prenatal Alcohol Exposure Using the Voluntary Drinking Paradigm

Pregnant female rat dams were given either ethanol or saccharin throughout pregnancy until birth according to the voluntary drinking paradigm previously described (Savage et al., 2010). Briefly, 3 to 4 month female Long-Evans rat breeders were acclimated for 4 hours per day, from 1000 to 1400 hours, to drinking water containing 0.066% (w/v) saccharin (Sac) that gradually increased in ethanol content from 0% (v/v) on Days 1-2, to 2.5% (v/v) on Days 3-4, to 5% (v/v) on Day 5 and thereafter for two weeks. It should be noted that regular drinking water is available at all times during housing. Thus, animals could

voluntarily choose to drink either saccharin sweetened water containing 5% ethanol or regular water during the four-hour drinking period. At the end of the two-week prepregnancy drinking phase, the mean daily ethanol consumption was determined for each rat and rats that consumed 1 standard deviation above or below the group mean were excluded from the study. Subsequently, female rats were assigned to either a 5% ethanol or Sac control drinking group such that the mean prepregnancy ethanol consumption was similar between groups. The females were then placed with proven male rat breeders until pregnant. No alcohol was consumed during the breeding period, which averaged between 1-2 days. Beginning on gestational day 1, rat dams were given either 0% (Sac) or 5% (PAE) ethanol in Sac water (4 hours/day). Sac control group rats were given a volume of 0% ethanol in Sac water that was matched to the mean volume voluntarily consumed by the 5% ethanol group. Total ethanol consumption was recorded for each dam, which averaged 2.04 g of ethanol/kg body weight/day. This level of drinking by rat dams produced a mean peak serum blood alcohol concentration of 0.06 g/dl. No significant differences were observed between prenatal treatment groups in dam weight gain during pregnancy, pup birth weights, or litter size, replicating previous reports (Savage et al., 2010). Offspring were weaned at 24 days of age and male offspring pair-housed with the exception of five single-housed rats due to incompatibility with a cage mate. For all experiments, 12-13 month prenatal alcohol or saccharin exposed animals were used. A total of 50 male offspring were used in these experiments. Behavioral testing of offspring was performed during the first three hours of the

light cycle to avoid the influence of elevated hormones under normal circadian rhythms.

Chronic constriction injury (CCI)

In adult (12-13 months) male Sac or PAE rats, sham or CCI aseptic surgical procedures were performed as previously described (Bennett and Xie, 1988; Noor et al., 2017) and modified in some experimental groups, as described here. Under isoflurane anesthesia (induction 5% vol. followed by 3.5% in oxygen), the sciatic nerve was carefully isolated with sterile glass prongs and snuggly ligated with 1 (minor injury) or 4 (standard injury; (Bennett and Xie, 1988)) segments of sterile 4-0 chromic gut sutures (Ethicon, Somerville, NJ) without pinching into the nerve. Sterile isotonic saline (0.9%) was applied to the nerve during the procedure to prevent dehydration. Sham surgery involved isolation of the sciatic nerve similar to CCI but without nerve ligation. The nerve was then gently placed back into position and the overlying muscle was sutured closed with two 3–0 sterile silk sutures (Ethicon, Somerville, NJ). Rats fully recovered from anesthesia within approximately 5 minutes and were monitored daily following surgery for any post-operative complications.

Behavioral Assessment of Allodynia

Allodynia was assessed using the von Frey fiber test as previously described (Dengler et al., 2014). Briefly, rats were first habituated to the testing environment by placing rats atop 2-mm thick parallel bars spaced 8-mm apart

allowing full access to the plantar hindpaw. Habituation occurred for approximately 45 min/day for 4 sequential days within the first 3 hours of the light cycle in a sound- and temperature-controlled dimly lit section of the colony room. Baseline responses were then assessed using the von Frey behavioral test. For these experiments, the scale range of the calibrated monofilaments was modified and included 3 monofilaments calibrated to bend at 0.027 g (2.44 log stimulus), 0.067 g (2.83 log stimulus) and 0.166 g (3.22 log stimulus). Thus, a total of 13 calibrated monofilaments were used in these studies. Additionally, these calibrated monofilaments (2.44–5.18 log stimulus intensity) were applied randomly to the plantar surface of the left and right hindpaw for a maximum of 8 seconds per application. A metronome placed in the room provided guidance at 1 tick/sec. Lifting, licking, or shaking of the paw was considered a response. In a similar manner to baseline (Hoyme et al.) evaluation, animals were re-assessed following CCI or sham surgery on days 3 and 10. The experimental tester was blind to the prenatal and surgical treatment groups.

Immunohistochemical (IHC) tissue sample preparation

All tissue was collected from behaviorally verified rats on Day 10 after sham or CCI surgery. Tissues were processed as described previously (Noor et al., 2017). Briefly, rats were overdosed with sodium phenobarbital (Sleepaway, Fort Dodge Animal Health, Fort Dodge, IA) and transcardially perfused with 0.1M phosphate buffered saline (PBS; pH = 7.4), initially at a rate of 28 mls/min, then increased to 32 mls/min (~10 min), followed by 4% paraformaldehyde (PFA; pH = 7.4; 28-34

mls/min, 8 min). Immediately following transcardial perfusion, the spinal vertebral column from C2-L6 with the spinal column intact within the vertebral column were collected and cut at vertebra T7 into a rostral and caudal half of the spinal vertebral column. All spinal cord sections underwent 48-hour post-fixation in 4% PFA at 4 °C. Approximately a third (initial N=12) of the total spinal cords collected for IHC underwent decalcification. The purpose for maintaining the spinal cord within the vertebral column was to identify possible immune cell and astrocytic endfeet changes that occur within the subarachnoid matrix known to house a sentinel and infiltrating immune cells. Our prior work employing this method documents our success in younger rats (3-4 month olds rats) (Wilkerson et al., 2012b; Wilkerson et al., 2012a). Decalcified spinal cords underwent unexpected prolonged tissue decalcification, possibly due to the age of the rats (1 year olds in the current study) that resulted in altered integrity of the Iba1 epitope as virtually no IR signal was detectable. To avoid this problem, spinal cords (N=24) collected from subsequent experiments did not undergo decalcification and were isolated as described below. Thus, each experimental condition consisted of sample sizes of N=6 rats.

For spinal vertebral columns that underwent decalcification, segments were placed in a 3-liter water bath containing 10% ethylenediaminetetraacetic acid (EDTA) (Sigma-Aldrich, St. Louis, MO), 0.01% sodium azide and 0.5% paraformaldehyde with gentle consistent stirring atop a stir plate, with the solution exchanged every 5 days. A fully decalcified spinal vertebral column was determined when no resistance occurred upon penetrating the dorsal and lateral

spinous processes with a 30-gauge hypodermic needle. At four months of decalcification, spinal cords were isolated from vertebral columns.

For non-decalcified and decalcified vertebral columns, entire spinal cord (T7- L6) was carefully isolated from the spinal vertebral column making sure to maintain an intact spinal cord. The isolated spinal cords were segmented and subsequently paraffin processed. L4-L5 paraffin-embedded blocks were subsequently sliced on a microtome with adjacent 7µm tissue sections mounted onto vectabond-treated slides**.

To investigate spinal augmented glial activation, we analyzed the expression of the astrocyte marker, glial fibrillary acidic protein (GFAP), and the microglial activation marker ionized calcium-binding adapter molecule 1 (Iba1) in L4-6 spinal segments reported previously (Wilkerson et al., 2012a). In addition, we analyzed the expression of the microglial specific marker, transmembrane protein 119 (TMEM119) as described below. Slides containing tissue from lumbar (L4-L6) spinal cord were chosen for glial staining to capture overall glial reactivity (Wilkerson et al., 2012a). Paraffin-processed tissues underwent deparaffinization followed by rehydration and antigen retrieval procedures in a rice cooker at 94-96°C allowing for a gentle and equal distribution of temperature warming throughout tissue sections. For antigen retrieval, GFAP required a Tris-based buffer at pH 9.5 (BioCare Medical, Concord, CA), Iba1 required a Tris-based buffer at pH 9.0 (Vector, Burlingame, CA), and TMEM119 required a citrate-based buffer at pH 6.0 (BioCare Medical, Concord, CA). All tissue sections were incubated with 5% normal donkey serum (NDS), PBS pH 7.4 for

2h, followed by overnight primary antibody incubation using rabbit anti-rat GFAP (Millipore, 1:1000)(Wilkerson et al., 2012a), rabbit anti-rat Iba-1 (Wako, 1:300) (Wilkerson et al., 2012a), or rabbit anti-rat TMEM119 (Abcam, 1:100) (Satoh et al., 2016) in a humidity chamber at 4 °C. Tissues were washed 3x with 0.1M PBS pH 7.4 followed by donkey-anti rabbit FITC- or TRITC- conjugated secondary antibody incubation for 2h in a humidity chamber at room temperature, and rinsed in 0.1 M PBS. Tissues were then stained with the nuclear stain 4,6-diamidino-2-phenylindole (DAPI) (Vector Labs, Burlingame, CA) separately before cover slipping. These slides were left at room temperature overnight before proceeding with image acquisition and microscopy analysis.

Microscope spectral imaging for immunofluorescent quantification

Image acquisition for spectral analysis was preformed using the Nuance spectral imaging system (http://www.cri-inc.com/products/nuancew.asp; Perkin Elmer, Waltham, MA) as described previously (Noor et al., 2017). Briefly, images of dorsal horn spinal cord were obtained using a 20X objective with a Zeiss Axioplan2 inverted fluorescence microscope. Flat-field correction was applied in order to produce a uniform illumination during image acquisition. Image cubes were obtained from multi-labeled tissue containing DAPI, conjugated secondary antibody, as well as autofluorescence. A spectral library was then created using single-labeled slides for each fluorophore (e.g. FITC or TRITC) and a label-free (autofluorescence) slide. A computed spectrum (420 nm – 720 nm) was obtained by separating the known spectrum (autofluorescence) from mixed spectrum

(single labeled) to produce pure spectrum of each fluorophore. This allowed the separation of spectrum from multi-labeled slides (e.g. DAPI + TRITC) to obtain composite images containing only labels of interest. These composite images were then used for further analysis using Slidebook 6 software (below). Twelve to twenty-four images per experimental group (4 sections per animal, 3-6 animals per condition) per side (ipsilateral and contralateral) of sciatic manipulation were acquired and analyzed. In addition, the Nuance spectral imaging system was used for representative acquired images of TMEM119 shown in Figure 3e. 20X and 60X objectives were used to produce representative images.

Slidebook software image analysis

Composite images were analyzed using Slidebook 6 software (Intelligent Imaging Innovations, Denver, CO, USA). To eliminate signals originating from artifacts, the experimenter determined an acceptable threshold of very low-level emission fluorescent intensity per each experimental condition (e.g. Sac+Sham, PAE+Sham, etc.) by closely replicating the on-screen composite computer image with that observed through the microscope eyepiece, as described previously (Noor et al., 2017). In addition, the dorsal horn of the spinal cord (region of interest (ROI)) was outlined for analysis eliminating the surrounding white matter and peri-spinal blank space (intrathecal space). The image was then refined to include the predetermined threshold within the outlined area. The 'Sum Intensity' (the total signal within the outlined area in the dorsal horn) was determined and divided by the 'Area' (total area in micrometers squared (μm^2)) to obtain the

'Fluorescence Intensity'. The average of four adjacent sections from a single slide (representing a single animal) was calculated to determine the value for each animal. Finally, averages for each slide within the same condition were calculated along with the standard deviation and standard error of the mean. Data are analyzed as "Sum Intensity of ROI/μm^2. Fluorescence intensity was characterized from these thin sections to capture staining density and intensity of both astrocytes and microglia at the dorsal lamina (I-V) within a single lumbar segment to assess the overall highly localized profile, as both GFAP and Iba1 are well-documented to upregulate these markers upon increased cellular activation (Ito et al., 2001; Zamanian et al., 2012).

Preparation of single cell suspensions of peripheral immune cells for flow cytometry.

Surgically-naive rats (Sac- control and PAE) were deeply anesthetized with Isoflurane (Piramal Healthcare, Mumbai, India) (8-10 min, 5% vol. in oxygen). Peritoneal exudate cells (PECs), peripheral blood, thymus, spleens, and medial iliac lymph nodes were collected and immediately placed on ice. Medial iliac lymph nodes are draining lymph nodes for sciatic nerves and the immune cells from these lymph nodes were examined (Van den Broeck et al., 2006; Harrell et al., 2008). Single cell suspensions from PECs, spleens and peripheral blood were prepared identically, as described previously (Noor et al., 2017). Briefly, PECs were collected using ice-cold Iscove's media (Sigma-Aldrich, St. Louis, MO) and pelleted by centrifuge at 300xg at 4 °C for 8 min. The resultant cell pellet was

incubated with 2 ml hypotonic salt solution (ACK lysis buffer; Sigma-Aldrich, St. Louis, MO) for 5 minutes on ice to lyse red blood cells (RBCs). One million cells were resuspended in 2 ml ice-cold 0.1M PBS (pH=7.4) and processed for flow cytometry as described here. The remaining cells were used for *in vitro* stimulation experiments described below.

Spleens were harvested in RPMI 1640 media (medium originally developed by Roswell Park Memorial Institute, purchased from Sigma-Aldrich, St. Louis, MO) and homogenized via passage through a 40 μm cell strainer (Corning^{TM} sterile cell strainers, Fisher Scientific, USA) to prepare a single-cell suspension. RBCs were lysed similarly to that conducted with PECs. Splenocytes were used for flow cytometry described below**.** Single cell suspensions from lymph nodes and thymus were prepared using 40 μm cell strainers, conducted similarly to the preparative procedures described for isolating splenocytes. However, the RBC lysis step was not performed for lymph node and thymus samples.

Peripheral blood was collected (in BD vacutainer^{R} K$_2$EDTA blood collection tube) through cardiac puncture immediately after PECs collection. Peripheral blood (PBMNs) were isolated using Ficol Premium 1.84 (GE Healthcare Life Sciences, PA, USA) according to the manufacturer's instructions. Briefly, 1 ml blood was diluted to 4 ml with PBS (w/o Ca/Mg) and layered on 3 ml Ficol in a 15 ml conical tube and centrifuged at 400xg for 30 min at 20 °C, without brakes. PBMNs were collected from the interface and washed twice with PBS at 400xg for 10 min at 20 °C. Cells were resuspended in 2ml of 0.1 M PBS pH 7.4

on ice until proceeding to identify live cells (described below; viability dye staining).

Flow cytometry data acquisition and analysis of immune cell profiles in PAE rats.

Using flow cytometry, major immune cell subtypes in Sac and PAE rats were identified using the following gating strategy: live cells were identified based on absence of cell viability dye, B and T cells contained positive CD3 and CD45RA expression respectively, NK cells contained positive CD161 expression, and myeloid cells were positive for CD11b/c expression.

Live cells were counted on a hemocytometer using the trypan blue staining exclusion criteria. Between 0.5×10^6 - 1×10^6 cells were transferred in a FACS tube (BD Falcon^{TM}, MA, USA) and pelleted by centrifugation at 300xg for 5 min at 4 °C, with the supernatant discarded. Cells were then resuspended in PBS (without calcium and magnesium; Sigma-Aldrich, St. Louis, MO) and stained with Viability Dye eFluor® 450 (eBioscience, San Diego, CA) for 30 min, washed with FACS buffer (1x PBS containing 1.0% bovine serum albumin, and 1 mM EDTA) and incubated with a saturating solution of Fc block (BD Biosciences, San Jose, CA, USA) for 10 min followed by staining with fluorochrome-conjugated antibodies for 30 min. All of these steps were conducted on ice. Antibodies against rat CD3 (cluster of differentiation 3, clone IF4) and CD45 RA (clone OX-33) were purchased from BD Biosciences (San Jose, CA, USA). CD11b/c (clone OX-42, recognizes a common epitope shared by Integrin αM and αX chains) and

CD161 (clone 10/78) were purchased from Affymetrix (Santa Clara, CA, USA). These antibodies were used for 0.125-0.5 μg/10^6 cells, as recommended by the manufacturer. Following antibody staining, cells were washed and resuspended in 300 μl FACS buffer and then passed through a 40 μm cell strainer immediately prior to analysis to avoid cell clumping. At least 50,000 live cell events were collected for each sample. Data were acquired using the BD LSR Fortessa cell analyzer (BD Biosciences, San Jose, CA) and analyzed using FlowJo software v.8.7.4 (Treestar Inc., Ashland, USA). Live, intact healthy cells were identified based on their size (Forward Scatter (FSC-A)) versus granularity (Side Scatter (SSC-A)). Dead cells were further excluded by the presence of positive viability dye staining and only cells displaying the absence of viability dye were included for flow cytometry analysis for different immune markers. T cell and B cell proportions were determined by positive expression of CD3 (T cell co-receptor) and CD45 RA (CD45 isoform expressed by only B cells) respectively. Natural killer cells (NK) were identified by negative expression of T/B cell markers and positive expression of CD161 (expressed predominantly on NK cells and involved in activating NK-cell-mediated toxicity (Ryan et al., 1995; Warren and Smyth, 1999). Myeloid cells (e.g. macrophages, monocytes, dendritic cells and neutrophils) were identified by positive expression of CD11b/c and negative expression for lymphoid cell (T cell, B cells and NK cells) markers.

Intracellular detection of TNFα from splenocytes by flow cytomtery.

To examine the production of the proinflammatory cytokine tumor necrosis factor-α (TNFα), splenocytes collected from each rat were stimulated *in vitro,* as described previously (Noor et al., 2017). Briefly, splenocytes were collected from rats and resuspended in RPMI 1640 complete medium supplemented with 10% (v/v) fetal bovine serum (FBS) (Sigma), 2.0 mM L-glutamine (Thermos Fisher Scientific, PA, USA), 50 µM 2-mercaptoethanol (Sigma-Aldrich), 100 U/ml penicillin and 100 µg/ml streptomycin (Thermos Fisher Scientific, PA, USA) to a cell density of $1x10^6$/ml. Splenocytes were plated in a 24-well culture plate (Corning Costar, Sigma-Aldrich) $1x10^6$ cells/well, and each well was stimulated with 50 ng PMA (a phorbol ester, Protein Kinase C activator, 50 ng/ml) and ionomycin (a calcium ionophore, 1 µg/ml), incubated for 5 hours at 37 °C and 5% CO_2. In order to block secretion of cytokines from activated splenic leukocytes, 2 µl/ml protein transport inhibitor cocktail (containing brefildin A and monensin, from eBioscience) was simultaneously added with PMA/ionomycin (PMA/Io) solution at the beginning of the cultures. Following 5 hr of stimulation, splenic cells were gently removed from the wells, washed twice with PBS and stained with viability dye and surface marker CD11b/c, as described above. Cells were fixed with 4% PFA (Sigma-Aldrich) for 10 min at room temperature. Following fixation, cells were permeabilized with 0.3% saponin (Sigma-Aldrich) in FACs buffer followed by incubation with anti-rat TNFα at 1 µg/10^6 cells (Affymetrix, Santa Clara, CA, USA) for 40 min on ice in the dark. Cells were then washed twice in saponin-FACs buffer and processed for flow cytometric data acquisition.

Viable cells were identified as described above. Cd11b/c cells expressing TNFα are represented. Proportions of TNFα+ leukocytes were evaluated based on the isotype control staining.

IL-1β and TNF-α detection by enzyme-linked immunosorbent assay (ELISA)

PECs from each animal were plated in a 24-well tissue culture plate at 2×10^5 cells per well, in duplicate followed by stimulation or control treatment. Cells were stimulated with 1 µg/ml lipopolysaccharide at 37 °C (LPS, major cell-membrane component from gram-negative bacteria) purchased from Sigma-Aldrich, St. Louis, MO, USA. LPS (diluted in RPMI). Following a 24 hr stimulation, plates were spun at 300xg, 5 min and cell-free supernatants collected and stored at -80 °C until assaying. Cells were washed 2x with ice-cold PBS. PBS was aspirated and cell lysates were prepared using a whole cell lysis buffer (Pierce^R IP lysis buffer, Thermo Fisher Scientific, Waltham, MA, USA). Briefly, for each well, cells were treated with 120 µl of cell lysis buffer, on ice, for 10 mins. To remove cell debris, cell lysates were transferred to microcentrifuge tubes and spun at 13,000xg, 10 mins, 4 °C. Cell lysates were collected and stored at -80 °C, avoiding freeze/thaw cycles. TNFα and interleukin 1β (IL-1β) levels were measured using commercially available ELISA kits (R&D Systems, Minneapolis, USA). Each experimental well (from the tissue culture plate) was run in duplicate on the 96-well ELISA plate. All experiments and data analysis were performed according to the manufacturer's instructions.

Statistical analysis

SPSS (IBM, Chicago, IL, USA) was used for all behavioral analysis. At BL, a 2-way (2 x 3) analysis of variance (ANOVA) was used for analysis of the between-subject factors of prenatal exposure (Sac versus PAE) and surgery (Sham versus minor CCI versus Standard CCI). Additionally, a 2-way (2 x 3) repeated measures ANOVA was used for analysis of the between-subject factors of prenatal exposure and surgery for days post-surgery. Data from acquired microscope images, flow cytometry, and ELISA were analyzed using GraphPad Prism version 7 software (Graphpad Software Inc., San Diego, CA, USA). IHC IR was analyzed using a 2-way (2 x 3) ANOVA followed by Fisher's LSD test for post-hoc examination. A total of N=6; Sac and N=8; PAE rats were used for characterizing peripheral immune cell phenotypes and their functional responses. To ensure healthy "live" single cell suspension and immediate flow cytometry data acquisition (without fixation), rats were equally divided into two different tissue collection days (N=3/day; Sac and N=4/day; PAE, per experiment yielding a total of 5 different tissue samples per animal), which is a standard number of animals used in flow analysis ((Vorderstrasse et al., 2003; Ghasemlou et al., 2015; Jatana et al., 2017; Prasad et al., 2017)). Each tissue digestion and flow cytometry data collection day was considered an independent biological experiment. Data from each experiment was combined to generate N=6 for Sac and N=8 for PAE. Data comparing surgically-naïve Sac and PAE groups were analyzed with unpaired t-tests. ELISA data for pro-inflammatory cytokine production were analyzed using two-way (2 x 2) ANOVA. To control the type I

error rate during multiple comparisons, reported with adjusted P values, Tukey's test was applied for post hoc examination. The threshold for statistical significance was set *a priori* at $\alpha = 0.05$ for all sets of multiple comparisons. In order to minimize unnecessary duplication, we used the minimum number of animals possible to make statistically significant conclusions, which was based on our previous publications (Wilkerson et al., 2012a; Dengler et al., 2014; Noor et al., 2017; Whitehead et al., 2017). These studies utilized sample sizes of N=3 (IHC analysis), and N=6 (behavioral analysis) to reliably produce statistically significant differences between treatment groups. Outliers were removed following Grubbs' Z-test (Grubbs, 1950). In all cases, the data are presented as the mean ± SEM.

Results

PAE induces long-lasting susceptibility to allodynia from even minor peripheral nerve damage

Under basal conditions, light touch sensory thresholds appear similar in both PAE and Sac offspring with hindpaw responses occurring at approximately 10 grams of touch stimuli. In uninjured rats (sham treatment), sensory thresholds remained near their BL values on Day 3 and 10 indicating that repeated stimulation to the hindpaws during von Frey behavioral testing does not affect threshold responses. In addition, following minor sciatic nerve 1-suture CCI in Sac rats, ipsilateral hindpaw responses remained close to their BL values on Day 3, with sensory thresholds measured on Day 10 that completely overlapped

Sham-treated rats. However, striking allodynia was observed as measured by increased sensitivity of the ipsilateral hindpaw on Day 3 and 10 after surgery (Fig 1a). While threshold responses of the contralateral hindpaw remained stably near BL values in Sham-treated and Sac - 1 suture CCI rats, PAE rats with 1 suture CCI revealed a subtle but significant increase in contralateral hindpaw thresholds on Days 3 and 10 (Fig 1b). Thus, these initial data support that the enduring pathological consequences of PAE are revealed only after a minor nerve injury, where allodynia was clearly observed in 1 year aged rats. These data indicate that PAE creates long-lasting susceptibility to developing neuropathies, such as allodynia, following minor challenges to the nervous system.

PAE results in long-term potentiation of allodynia following a standard chronic constriction injury

Using a standard 4-suture sciatic chronic constriction injury (CCI), we have previously reported that prenatal alcohol exposure (PAE) potentiates allodynia in young adult rats (4 months) compared to the levels of allodynia observed in saccharin (Sac) control offspring (Noor et al., 2017). The current data demonstrate that the susceptibility to standard injury persists into middle age (12-13 month-old rats). BL thresholds in both PAE and Sac-treated rats were similar prior to surgery replicating data shown in Fig 1a and b and prior work by Noor, et al (Noor et al., 2017). Following standard CCI, Sac rats develop typical bilateral allodynia whereas PAE rats develop potentiated bilateral allodynia (Fig. 1 c-d), also replicating our prior report in younger (4 month) adult rat offspring. Overall,

54

these findings suggest that the effects of PAE are long-lasting and result in enhanced allodynia following a standard CCI in middle-aged offspring.

PAE underlies enhanced spinal expression of astrocytic GFAP in neuropathic rats

Spinal astrocytes and microglia were evaluated in middle-aged Sac exposed or PAE offspring that had undergone standard or minor CCI. Behavioral assessment in these rats (data shown in Fig. 1) was terminated on Day 10 post-surgery followed by spinal tissue collection and preparation for immunohistochemistry (IHC) to determine the immunoreactivity (IR) of the astrocyte 'activation' marker glial fibrillary acidic protein (GFAP). Standard 4-suture CCI induced exaggerated astrocyte responses in both the ipsilateral and contralateral dorsal horn of the spinal cord relative to CCI in PAE rats that displayed bilateral allodynia compared to Sac rats (Fig. 2a-b). Minor 1-suture CCI also resulted in significantly elevated bilateral spinal astrocyte responses in PAE rats compared to sham conditions and Sac rats with minor injury. It is notable that spinal cord dorsal horn GFAP IR from PAE rats with minor injury was comparable to Sac rats with standard CCI and allodynia (Fig. 1c and Fig. 2a). Representative images (Fig. 2c) of Sac-treated sham, Sac standard CCI, and PAE standard CCI conditions for GFAP used for analysis are shown. The results suggest that PAE underlies elevated astrocyte activation only following a secondary injury such as either standard or minor sciatic nerve injury.

Elevated spinal microglial activation markers are only seen following standard CCI but not minor CCI

Spinal dorsal horn microglial responses in middle-aged offspring following IHC processing revealed the transmembrane protein 119 (TMEM119), characterized as a microglial specific proliferation marker (Bennett et al., 2016; Satoh et al., 2016), was significantly elevated bilaterally in PAE rats with standard CCI compared to PAE sham, PAE minor injury, and Sac standard CCI (Fig. 3a-b). Additionally, significant bilateral increases in spinal cord TMEM119 IR were observed in Sac rats with standard CCI compared to Sac offspring with sham treatment or minor CCI injury (Fig. 3a-b).

To provide parallel lines of evidence, we examined the expression of ionized calcium-binding adaptor molecule 1 (Iba1), a protein that is up-regulated in both microglia and macrophages upon increased activation. Significant bilateral increases in Iba1 IR from Sac and PAE offspring were observed in the spinal cord dorsal horn with standard injury compared to all sham-treated rats, Sac minor and standard CCI and PAE with minor CCI. (Fig. 3d-e). Images of TMEM119 (Fig. 3c) and Iba1 (Fig. 3f) represent Sac sham, Sac standard CCI, and PAE standard CCI conditions. Insets for TMEM119 provide a representation of microglia surrounding nearby nuclei. Overall, these results suggest microglia may not be the key cell type responsible for primed spinal cord responses in PAE that lead to enhanced susceptibility to allodynia (Fig. 1c-d). It should be noted that our 7 µm tissue sections do not provide the thickness needed to display the multi-level microglial branching processes that TMEM119 IR has previously

shown (Bennett et al., 2016). However, thin 7-um sections allows for adjacent sections within the same anatomical regions of interest to be stained for different cellular markers. Additionally, decalcified spinal cords described above, underwent prolonged tissue decalcification that resulted in altered integrity of the Iba1 epitope. As a result, data for Iba1 IR from decalcified tissue was not included in the final Iba1 data set (Fig. 3c-d), as virtually no IR signal was detectable. To avoid artificially losing Iba-1 IR, a separate group of spinal cord tissue that did not undergo decalcification were isolated as described above. Subjects were removed if values fell 2 standard deviations +/- mean. N=2 subjects were removed A total of 7 subjects (N=2 Sac 1-Sut, N=2 Sac 4-Sut, N=2 PAE 1-Sut, N=1 PAE 4-Sut) were removed from the ipsilateral data set and 6 subjects (N=2 Sac 1-Sut, N=3 Sac 4-Sut, N=1 PAE 4-Sut) were removed from the contralateral data set in Fig. 3 (a-b).

PAE alters the peripheral immune cell profile in middle-aged offspring.

In addition to spinal astrocytes and microglia, peripheral leukocytes, known to traffic to the level at the spinal cord where incoming nociceptive signals from damaged peripheral nerves communicate to pain projection neurons, may be important contributors of neuropathic pain. Our prior work revealed that PAE potentiates peripheral immune responses from the sciatic nerve following nerve injury in young-adults. Thus, the phenotype of peripheral leukocytes in specific immune organs prior to trafficking to the spinal cord were examined for elevations in their specific populations or activation markers as an indication of a

primed state at basal levels. Thus, general immune cell populations in the primary lymphoid organ (thymus) and secondary/peripheral lymphoid organs (spleen, lymph node) in middle-aged PAE offspring were characterized. In addition, immune cell composition was characterized in the circulating/peripheral blood and the peritoneal cavity. The major immune cell subsets, T cells, B cells, NK cells and myeloid cells in these immune compartments were identified using the gating strategy represented in Fig 4 (a-e). In the thymus, the majority of viable cells were mature T cells (Fig. 4f) with no differences between cells collected from Sac or PAE rat offspring. Note that the thymus is primarily involved in T cell maturation, therefore, it was not unexpected that other immune cell subsets were not reliably detected in the thymus (data not shown). T cells (about 30-65%) and B cells (2-40%) were identified in the spleen, lymph node, PECs and the peripheral blood (Fig. 4f-g) with no differences in their proportions from Sac or PAE treated rat offspring. Interestingly, compared to Sac-treated rats, NK cells collected from PAE rats were significantly increased in the lymph node, whereas the NK cell population was significantly decreased in the PECs (Fig. 4h). While there was a strong trend toward decreased NK cells in the PBMNs, the proportion of NK cells in the spleen from PAE and Sac rats were virtually the same (Fig 4h). Combined, these data suggest that of the immune cell examined, NK derived from PAE cells are somewhat primed under basal conditions and may contribute to enhanced trafficking following a secondary challenge, as they have already migrated to tissue areas where antigen presentation of pathogen- or danger-associated molecular patterns takes place.

Myeloid cell proportions from middle-aged PAE offspring are elevated in secondary lymphoid organs

The composition of myeloid immune cells was compared from the immune compartments, the spleen, lymph node, PECs and PBMNs using the gating strategy described in Fig. 4 (a-e). Compared to Sac offspring, data revealed significant increases in myeloid cell proportions in the spleen and the lymph node of PAE rats (Fig. 5a-b for representative plots). More importantly, though CD11b/c expression is considered a general myeloid cell marker, expression and up regulation of CD11b/c often corresponds with leukocyte activation. Therefore, these data suggest a chronic basal increase in the programming of myeloid cell activation in peripheral lymphoid organs that occurs as a consequence of PAE. While the proportions of myeloid cells in the PBMNs and PECs were comparable between Sac and PAE groups (Fig. 5b), these data further support that immune cell responses in later life may be heightened following minor challenges.

PAE primes peripheral immune cells resulting in augmented pro-inflammatory cytokine production

The current report demonstrates alterations in peripheral immune cell populations (Fig. 4-5) of PAE rats that suggest the functional leukocyte responses to typical immune stimulators may be exacerbated to typical challenges. Leukocyte responses were evaluated in a mixed population of immune cells collected from Sac or PAE rats. PMA/Io (for splenocytes) and LPS

(myeloid cells) stimulation was used to examine the protein production of the classic pro-inflammatory cytokines, TNFα and IL-1β, which are key in mediating allodynia following sciatic nerve damage. Data revealed a profound enhanced cellular response from 1 year-old PAE offspring compared to cellular responses from Sac offspring. Leukocytes were isolated from the spleen and peritoneal cavity. Following PMA/Io stimulation, significant increases in the proportions of TNFα producing splenic leukocytes was observed in cells from PAE compared to cells collected from the Sac group (Fig. 6 a-b). Compared to leukocytes without LPS stimulation, LPS stimulation significantly induced TNFα and IL-1β protein levels in leukocytes from Sac offspring, as expected (Fig. 6c-d). However, LPS stimulation of leukocytes from PAE offspring resulted in the greatest increase in TNFα production as detected in the cell culture supernatant (Fig. 6c) and cell lysate (data not shown). Similarly, compared to stimulated leukocytes from Sac offspring, IL-β levels from cell lysates were greatest from PAE leukocytes stimulated with LPS (Fig. 6d). Together, these data demonstrate that adult immune cells that have previously undergone PAE appear "normal" under basal conditions, but generate exaggerated cytokine responses to typical stimuli. Moreover, the primed immune cell programming induced by PAE persists throughout adulthood. These data indicate the potential contribution of the PAE-primed peripheral immune system underlying the susceptibility to neuropathy in middle-aged rats.

Discussion

Data from recent reports support the emerging idea that moderate drinking during pregnancy, which results in mean maternal peak serum ethanol levels of 60-80 mg/dL, exacerbates later-life central nervous system (CNS) dysfunction upon subsequent challenge either from immune activation or nervous tissue damage (Terasaki and Schwarz, 2016a; Noor et al., 2017). These reports demonstrate that long-term PAE-related adverse outcomes ranging from cognitive deficits to potentiated peripheral neuropathy are associated not only with elevated CNS glial reactivity, but also adult-onset injury-induced exaggerated peripheral immune cell responses suspected to participate in ongoing peripheral neuropathies. A recent study using moderate PAE in rats conducted by Noor et al. (Noor et al., 2017) reported the striking observation of identical baseline sensory responses in saccharin and PAE offspring, suggesting the pathological consequences of PAE are not necessarily overt, but rather, can be unmasked following a secondary insult. These results further suggest PAE may create risks associated with later-life CNS pathology (i.e. neuropathy) triggered by challenges typically unnoticed and resolved in non-PAE individuals. The current work demonstrates that in later-life adult PAE offspring, PAE creates susceptibility to adult-onset peripheral neuropathy despite a substantial reduction in sciatic nerve injury not typically observed in the absence of prenatal alcohol exposure (Fig. 1).

In the current report, analysis of the dorsal horn of the spinal cord collected from the same rats examined for peripheral neuropathy revealed that

61

standard (4-suture) CCI induces exaggerated bilateral microglial activation and proliferation, as assessed by immunoreactivity (IR) of two microglial markers Iba1 and TMEM119, providing converging lines of evidence (Fig. 3 A-E). Elevated bilateral spinal astrocyte activation was observed concurrently, as measured by GFAP IR (Fig 2). These data agree with previous reports that have demonstrated that both astrocytes and microglia mediate allodynia through their activation and release of proinflammatory cytokines (Milligan et al., 2003). Interestingly, spinal cords from PAE offspring with minor CCI (and corresponding allodynia) revealed no changes from sham conditions in microglial activation, as measured by both Iba1 and TMEM119, yet bilateral astrocyte activation was observed as significant increases in GFAP IR compared to Sac control rats (Fig 2A and B) were evident. Together, these data suggest that spinal astrocytes and not microglia are playing a key role in mediating a PAE-associated increased risk for developing allodynia following minor injury. This notion is supported in previous studies showing no microglial activation in PAE animal within the visual cortex (Wong et al., 2017).

Further characterization of immune cell populations collected from surgically-naïve saccharin and PAE offspring provided insight into the PAE-induced priming on immune subsystems, such as the adaptive immune system that requires the action of both B and T cells and the innate immune system that can initially act without T and B cell involvement (Janeway et al., 2017). Our T and B cell data revealed normal distribution patterns regardless of whether these cells were derived from Sac or PAE rats (Fig. 4f-g), which is consistent with prior reports (Norman et al., 1991; Basham et al., 1998; Moscatello et al., 1999).

However, other studies that ranged from a moderate PAE (Jerrells and Weinberg, 1998; Zhang et al., 2012) to a chronic life-long PAE (McGill et al., 2009) have shown cellular activation states and altered adaptive immune responses prior to subsequent challenge in adult rodents following PAE. The work in the current report support that further exploration into the possible effects of PAE on inflammatory versus anti-inflammatory T cell phenotypes underlying chronic neuropathy is needed, Using recently developed flow cytometry techniques, such as mass cytometry and imaging flow cytometry, would be beneficial (Korn et al., 2007; Jäger and Kuchroo, 2010; Barteneva et al., 2012; Carvajal et al., 2017; McFarlin and Gary, 2017).

Cellular populations critical to the function of the innate immune system revealed significantly different levels between Sac and PAE treatment groups (Fig. 4h). NK cells play a role similar to that assigned to T cytotoxic lymphocytes and provide rapid immune responses to tissue injury such as sciatic nerve damage, or infection (Janeway et al., 2017). NK cells populate/migrate to lymph nodes when activated and may influence adaptive immune cell differentiation (Fehniger et al., 2003; Martín-Fontecha et al., 2004). Thus, observing elevated NK cell populations in PAE lymph nodes suggests these cells are in a state of increased activation after trafficking from peripheral regions where they may reside in less differentiated and activated states.

Myeloid cell proportions were heightened in PAE rats specifically in the spleen and lymph node compared to Sac controls (Fig 5), further supporting an increase in an activated phenotype. In general, myeloid cells act as potent

antigen-presenting cells and upon immune activation, which can occur following recognition of altered self-antigens (i.e. damaged sciatic nerve axons), they acquire a "mature" differentiated state and relocate to secondary lymphoid organs to induce T cell mediated immune responses (Martín-Fontecha et al., 2009). In light of what is currently understood about myeloid cell function, the data reported here support the idea that cells from PAE rats are in a state of chronic mild heightened activation in key immune tissue systems. Given reported data here show elevated immune surveillance, the functional significance of these alterations was further explored and revealed that following *in vitro* stimulation, PAE-derived leukocytes show significant increases in TNFα and IL-1β protein (Fig. 6). Together, these data suggest that PAE alters the distribution of cells as well as their functional reactivity to immune stimulators that persists into middle age in PAE rats. A second insult results in heightened immune responses inducing allodynia.

The results of these data may extend beyond neuropathic pain and may apply to other peripheral inflammatory and CNS conditions. Additionally, the long-term clinical implications of these results suggest that some adverse consequences of *in utero* alcohol exposure only occur upon a secondary insult sometime after prenatal alcohol exposure. This possibility is supported by studies in animal models of PAE where enhanced severity and disease outcomes are associated with influenza virus (McGill et al., 2009), adjuvant-induced arthritis (Zhang et al., 2012), or following sciatic nerve damage in young adult PAE animals that display heightened allodynia and exaggerated glial activation (Noor

et al., 2017). Clinically, children with FASD display alterations in peripheral immune responses and show overall increased susceptibility to developing infections (Johnson et al., 1981). Collectively, these reports provide intriguing evidence that the effects of PAE on adult-onset disease are not observed until a secondary insult.

Astrocytes have been well-characterized to act as key mediators of enduring allodynia following peripheral neuropathy (Zhuang et al., 2005; Milligan and Watkins, 2009; Ji et al., 2013), and this possibility is further supported by current data from PAE rats with allodynia. Prior work demonstrated that moderate PAE downregulates the expression of the astrocyte specific glutamate transporter, glutamate aspartate transporter or GLAST (Danbolt, 2001; Brolese et al., 2015) , which may underlie the observed elevation in spinal astrocyte activation in PAE allodynia rats described in the current report. Indeed, following CCI in rats, spinal astrocyte-specific glutamate transporters downregulate leading to the induction of allodynia (Sims and Robinson, 1999), which is thought to occur as a consequence of reduced glutamate clearance and enhanced glutamate action on spinal pain projection neurons. In addition, prior reports have shown that inhibition of astrocyte glutamate transporters results in potentiated allodynia (Sung et al., 2003). Together these data suggest that PAE-induced allodynia may be a result of alterations within astrocyte-specific glutamate transporters.

In PAE rats with minor injury, astrocyte but not microglial activation in the contralateral dorsal horn of the spinal cord are significantly elevated compared to

sham conditions, coinciding with slight increases in contralateral hindpaw sensitivity. Previous publications suggest that contralateral allodynia is a result of astrocyte activation and subsequent release of proinflammatory cytokines (Milligan et al., 2003) that spread to the contralateral spinal cord via communication through astrocyte-specific gap junctions (Spataro et al., 2004). Thus, it is possible that following minor CCI in PAE rats, elevated contralateral spinal cord astrocyte activation is sufficiently elevated to induce small increases in contralateral hindpaw sensitivity. This data supports the notion that a sufficient threshold of astrocyte activation is needed to induce bilateral allodynia. It should be noted that microglial activation is also observed following standard CCI. Previous reports have suggested that elevated microglial activation plays a greater role in the induction of contralateral allodynia (Gallo et al., 2017).Therefore, a combination of both astrocyte and microglial activation mat be required to generate robust bilateral allodynia observed following standard unilateral sciatic nerve injury.

Conclusions

In conclusion, the risks of PAE associated with pathological pain endure long into middle adulthood and can be unmasked following even minor injuries to the peripheral nervous system. A contributing factor in the PAE-induced susceptibility to peripheral neuropathy is heightened spinal astrocyte responses following minor CCI. Additionally, not only does PAE alter peripheral immune cell distribution, but also primes peripheral immune cell responses to immune stimuli

resulting in heightened cytokine production. Heightened immune-cytokine responses as a consequence of PAE may be the critical underlying factor rendering one susceptible to chronic adult-onset neuropathies from minor insults. The results demonstrate that some of the adverse effects of PAE occur via long-lasting pathologically-altered neuroimmune responses.
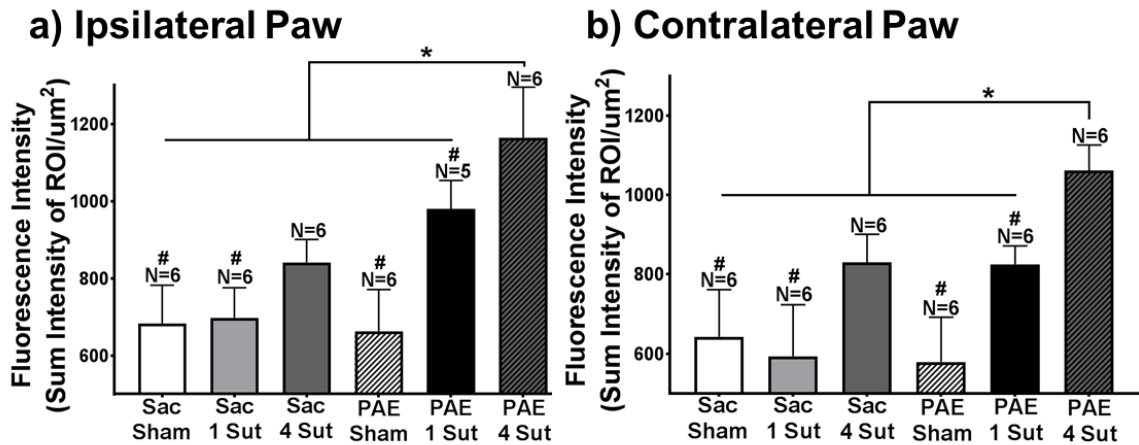
Figure 1
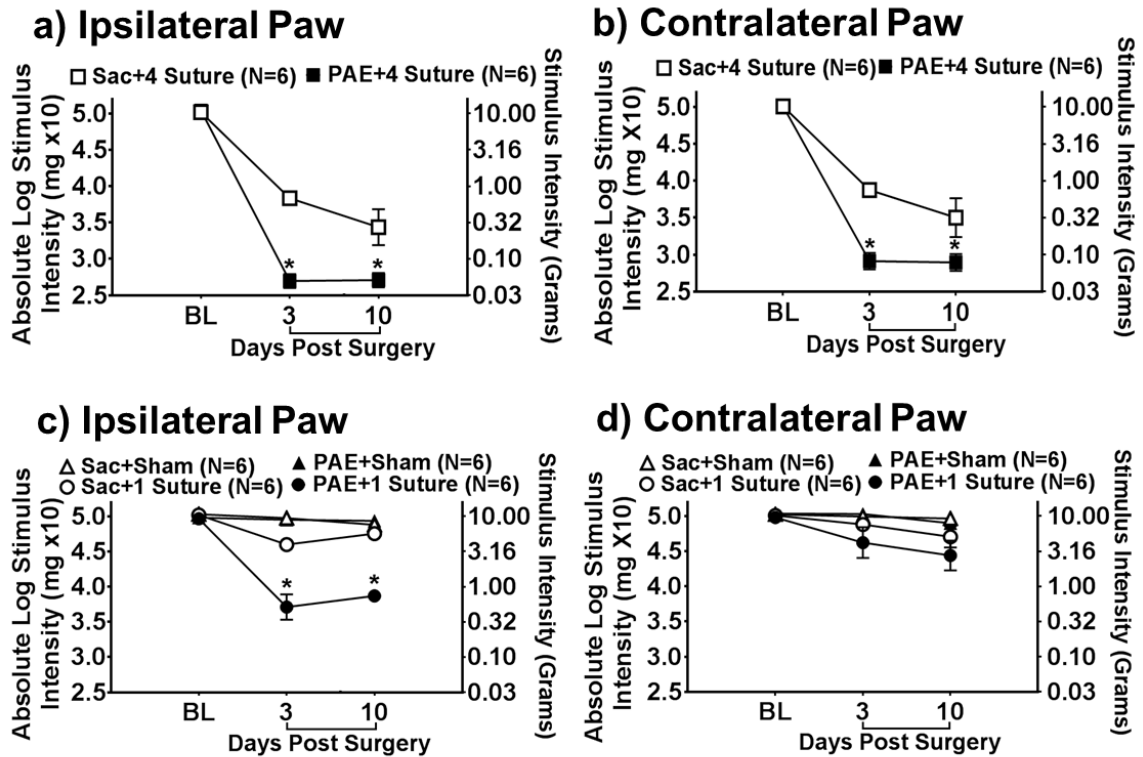
Figure 1. Prenatal alcohol exposure (PAE) causes *enhanced* allodynia following standard sciatic damage and allodynic *susceptibility* following minor nerve damage. Hindpaw response thresholds from (a-b) minor (1-suture) vs (c-d) standard (4-suture) unilateral sciatic nerve injury (CCI) in middle-aged PAE rats. (a-d), All Sac and PAE rats displayed similar baseline hindpaw sensitivity responses following application of mechanical stimuli. Following surgical sciatic nerve manipulation, a main effect of alcohol exposure, surg, and an interaction between alcohol exposure and surgery was seen. (a-b) Following minor CCI, PAE rats developed increased sensitivity whereas Sac rats did not. A main effect of alcohol exposure, surgery, as well as an interaction between alcohol exposure and surgery was revealed. Asterisks indicate $p < 0.05$. The data are presented as the mean ± SEM.

Figure 2

Astrocyte

a) Ipsilateral Paw
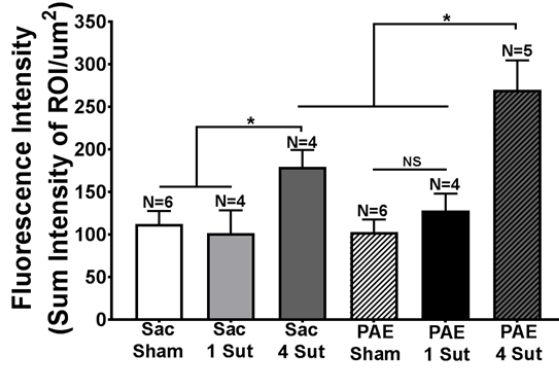

b) Contralateral Paw

Figure 2. PAE induces heightened spinal cord astrocyte activation following both standard and minor CCI. Quantification of immunoreactivity (IR) following immunohistochemical (IHC) procedures was applied to assess the degree of astrocyte activation (GFAP) following standard and minor CCI. Fluorescence intensity is defined as the total sum intensity within the dorsal horn spinal cord (identified as a region of interest - ROI) divided by the area of the ROI. (a-b) A main effect of alcohol exposure and surgery is seen in both ipsilateral and contralateral dorsal spinal cord relative to the side of sciatic nerve injury. PAE rats with standard 4-suture CCI had significantly elevated ipsilateral and contralateral GFAP IR compared to Sac control rats with standard 4-suture CCI. Following minor CCI, PAE rats had elevated ipsilateral and contralateral GFAP IR compared to PAE Sham, Sac Sham, Sac 1-suture. Minor CCI-PAE rats revealed comparable IR to Sac 4-suture. Representative images (c) of GFAP IR used in IHC analysis are shown for Sac Sham, Sac standard CCI, and PAE standard CCI conditions at 20x. N=5-6 rats per group. Asterisks indicate p < .05. Number sign indicates significance amongst groups at p < 0.05. The data are presented as the mean ± SEM.

Figure 3

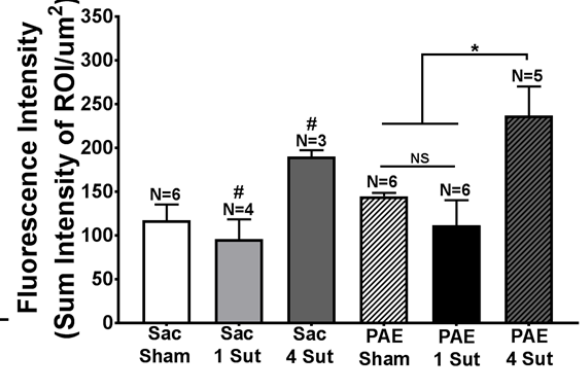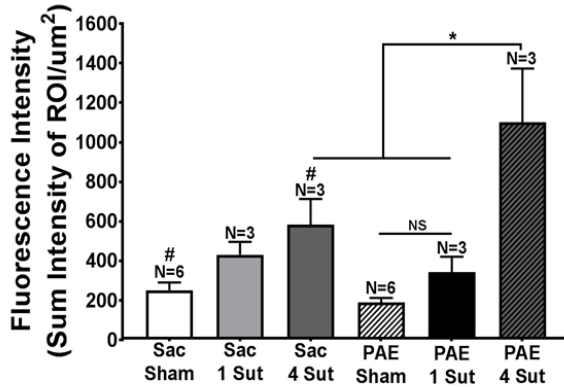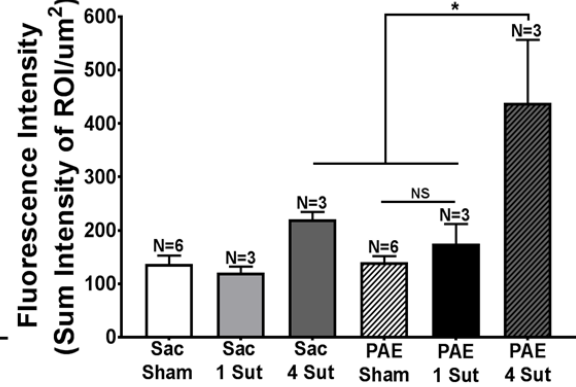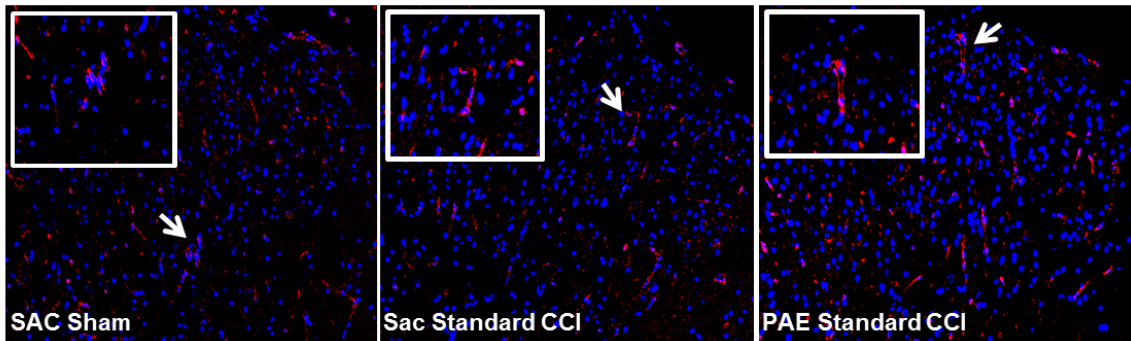Figure 3. Minor CCI does not augment microglial activation in PAE rats.
Applying IHC quantification following either standard CCI or minor CCI, two
markers to identify alterations in microglial activation were examined: the
microglial specific marker TMEM119 and the microglial and macrophage marker

Iba1. (a-b) TMEM119 IR revealed a main effect of surgery. Comparisons *a priori* of TMEM119 IR (a-b) showed that following standard CCI, PAE rats display elevated bilateral microglial activation compared to the PAE sham condition as well as PAE rats with minor injury. TMEM119 IR was also significantly elevated in PAE rats with standard CCI compared to Sac rats with standard CCI within the ipsilateral dorsal spinal cord. Sac rats with standard CCI displayed elevated TMEM119 IR within the ipsilateral dorsal spinal cord compared to Sac sham rats. These rats also revealed bilateral increases in TMEM119 IR compared to Sac rats with minor injury. No significant differences in TMEM119 IR were seen between PAE sham and PAE minor CCI conditions. (d-e) Iba1 results reveal a main effect of surgery. Iba1 comparisons *a priori* (c-d) revealed significantly elevated IR in PAE with standard CCI compared to PAE sham rats, PAE rats with minor injury, as well as Sac rats with standard CCI. Sac rats with standard CCI had significantly elevated Iba1 IR compared to Sac sham rats in the ipsilateral dorsal spinal cord and contralateral spinal cord. No significant differences were seen between PAE sham and PAE minor CCI conditions. (e) Representative images of TMEM119 IR and (f) Iba1 IR that were included in the IHC analysis are shown for Sac Sham rats, Sac rats with standard CCI, and PAE rats with standard CCI at 20x. Inset for TMEM119 is shown at 60x. Asterisks indicate $p < 0.05$. NS indicates not significant. The data are presented as the mean ± SEM.
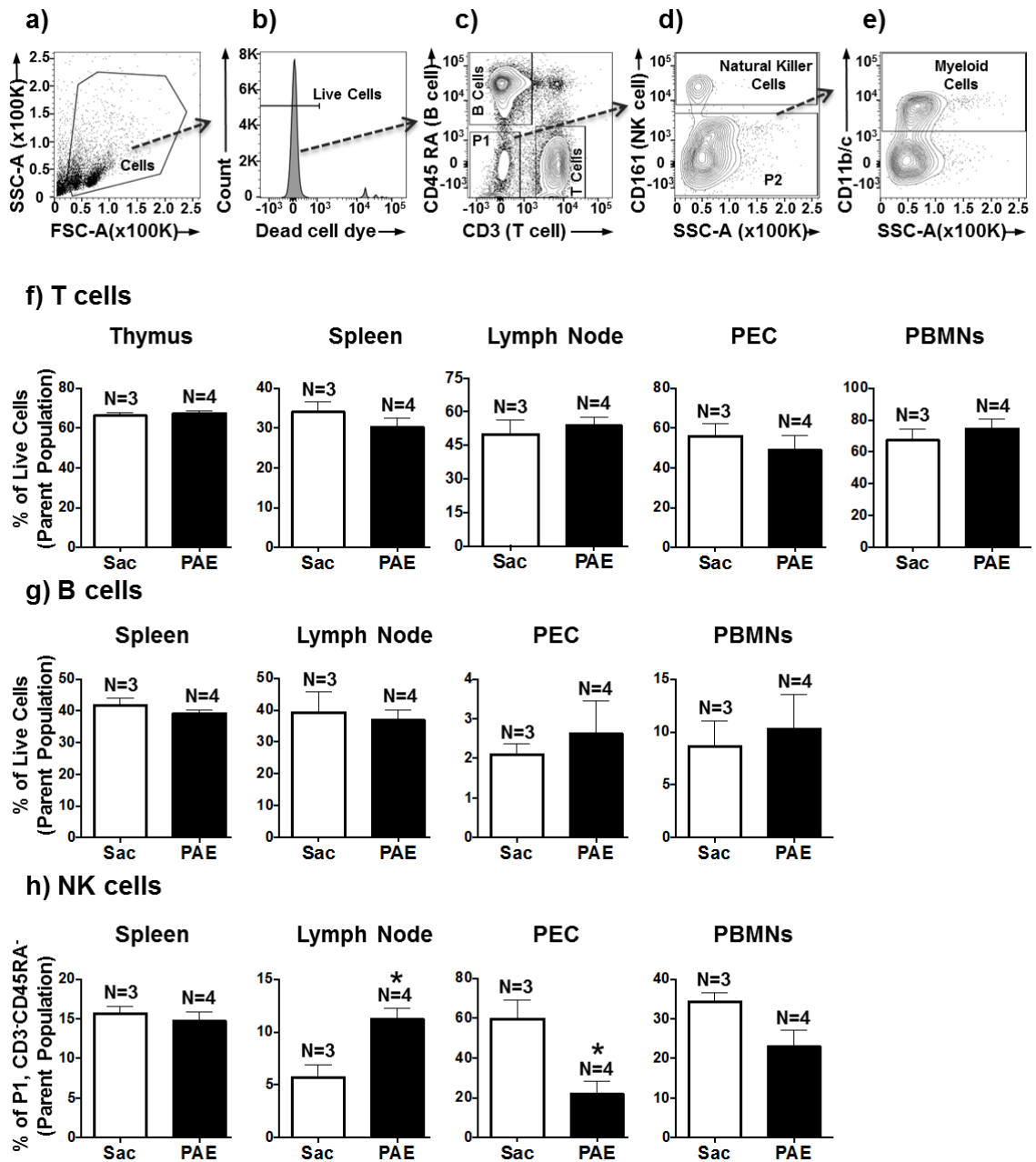
Figure 4. Characterization of major immune cell subsets in peripheral leukocytes as a consequence of PAE. (a-e) Representative flow cytometry plots and gating strategy to identify immune cell subsets in surgically-naive Sac and PAE rats. (a) The intact/healthy cells were identified based on their light scatter properties. (b) Only live cells (verified by the absence of viability dye) were included for subsequent analyses. (c) T cells and B cells were identified by positive expression of CD3 and CD45RA, respectively. The double negative cell population was identified as P1. (d) Within P1, NK cells were quantified by their

expression of CD161. The cell population not expressing CD161 was identified as P2. (e) P2 cells were further analyzed for the expression of CD11b/c (binds common epitope between CD11b and CD11c) to identify myeloid cells. Bar graphs represent proportions of (f) T cells, (g) B cells and (h) NK cells in leukocytes collected from thymus, spleen, lymph nodes, peritoneal cavity (PEC) and peripheral blood (PBMNs). Data are presented as percentages of their parent populations. A significant increase of NK cells was observed in the lymph node, whereas NK cells in the peritoneal cavity were reduced. Data are representative of two independent experiments. Sac (N=3 rats) and PAE (N=4 rats), in each experiment (total of Sac; N=6 and PAE; N=8). Asterisks indicate p < 0.05. The data are presented as the mean ± SEM.

Figure 5

a) Myeloid cells
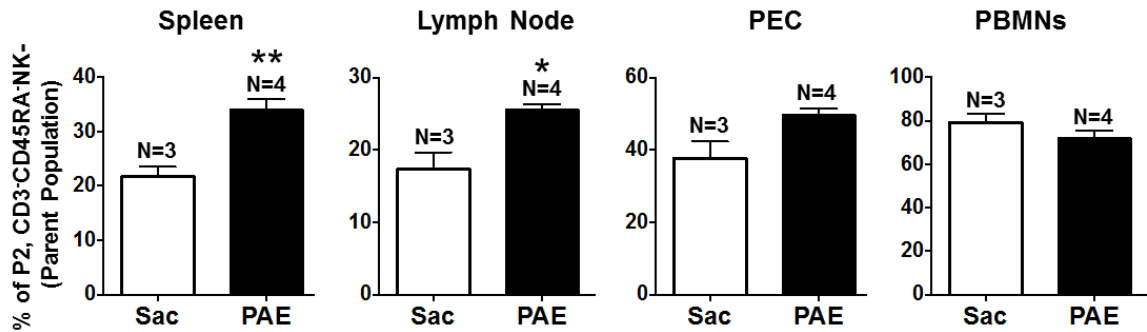
Figure 5. PAE induced myeloid cells in the secondary lymphoid organs. Leukocytes displaying negative expression of B cell, T cell and NK cell markers (P2 population in Fig. 4), were further analyzed for myeloid cell marker (CD11b/c) expression. (a) Bar graphs showing proportions of myeloid cells in the spleen, medial iliac lymph nodes, peritoneal cavity (PEC) and peripheral blood mononuclear cells (PBMN). Myeloid cell proportions were significantly increased in the spleen and in the lymph nodes in PAE rats. (b) Representative flow

cytometry plots of CD11b/c expression vs side scatter (SSC-A) in the spleen (top panels) and in the lymph node (bottom panels) from Sac and PAE rats is provided. Data are representative of two independent experiments. Sac (N=3 rats) and PAE (N=4 rats), in each experiment (total of Sac; N=6 and PAE; N=8). Asterisks indicate $P < 0.05$. The data are presented as the mean ± SEM.
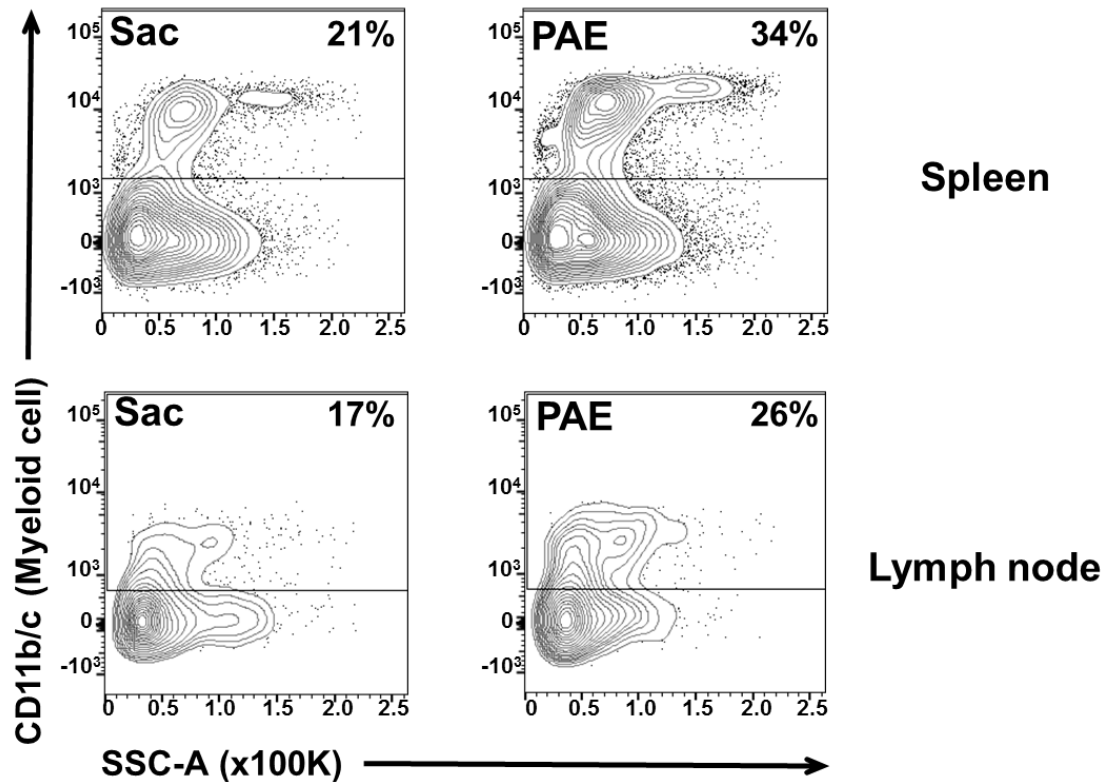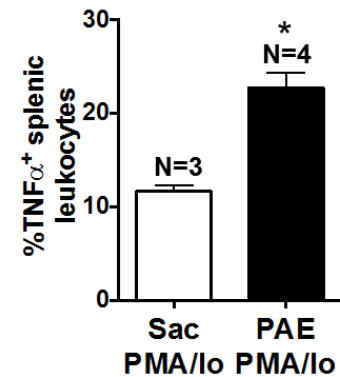
Figure 6

a) TNFα⁺ / Spleen

b)

c) TNFα / PECs
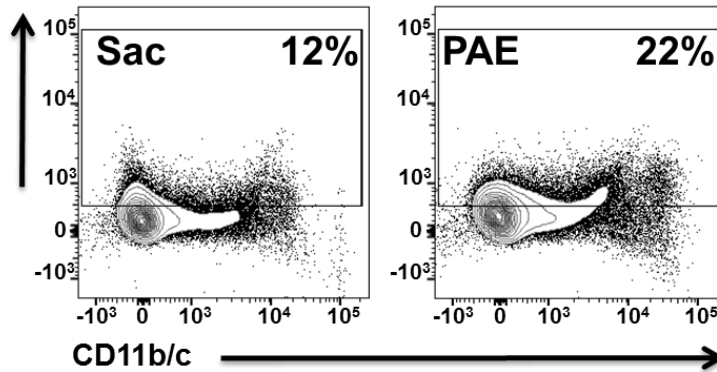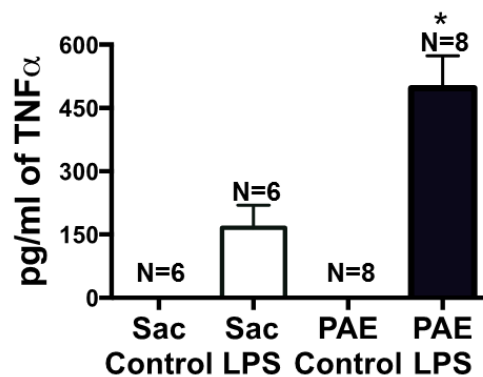
d) IL-1β / PECs
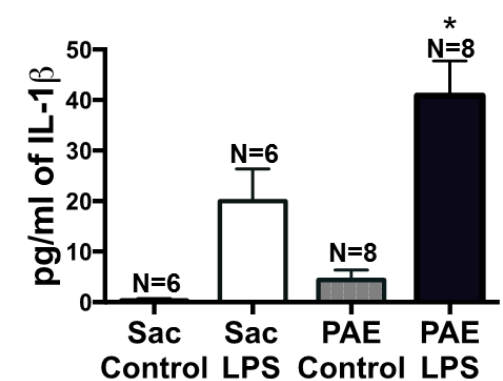
Figure 6. Peripheral immune cells in middle age PAE rats display augmented pro-inflammatory cytokine production. (a-b) Splenic leukocytes and (c-d) PEC were stimulated *in vitro* to examine their functional response profiles in proinflammatory cytokine production from Sac vs PAE rats. (a) Representative flow cytometry plots showing TNFα expression with CD11b/c expression on splenic leukocytes. (b) Bar graph of proportions of leukocytes displaying intracellular TNFα protein levels following 5 hrs of PMA/Io stimulation. Proportions of TNFα producing splenic leukocytes were significantly induced in PAE rats, (c) TNFα levels in the media/ cell-free supernatant after 24 hrs of LPS stimulation of PECs. Both LPS stimulation and PAE increased TNFα production. A significant interaction between LPS stimulation and PAE was observed ($F_{1,24} =$ 10.74, p = 0.0032). LPS stimulated leukocytes from PAE rats induced the greatest number of TNFα production than LPS stimulated leukocytes from Sac rats. (d) IL-1β levels in cell lysates of PECs following leukocyte stimulation with LPS. Both LPS stimulation and PAE increased IL-1β production. Following stimulation with LPS, IL-1β production was significantly increased in leukocytes from PAE than leukocytes from Sac rats. N=6 rats in Sac groups and N=8 rats in

PAE groups. Asterisks indicate $p < 0.05$. The data are presented as the mean ± SEM.

Chapter 3 - Targeting the β2-integrin LFA-1, reduces adverse neuroimmune actions in neuropathic susceptibility caused by prenatal alcohol exposure

Abstract

Recently, moderate prenatal alcohol exposure (PAE) was shown to be a risk factor for peripheral neuropathy following minor nerve injury. This effect coincides with elevated spinal cord astrocyte activation and *ex vivo* immune cell reactivity assessed by proinflammatory cytokine interleukin (IL) -1β protein expression. Additionally, the β2-integrin adhesion molecule, lymphocyte function-associated antigen-1 (LFA-1), a factor that influences the expression of the proinflammatory/anti-inflammatory cytokine network is upregulated. Here, we examine whether PAE increases the proinflammatory immune environment at specific anatomical sites critical in the pain pathway of chronic sciatic neuropathy; the damaged sciatic nerve (SCN), the dorsal root ganglia (DRG), and the spinal cord. Additionally, we examine whether inhibiting LFA-1 or IL-1β actions in the spinal cord (intrathecal; i.t., route) could alleviate chronic neuropathic pain and reduce spinal and DRG glial activation markers, proinflammatory cytokines, and elevate anti-inflammatory cytokines. Results show that blocking the actions of spinal LFA-1 using BIRT-377 abolishes allodynia in PAE rats with sciatic neuropathy (CCI). This effect is observed (utilizing immunohistochemistry; IHC, with microscopy analysis and protein quantification) in parallel with reduced spinal glial activation, IL-1β and TNFα expression, and elevated IL-10 in the spinal cord. DRG from PAE rats with neuropathy reveal significant increases in

satellite glial activation and IL-1β, with a reduction of IL-10. Further, blocking

spinal IL-1β with i.t. IL-1RA transiently abolishes allodynia in PAE rats,

suggesting that IL-1β is necessary for susceptibility to adult-onset peripheral

neuropathy caused by PAE. mRNA analysis reveal that BIRT-377 increased

CCL2 and CXCL1 at the damaged SCN in rats with CCI. These data

demonstrate that PAE creates life-long dysregulated IL-1β /IL-10 responses to

minor injury in the sciatic-DRG-spinal pain pathway. PAE creates a risk for

developing peripheral neuropathies, and LFA-1 may be a novel therapeutic target

for controlling dysregulated neuroimmune actions as a consequence of PAE.

Introduction

Fetal alcohol spectrum disorder (FASD), a condition that occurs as a result of prenatal alcohol exposure (PAE), results in cognitive and behavioral deficits (Mattson et al., 1998). Unfortunately, many of the central nervous system (CNS) deficits are not always apparent. By using animal models of FASD, many of the insidious effects of PAE have been uncovered. Interestingly, a growing body of evidence shows that PAE alters immune function and reactivity. Specifically, the viability of microglial cells within the cerebellum is decreased as a consequence of developmental ethanol exposure (Kane et al., 2011). Additionally, a separate study demonstrates that hippocampal glial cells are increased in their activation state, which coincides with heightened expression of the proinflammatory cytokine interleukin (IL)-1β (Topper et al., 2015). These and other PAE studies utilize high levels of alcohol exposure to mimic the effects of binge alcohol consumption, leaving the question of whether low-to-moderate levels of PAE adversely impacts the function of the central nervous system in adulthood. Recent reports aim at understanding whether PAE alters spinal cord pain processing by utilizing an animal model of neuropathic pain. These studies demonstrate that moderate PAE alters both peripheral and spinal neuroimmune function, which are immune processes well-characterized to mediate pathological pain. Additionally, these reports demonstrate that the immune responses becomes 'primed' (i.e. sensitized) such that applying a sciatic nerve (SCN) injury generates potentiated microglial and astrocyte responses at the spinal cord, as well as enhanced expression of proinflammamtory cytokines, such as tumor

80

necrosis factor-α (TNFα) and IL-1β, at the damaged SCN (Noor et al., 2017; Noor and Milligan, 2018). Additionally, blunted expression of the anti-inflammatory cytokine IL-10, which suppresses neuropathic pain (Wilkerson et al., 2012a; Khan et al., 2015), is observed in PAE rats compared to controls at both the dorsal root ganglia (DRG) and the SCN (Noor et al., 2017). These data suggest that PAE results in heightened pro-nociceptive and proinflammatory neuroimmune responses creating enduring susceptibility to developing pathological pain.

In an effort to address the possible risk of developing neuropathy created by PAE, the injury to the SCN was substantially reduced in an effort to unmask the effects of moderate PAE on glial and immune priming (Sanchez et al., 2017). This reduction uncovered an alteration in spinal astrocytes, as the astrocyte marker, glial fibrillary acidic protein (GFAP) is significantly elevated in PAE rats with neuropathy (Noor et al., 2017; Sanchez et al., 2017), while evidence for microglial activation was not observed. In support of a role for peripheral immune cells in sensitized responses to minor injury/challenge, heightened expression of TNFα and IL-1β was observed in leukocytes from PAE rats (Sanchez et al., 2017). Together, these data suggest that the PAE leads to hyper-reactive neuroimmune response which may render one vulnerable to developing neuropathic pain.

Interestingly, the chemokine CCL2 and the β_2-integrin, lymphocyte function-associated antigen-1 (LFA-1) is altered in PAE rats (Noor et al., 2017). CCL2 activates the surface receptor, intercellular adhesion molecule-1 (ICAM-1)

that is expressed on endothelial cells and critically interacts with LFA-1 (Dustin and Springer, 1988), a process underlying transendothelial leukocyte migration into CNS sites expressing CCL2. LFA-1 is expressed by peripheral leukocytes (e.g. macrophages and T-cells) and microglia (Hailer et al., 1997; Evans et al., 2006). Following peripheral nerve damage, peripheral leukocytes utilize ICAM-1-LFA-1 interactions to extravasate into the spinal cord where projections of the damaged nerve terminate onto spinal pain projection neurons and release CCL2. Thus, high CCL2 expression occurs in the spinal regions where excitatory neuronal communication and pain relays occur, further aiding in the induction of allodynia. Interestingly, LFA-1 expression can potentially influence IL-10 expression (Labuda et al., 1998; Emoto et al., 2003). A separate study looking at the influence of LFA-1 on cytokine activity demonstrate that pretreating cultured macrophage cells (RAW267) stimulated with lipopolysaccharide (LPS) using an LFA-1 antagonist, BIRT-377, results in a dose-dependent increase in IL-10 protein release with a simultaneous decrease in IL-1β and TNFα protein release (Lam et al., 2014). Therefore, the present study examines whether blocking LFA-1 activation can generate an anti-inflammatory phenotype within the DRG and spinal cord resulting in reversal of chronic allodynia in neuropathic susceptible PAE rats.

The present report utilizes a rodent model of peripheral neuropathy referred to as chronic constriction injury (CCI), but modified with significantly reduced injury by applying a single suture (minor CCI) rather than the established 4-suture paradigm. By applying a minor CCI to a characterized rat model of

moderate PAE, allodynia is induced only in PAE rats, replicating prior findings (Sanchez et al., 2017). Following CCI, BIRT-377 is injected intrathecally followed by behavioral assessment. At maximal efficacy of BIRT-377 on suppression of allodynia, tissue is collected from the SCN, DRG, and dorsal horn of the spinal cord to characterize the proinflammatory cytokine and chemokine profile using IHC, electrochemiluminescence (for protein quantification assays), and mRNA gene expression. Additionally, IL-1 receptor antagonist (IL-1RA) is administered via the intrathecal (i.t.) route to determine whether spinal IL-1β is necessary to induce allodynia following minor injury. The goals of these studies are to determine the SCN, DRG, and spinal immune factors altered and whether controlling the spinal cord cytokine/chemokine environment can reverse PAE induced sensitivity to allodynia.

Materials and Methods

Animals and Study Group Strategy

All procedures were approved by the Institutional Animal Care and Use Committee (IACUC) of the University of New Mexico Health Sciences Center and closely adhered to guidelines from the International Association for the Study of Pain for the use of animals in research. Long-Evans rat breeders purchased from Harlan Industries (Indianapolis, IN) were maintained in a breeding colony on a 12:12-hour reverse light/dark schedule (lights on from 2100 to 0900 hours), and fed Harlan Teklad rat chow and water, available *ad libitum*. For all experiments, 5-8-month old male prenatal alcohol or saccharin exposed (described below) rat

offspring derived from 56 litters were used. Offspring were transferred to a standard light/dark cycle (lights on from 0600 hours to 1800 hours) and allowed to acclimate to these conditions for at least 30 days before commencing experiments. Additionally, rats were kept in these conditions for the duration of the study.

Moderate Prenatal Alcohol Exposure Using the Voluntary Drinking Paradigm. Pregnant female rat dams are given either ethanol or saccharin throughout pregnancy until birth according to the voluntary drinking paradigm previously described (Savage et al., 2010). Briefly, 3- to 4-month-old female Long-Evans rats are acclimated for 4 hours per day, from 1000 to 1400 hours (during their active phase), to drinking water containing 0.066% (w/v) saccharin (Sac) that gradually increased in ethanol content from 0% (v/v) on Days 1-2, to 2.5% (v/v) on Days 3-4, to 5% (v/v) on Day 5 and thereafter for two weeks. It should be noted that regular drinking water is available at all times during housing. Thus, animals could voluntarily choose to drink either saccharin sweetened water containing 5% ethanol or regular water during the 4-h drinking period. At the end of the 2-week pre-pregnancy drinking phase, the mean daily ethanol consumption is determined for each rat and rats that consumed 1 standard deviation below the group mean are excluded from the study. Subsequently, female rats are assigned to either a 5% ethanol or Sac control drinking group such that the mean pre-pregnancy ethanol consumption was similar between groups. The females are then placed with proven male rat breeders until pregnant (~2-5 days). No alcohol is consumed during the breeding

84

period. Beginning on gestational day 1, rat dams are given either 0% (Sac) or 5% (PAE) ethanol in Sac water (4 hours/day, during the active phase). Sac rats are given a volume of 0% ethanol in Sac water that is matched to the mean volume voluntarily consumed by the 5% ethanol group. Total ethanol consumption is recorded for each dam, which averaged 2.04 g of ethanol/kg body weight/day. This level of drinking by rat dams produced a mean peak serum blood alcohol concentration of 60.8mg/dl (Savage et al., 2010). No significant differences are observed between prenatal treatment groups in dam weight gain during pregnancy, pup birth weights, or litter size, replicating previous reports (Savage et al., 2010; Noor et al., 2017; Sanchez et al., 2017). Offspring are weaned at 24 days of age and male offspring pair-housed with the exception of five single-housed rats due to incompatibility with a cage mate. For all experiments, 5-8-month-old prenatal alcohol or saccharin-exposed animals are used. Behavioral testing of offspring is performed during the first three hours of the light cycle (inactive phase) to avoid the influence of elevated hormones under normal circadian rhythms.

A total of 108 male offspring are used in all experiments. Offspring are predominantly pair-housed with 5 rats single-housed due to incompatibility with a cage mate. Rat offspring are split into three groups. It should be noted that none of the experimental groups contained more than one subject from a given litter to avoid "litter effects". The first group and second group consists of 43 (24 with prenatal saccharin exposure, Sac; and 19 with prenatal alcohol exposure; PAE) and 51 (23 Sac and 28 PAE) rats, respectively, and are used for behavioral

examination of hindpaw sensitivity following i.t. treatment of BIRT-377 and its effects on neuropathy produced by minor peripheral nerve injury. Following behavioral verification for allodynia, Group 1 rats are used for protein and mRNA analysis whereas Group 2 rats are used for spinal cord and DRG immunohistochemical (IHC) analysis. Group 3 consisted of 14 (PAE) rats and are used to examine the effects of an i.t. administration of IL-1 receptor antagonist (IL-1RA) on CCI-induced allodynia. In all cases, experimenter is blinded to the group identities of all experimental conditions.

Chronic constriction injury (CCI)

In adult male Sac or PAE rats, sham or CCI aseptic surgical procedures are performed as previously described (Bennett and Xie, 1988; Noor et al., 2017; Sanchez et al., 2017) and modified, as described here. Under isoflurane anesthesia (3% volume in oxygen), the sciatic nerve is carefully isolated with sterile glass prongs and snuggly ligated with 1 (minor CCI) segment of sterile 4-0 chromic gut suture (Ethicon, Somerville, NJ) without pinching into the nerve. Sterile isotonic saline (0.9%) is applied to the nerve during the procedure to prevent dehydration. Sham surgery involves isolation of the sciatic nerve similar to CCI but without nerve ligation. The nerve is then gently placed back into position and the overlying muscle is sutured closed with two 3–0 sterile silk sutures (Ethicon, Somerville, NJ). Rats fully recover from anesthesia within approximately 5 minutes and are monitored daily following surgery for any post-operative complications. Two rats (1.8%) were excluded from the study due to

the presence of hindpaw autotomy.

Behavioral Assessment of Allodynia

Allodynia was assessed using the von Frey fiber test as previously described (Dengler et al., 2014; Sanchez et al., 2017). Briefly, habituation to the testing environment required placing rats atop 2-mm thick parallel bars spaced 8-mm apart allowing full access to the plantar hindpaw. Habituation occurres for approximately 45 min/day for 4 sequential days within the first 3 hours of the light cycle (inactive phase) in a sound- and temperature-controlled dimly lit section of the home colony room. Baseline (BL) responses are then assessed using the von Frey behavioral test. A total of 13 calibrated monofilaments are used in these studies. Additionally, these calibrated monofilaments (3.61–5.18 log stimulus intensity) are applied to the plantar surface of the left and right hindpaw for a maximum of 8 seconds per application. Random order between left and right hindpaw assessment is conducted. A metronome placed in the room provided guidance at 1 tick/sec. Lifting, licking, or shaking of the paw is considered a response. In a similar manner to BL evaluation, one group of rats is re-assessed following CCI or sham surgery through Day 10 prior to drug treatment. A second group of rats is assessed through Day 28 prior to drug treatment. The experimental tester was blind to the prenatal and surgical treatment groups. At either Day 10 or Day 28, rats are given an i.t. injection of drug or vehicle (described below) and behavioral re-assessment occurs daily for 4 sequential

days post-injection to examine the effects of i.t. BIRT-377, or at 1, 2, 2.5, 3, and 24hrs post-injection to examine the effects of i.t. IL-1RA.

Drug preparation

BIRT-377 is a small molecule characterized as a non-competitive inhibitor of leukocyte function-associated antigen-1 (LFA-1) that minimizes the active conformation of this transmembrane β_2-adhesion receptor expressed on leukocytes (e.g. T cell and myeloid cells). BIRT-377 (Tocris, Bristol, UK) was initially reconstituted in 100% ethanol as a stock solution at a concentration of 22.156mg/ml, aliquoted into 0.5 ml sterile Eppendorf tubes and stored in a clean sealed container at 4°C for later use. On the day of i.t. injection, sterile ddH_20 is warmed in a water bath and BIRT-377 is added to reach a concentration of 500 ng/20µl for i.t. injection and vortexed for 2 min. Vehicle consisted of sterile ddH_2O. Animals are injected within the hour following drug dilution.

IL-1 receptor antagonist (IL-1RA) (R&D systems, Minneapolis, MN) is reconstituted in sterile ddH_20 at a stock concentration of 50 mg/ml, aliquoted into 0.5 ml sterile Eppendorf tubes and stored at -20°C for later use. On day of i.t. drug injection, IL-1RA is diluted in 0.1% rat serum albumin (RSA) in sterile phosphate buffered saline (PBS) to a concentration of 1µg/µl containing 0.01% RSA. Therefore, each rat receives 20µg of IL-1RA in 20µl i.t. Vehicle consists of 0.1% RSA in sterile PBS.

Intrathecal (i.t.) Injection

BIRT-377, IL-1RA or vehicle is administered using an i.t. catheter on Day 28 (BIRT-377) or Day 10 (BIRT-377 or IL-1RA) post-surgery as described previously (Milligan et al., 2005). Briefly, under isoflurane anesthesia (3% volume in oxygen), the beveled needle end of an 18-gauge sterile (Bectin Dickson, Franklin Lakes, NJ) needle with the plastic hub removed is inserted between lumbar vertebrae L5-L6. PE-10 tubing (Fisher Scientific, Hampton, NH) is fitted with a 30-gauge sterile needle (Bectin Dickson, Franklin Lakes, NJ) containing a Hamilton syringe at one end and labeled with a marking at 7.7 cm at the opposite end. Drug or equivolume of vehicle (20 µl) is withdrawn from the open side of the PE-10 tubing. The open end of the tubing is then threaded into the 18-gauge needle until the 7.7 cm marking is reached. This position corresponds to the lower lumbar L4-L5 region of the spinal cord. Correct placement of the PE-10 is determined by twitching of the hindleg and/or tail during catheter advancement, as well as cerebrospinal fluid efflux from the externalized portion of the needle. Drug is administered over a 25 second interval. Immediately following drug or vehicle administration, tubing is removed followed by removal of the needle and rats are allowed to recover before being placed in their home cage. Rats fully recover from anesthesia within 5 minutes and 100% motor recovery is observed following injection.

Immunohistochemical (IHC) tissue sample preparation

All tissue from rats behaviorally verified for allodynia on Day 4 (Day 32 post-surgery) after i.t. BIRT-377 injection are collected for IHC processing as

described previously (Noor et al., 2017; Sanchez et al., 2017). Briefly, rats are overdosed with sodium phenobarbital (390 mg/ml Sleepaway, Fort Dodge Animal Health, Fort Dodge, IA) and transcardially perfused with 0.1 M phosphate buffered saline (PBS; pH = 7.4), initially at a rate of 28 ml/min, then increased to 32 ml/min (~10 min), followed by 4% paraformaldehyde (PFA; pH = 7.4; 28-34 ml/min, 8 min). Immediately following transcardial perfusion, the spinal vertebral column from C2-L6 with the spinal cord intact within the vertebral column are collected and cut at vertebra T7 into a rostral and caudal half of the spinal vertebral column. All spinal cord sections undergo 48-hour post-fixation in 4% PFA at 4 °C.

Following post-fixation, the entire spinal cord (T7- L6) is carefully isolated, and separately, the corresponding L4-L6 dorsal root ganglia (DRG), making sure to maintain tissue integrity. The isolated spinal cords are then subsequently paraffin processed. At a later time, DRGs are individually dissected and paraffin processed. Paraffin-embedded blocks are then subsequently sliced on a microtome with adjacent 7 μm tissue sections mounted onto vectabond-treated slides**.

To investigate spinal augmented neuroimmune activation, we analyze the expression of the astrocyte marker, glial fibrillary acidic protein (GFAP), the microglial activation marker ionized calcium-binding adapter molecule 1 (Iba1), the proinflammatory cytokine marker IL-1β, and the anti-inflammatory marker IL-10 in L4-6 spinal segments, as reported previously (Wilkerson et al., 2012a). Slides containing tissue from lumbar (L4-L6) spinal cord and (L4-L6) DRG are

chosen for staining to capture overall reactivity (Wilkerson et al., 2012a). Paraffin-processed tissues undergo deparaffinization followed by rehydration and antigen retrieval procedures in a standard rice cooker at 94-96° C allowing for gentle and equal distribution of temperature warming throughout tissue sections. For antigen retrieval, polyclonal GFAP required a Tris-based buffer at pH 9.5 (BioCare Medical, Concord, CA), Monoclonal GFAP, Iba1, and IL-1β required a Tris-based buffer at pH 9.0 (Vector, Burlingame, CA), and IL-10 required a citrate-based buffer at pH 6.0 (BioCare Medical, Concord, CA). All tissue sections are incubated with 5% normal donkey serum (NDS), PBS pH 7.4 for 2h, followed by overnight primary antibody incubation using rabbit anti-rat polyclonal GFAP (Millipore, 1:1000), rabbit anti-rat monoclonal GFAP (Abcam. 1:400), rabbit anti-rat polyclonal Iba-1 (Wako, 1:300), or rabbit anti-rat polyclonal IL-1β (Santa Cruz, 1:100), or goat anti-rat polyclonal IL-10 (Vector Labs, 1:250) in a humidity chamber at 4° C. Tissues are washed 3x with 0.1M PBS pH 7.4. All tissues, except those containing IL-10 antibody, are incubated with donkey-anti rabbit FITC- or TRITC- conjugated secondary antibody incubation for 2 hr in a humidity chamber at room temperature and rinsed in 0.1 M PBS. IL-10 spinal cord and DRG sections are incubated with a biotinylated donkey anti-goat secondary antibody (Vector Labs, 1:1300) for 1 hr followed by a 1h incubation with Vectastain ABC Elite kit (Vector Labs, Burlingame, CA). Sections are incubated for 10 min with TSA plus Fluorescein System (PerkinElmer Life Sciences, Waltham, MA,). All tissues are stained with the nuclear stain 4,6-diamidino-2-phenylindole (DAPI) (Vector Labs, Burlingame, CA) separately

before cover slipping. These slides are left at room temperature overnight and then placed at 4° C until proceeding with image acquisition and microscopy analysis (Wilkerson et al., 2012a; Sanchez et al., 2017).

Microscope spectral imaging for immunofluorescent quantification

Image acquisition for spectral analyses is performed using the Nuance spectral imaging system (http://www.cri-inc.com/products/nuancew.asp; Perkin Elmer, Waltham, MA) as described previously (Noor et al., 2017; Sanchez et al., 2017). Briefly, images of dorsal horn spinal cord are obtained using either a 20X or 40X (IL-10 spinal cord sections) objective with a Zeiss Axioplan2 inverted fluorescence microscope. A flat-field correction is applied to correct for uneven illumination during image acquisition. Image cubes are obtained from multi-labeled tissue containing DAPI, conjugated secondary antibody, as well as autofluorescence. A spectral library is then created using single-labeled slides for each fluorophore (e.g. FITC or TRITC) and a label-free (autofluorescence) slide. A computed spectrum (420 – 720 nm) is obtained by separating the known spectrum (autofluorescence) from mixed spectrum (single labeled) to produce a pure spectrum of each fluorophore. This allowed the separation of spectrum from multi-labeled slides (e.g. DAPI + TRITC) to obtain composite images containing only labels of interest. These composite images are then used for further analysis using Slidebook 6 software (below). For dorsal horn spinal cord sections ipsilateral to sciatic manipulation, sixteen to thirty-two images per experimental group (4 sections per animal, 4-8 animals per condition) were acquired and

analyzed. For L4-L6 DRG sections ipsilateral to the sciatic manipulation, thirty images per experimental group (6 sections/rat, 5 rats per condition) were acquired and analyzed. It should be noted that the 6 sections per animal were made up of the L4, L5, and L6 DRG and contained two images per DRG level. Representative acquired images from the Nuance spectral imaging system from the dorsal horn spinal cord of GFAP immunoreactive (IR) and Iba1 IR regions are shown in Fig. 2c-d, as well as IL-1β and IL-10 shown in Fig. 3c-d; and in DRG of satellite glial cells (SGCs), IL-1β, and IL-10 in Fig. 5. 20x and 40x objectives are used to produce representative images.

SlideBook6 software image analysis

Composite images are analyzed using SlideBook6 software (Intelligent Imaging Innovations, Denver, CO, USA) as described previously (Sanchez et al., 2017). Briefly, to discriminate signals originating from artifacts, the experimenter determined an acceptable threshold of very low-level emission fluorescence intensity per each experimental condition (polyclonal GFAP and Iba1 analysis), or per individual animal (monoclonal GFAP, IL-1β and IL-10 analysis). This was done by closely replicating the on-screen composite computer image with that observed through the microscope eyepiece, as described previously (Noor et al., 2017; Sanchez et al., 2017). In addition, for spinal cord sections, the dorsal horn (region of interest (ROI)) is outlined for analysis eliminating the surrounding white matter and peri-spinal blank space (intrathecal space). For DRG sections, ROI included all cell bodies found within the composite image. The image is refined to

include the predetermined threshold within the outlined area. The 'Sum Intensity' (the total signal within the outlined area in the dorsal horn) is determined and divided by the 'Area' (total area in micrometers squared (μm^2)) to obtain the 'Fluorescence Intensity'. The average of the adjacent sections from a single slide (representing a single animal) is calculated to determine the value for each animal. Finally, averages for each slide within the same condition are calculated along with the standard deviation and standard error of the mean. Data are analyzed as "Sum Intensity of ROI/μm^2.

Tissue collection and total RNA isolation

Following behavioral assessment on Day 4 post-injury (Day 14 post-surgery), rats are deeply anesthetized with isoflurane (induction 3% vol. followed by 5% in oxygen) for 10 -12 minutes. Rats are then transcardially perfused with ice cold 0.1M PBS pH 7.4 for 3 min at a rate of 24 ml per minute. The perfused body is placed on a frozen gel refrigerant pack (Glacier Ice, Pelton Shepherd Industries, Columbus, OH). Laminectomy and tissue dissection is performed to collect both ipsilateral and contralateral lumber L4-L6 spinal cord, followed by L4-L6 dorsal root ganglia, and finally ipsilateral sciatic nerve. All samples are placed in DNase/RNAse-free 1.5 ml centrifuge tubes (VWR International, Radnor, PA), flash frozen on dry ice, and stored at -80 °C for future analysis.

Flash frozen tissues are transferred to ice and 100 µl sterile 1 x PBS was added. It should be noted that, in contrast to spinal cord and DRG tissue, sciatic nerve is quickly chopped with scissors for ~2 minutes on ice. All tissues are then

homogenized using a motorized VWR disposable Pellet Mixer and motor pestle system (VWR International, Radnor, PA) for about 30 seconds. 60% of the tissue homogenate is then processed for protein analysis (described below). The remaining 40% of the homogenate is added to chilled Qiazol Lysis Reagent (Qiagen, Hilden, Germany) for total RNA isolation (described below). It should be noted that, due to the small quantity of DRG tissue collected, 100% of tissue homogenate is used for RNA isolation and not protein analysis.

Tissue lysate preparation and Meso Scale Discovery (MSD) Multi-Spot Assay System

Flash frozen ipsilateral sciatic nerve and ipsilateral and contralateral lower lumbar L4-L6 spinal cord sections collected from animals are prepared for MSD Multi-Spot Assay system as previously described (Noor et al., 2017). Briefly, tissues are allowed to thaw on ice and homogenized using a Fisherbrand Disposable Pestle system (Fisher Scientific, Hampton, NH). Samples are then sonicated in buffer containing protease inhibitors per instructions of manufacturer. All samples are then centrifuged at 4200 g, at 4 °C, for 10 minutes. Lysate is collected from samples and Bradford protein assay (Biorad, Hercules, Ca) is used to determine protein concentrations. Using a V-PLEX immunoassay (MesoScale Discovery, Gauthersburg, MD), 100 μg protein of all samples is used to determine cytokine expression levels for TNFα, IL-1β, IL-10, and CXCL1 as previously validated (Maxwell et al., 2015; Noor et al., 2017; Robinson et al., 2017).

Total RNA isolation and mRNA analysis by quantitative real-time PCR

Total RNA is extracted from ipsilateral sciatic nerve, ipsilateral and contralateral spinal cord, and ipsilateral DRG. Tissue is placed in chilled Qiazol Lysis Reagent (Qiagen, Hilden, Germany) and homogenized for 15 seconds. Total RNA is then extracted using a miRNeasy Micro Kit (Qiagen, Hilden, Germany) per manufacturer's instructions. It should be noted that an additional buffer RPE and 80% EtOH wash steps is added to remove any additional salt contaminants added from the PBS step. Tissue is centrifuged at 15,000 rpm for 1.5 min at 4° C. PBS is aspirated and 35 µl of protease inhibitor solution (MesoScale Discovery System) is added and samples were stored on dry ice and later stored at -80° C for future analysis (described below).

RNA concentration and quality is assessed using Nanodrop (ThermoFisher Scientific, Walham, MA). RNA samples are then diluted to standardized RNA concentrations of 195 ng/µl for ipsilateral DRG, 137ng/µl for ipsilateral and contralateral lumbar spinal cord, and 100 ng/µl for ipsilateral sciatic nerve. Standardized samples are then transcribed to cDNA at 2,145 ng for ipsilateral DRG, 950 ng for ipsilateral SCN, and 1,438.5 ng for ipsilateral and contralateral lumbar spinal cord. Reverse transcription is performed for all tissue types using a Superscript IV VILO cDNA Synthesis Kit (Invitrogen, Carlsbad, CA).

Levels of mRNA expression is measured and analyzed as described previously (Mellios et al., 2014). For assessment of transcripts, a dilution factor of 1:2.5 is applied to cDNA samples for ipsilateral DRG, 1:2 for ipsilateral SCN, and

1:2.2 for ipsilateral and contralateral lumbar spinal cord. cDNA dilution for assessment of rat 18S rRNA normalizer is 1:200 for all tissue types. Levels of mRNA and "Normalizer" rat 18s rRNA (Rn18s, Taqman Assay ID#: Mm03928990_g1), is assayed in triplicate using quantitative real-time PCR (qRT-PCR) with Taqman Gene Expression Assays (ThermoFisher Scientific, Waltham, MA). Gene expression assays are deemed to be "best coverage" assay by the manufacturer and is analyzed with the formula $C = 2^{\wedge}CT^{Normalizer}/2^{\wedge}CT^{Target}$ in order to exclude detection of genomic DNA (Livak and Schmittgen, 2001; Schmittgen and Livak, 2008). Chemokines chosen for qRT-PCR include CCL2 (Taqman Assay ID#: Rn00580555_m1), CXCL10 (Taqman Assay ID#: Rn01413889_g1), CXCL1 (Taqman Assay ID#: Rn00578225_m1), and CX3CL1 (Taqman Assay ID#: Rn00593186_m1). These chemokines have been previously shown to be upregulated during neuropathic pain conditions (Lindia et al., 2005; Akimoto et al., 2013; Zhang et al., 2013; Jiang et al., 2016), and additionally, CCL2 and CX3CL1 have been shown to be altered following PAE (Roberson et al., 2011; Noor et al., 2017).

Statistical analysis

SPSS (IBM, Chicago, IL, USA) is used for all behavioral analysis. At baseline (BL), a 3-way (2 x 2 x 2) analysis of variance (ANOVA) is applied to assess differences between prenatal exposure (Sac versus PAE), surgical treatment (Sham versus minor CCI) and drug injection (vehicle versus BIRT-377). Additionally, a 3-way (2 x 3) repeated measures ANOVA is used for analysis of

the between-subject factors of prenatal exposure, surgery, and injection for days post-surgery as well as days post-injection. Furthermore, 3-way (2 x 2 x 2) ANOVA is used for analysis of all IHC immunoreactivity (IR) data. Data acquired from V-Plex immunoassay and qRT-PCR are analyzed using GraphPad Prism version 7 software (GraphPad Software Inc., San Diego, CA, USA). *Post-hoc* examination of IHC IR is analyzed using Fisher's LSD test. The threshold for statistical significance was set *a priori* at α = 0.05 for all sets of multiple comparisons. In order to minimize unnecessary duplication, we use the minimum number of animals possible to make statistically significant conclusions, which is based on our previous publications (Wilkerson et al., 2012a; Dengler et al., 2014; Noor et al., 2017; Sanchez et al., 2017; Whitehead et al., 2017). Outliers were removed following Grubbs' Z-test (Grubbs, 1950). In all cases, the data are presented as the mean ± SEM. All figures are created in GraphPad Prism version 7 software (GraphPad Software Inc., San Diego, CA, USA).

Results

i.t. injection of BIRT-377 reverses enduring allodynia resulting from minor CCI in PAE rats.

Previous studies show that PAE-induced sensitivity to allodynia is enduring for at least 28 days after CCI (Noor et al., 2017). Thus, we want to determine whether blocking the activated LFA-1 altered enduring PAE induced sensitivity to allodynia. To accomplish this, i.t. BIRT-377 is administered at Day 28 post-surgery. Interestingly, all rats reveal similar hindpaw sensitivity at BL, indicating

that PAE alone does not induce allodynia, but rather, it is not until a second insult is applied that the effects of PAE are unmasked, which replicates prior findings (Zhang et al., 2012; Noor et al., 2017; Sanchez et al., 2017) (Fig. 1). Normal sensitivity is maintained throughout the 28-day time-course following sham or minor (1-suture) CCI surgery in healthy Sac control rats (Fig. 1a). In contrast, compared to PAE rats with sham surgery that maintain normal sensitivity through day 28 post-surgery, minor CCI results in robust and enduring unilateral allodynia (Fig. 1b). At Day 28, all rats received BIRT-377 or vehicle injection. Chronic allodynia is reversed in PAE rats with hindpaw responses similar to BL levels following BIRT-377, with maximal reversal seen by day 4 post-injection (Fig. 1b). No changes in hindpaw sensitivity are observed in sham groups or Sac-minor CCI. Additionally, no significant differences are seen in contralateral hindpaw responses (Fig. 1c-d). These data suggest that the blockade of activated LFA-1 may alter the pronociceptive glial and immune cytokine/chemokine spinal milieu such that a full reversal from chronic allodynia in PAE rats occurs.

Spinal BIRT-377 treatment blunts spinal glial activation.

To further explore how BIRT-377 works to reverse enduring (Day 28 post-CCI surgery) allodynia in PAE rats, spinal cords are collected and processed for IHC and image analysis from all rat groups (rats from data shown in Fig. 1) for evaluation of glial activation (Fig. 2), cytokine expression (Fig. 3) and LFA-1 expression (Fig. 4) immediately following behavioral characterization of the effects of i.t. BIRT-377 (BIRT) on allodynia. Analysis of GFAP IR reveal elevated

spinal astrocyte responses in Sac and PAE rats with minor CCI given vehicle

(Veh) injection compared to their corresponding sham groups (Fig. 2a).

Additionally, minor CCI result in significant differences in astrocyte activation in

PAE and Sac rats given vehicle (Fig. 2a). However, spinal cord astrocyte

responses are decreased in BIRT-377 treated rats (Fig. 2a). Interestingly, spinal

microglial responses were increased in both PAE and Sac rats with minor CCI

given vehicle compared to their corresponding sham groups (Fig. 2b) despite

ongoing allodynia only in PAE rats. BIRT-377 injection results in significant

decreases in microglial activation (Fig. 2b), suggesting that processes underlying

allodynia do not have to be present for BIRT-377 to exert Iba-1 expression on

activated microglia. Representative images (Fig. 2c-d) for GFAP and Iba1 are

from Sac/Sham/Veh, Sac/1-Sut/Veh, Sac/1- Sut/ BIRT, PAE/Sham/Veh, PAE/1-

Sut/Veh, and PAE/1-Sut/BIRT. These data suggest that PAE-induced allodynia

requires mechanisms in addition to microglial activation because elevated

microglial activation is observed in non-allodynia Sac/1-Sut/Veh rats. From these

data, it is plausible that astrocyte actions play a greater role in PAE susceptibility

to allodynia from minor injury.

PAE blunts normal IL-10 responses following minor CCI

Both IL-1β and IL-10 IR in the dorsal horn of the spinal cord are assessed for

changes following i.t. BIRT-377 injection (Fig. 3a-b). Compared to sham groups,

PAE rats with minor CCI given vehicle reveal elevated levels of IL-1β (Fig. 3a).

Interestingly, this elevation is also seen in Sac rats with minor CCI given vehicle

injection despite the absence of allodynia (Fig. 1a and 3a). Furthermore, BIRT-377 is sufficient to significantly decrease spinal IL-1β IR (Fig. 3a). In healthy Sac control rats, elevated levels of IL-10 IR are measured following minor CCI given vehicle compared to Sac-sham rats given vehicle (Fig. 3b). Interestingly, PAE CCI rats with ongoing allodynia (e.g. given vehicle) do not show a significant increase in IL-10 IR expression, an observation that is present in Sac CCI rats without allodynia. The elevated IL-10 IR in healthy rats (Sac) with CCI suggests the increase is in response to minor damage to maintain homeostasis and consequent non-neuropathy. In contrast, it is possible that in PAE rats, IL-10 fails to upregulate, thereby allowing for the development of allodynia following minor CCI (Fig. 3b). IL-10 IR is significantly greater in Sac-minor CCI rats given vehicle compared to PAE-minor CCI rats given vehicle (Fig. 3b). Intrathecal BIRT-377 results in slight non-significant increases in IL-10 IR. Images of IL-1β (Fig. 3c) and IL-10 (Fig. 3b) represent Sac/Sham/Veh, Sac/1-Sut/Veh, Sac/1-Sut/BIRT, PAE/ Sham/Veh, PAE/1-Sut/ Veh, and PAE/1-Sut/BIRT is shown. These results demonstrate that PAE alters healthy IL-10 responses demonstrated by Sac control rats following minor sciatic nerve injury. Additionally, the data demonstrate that BIRT-377 may reverse chronic allodynia by reducing glial activation (Fig. 2a-b) and decreasing IL-1β (Fig. 3a).

LFA-1 expression is dysregulated in PAE rats

Immunoreactivity for Cd11a (LFA-1) is analyzed in the dorsal horn of the spinal cord in rats behaviorally verified for allodynia. Data show a significant increase in

LFA-1 IR occurs in PAE-sham rats given vehicle compared to Sac-sham rats given vehicle (Fig. 4). Importantly, PAE-sham rats have not undergone a second insult, suggesting that the effects of PAE alone alter the LFA-1 levels. No significant differences are observed between PAE-sham rats given vehicle and PAE-minor CCI given vehicle (Fig. 4). The data suggest that PAE dysregulates the basal expression of LFA-1, which may be an underlying neuroimmune factor in the "primed" spinal cord of PAE rats leading to susceptibility upon a second challenge. While BIRT-377 significantly decreases LFA-1 in PAE rats, these levels are similar to those under basal conditions (Fig. 4), suggesting that "resetting" LFA-1 to basal levels is sufficient to ultimately control PAE-induced sensitivity to allodynia.

Alteration of normal SGC and cytokine responses is seen in DRGs of PAE rats following minor CCI

The critical action of IL-1β underlying chronic neuropathy to minor damage may occur in more than a single anatomical region of the pain pathway. That is, it is possible that L4-L6 DRGs of damaged sciatic nerve axons may respond to damage signals in an exaggerated manner acting to exacerbate events occurring in the spinal cord. GFAP IR for satellite glial cells (SGCs), IL-1β, and IL-10 in the L4-L6 DRGs is analyzed. Thus, the goal of this experiment is to identify neuroimmune factors influenced by PAE that may underlie susceptibility. Therefore, rats treated with BIRT-377 were intentionally omitted from this analysis. Large and significant increases in the expression of GFAP in PAE rats

with minor CCI compared to controls are observed (Fig. 5a), suggesting that SCGs are more reactive/activated than in non-neuropathic controls inclusive of PAE/Sham rats. Additionally, data show significant increases in IL-1β only in PAE rats following minor CCI (Fig. 5b). Interestingly, compared to Sac-sham rats displaying basal levels of IL-10 IR, PAE-sham rats display dramatically reduced basal levels of IL-10 IR (Fig. 5c) with no compensatory IL-10 elevation under neuropathy (Fig. 5c). These data provide further support that PAE leads to dysregulated IL-10 responses to injury (Fig. 3b and 5c). Representative images (Fig. 5d-f) of SGCs, IL-1β, and IL-10 are shown for Sac/Sham/Veh, Sac/1-Sut/Veh, PAE/Sham/Veh, and PAE/1-Sut/Veh. These data suggest that PAE induced sensitivity to allodynia may be a result of significant increases in IL-1β in combination with a diminished capacity of IL-10 expression and action in the DRG.

Spinal IL-1β is necessary for induction of allodynia in PAE rats

Following minor CCI, Sac and PAE rats display elevated IL-1β despite the absence of allodynia in Sac-minor CCI rats (Fig. 3a). A number of prior reports that indicate the action of spinal IL-1β is necessary for the early and chronic phase of allodynia, the goal of the current experiment is to assess whether spinal IL-1β is necessary for allodynia susceptibility in PAE rats induced by minor peripheral nerve injury. All rats are assessed prior to surgery to determine BL responses and demonstrated no significant differences between groups (Fig. 6a-b). Following minor CCI, all PAE rats develop allodynia when comparing hindpaw

response to their BL values (Fig. 6), replicating prior findings (Fig. 1 and 7).

However, on Day 10 immediately following hindpaw threshold values, that action

of IL-1β in the spinal cord is blocked by an i.t. injection of IL-1 receptor antagonist

(IL-1RA). Compared to vehicle, allodynia is reversed with hindpaw sensitivity

initially changing within 1 hr after the injection. This reversal is sustained

reversal for at least 3 hours post-injection (Fig. 6). Allodynia returns by 24 hours

post-injection replicating prior reports of the duration of action of IL-1RA. No

significant differences are seen in sensitivity within the contralateral hindpaw

throughout the behavioral time-course (Fig. 6b). These data demonstrate that IL-

1β is a critical factor underlying the susceptibility for developing allodynia in PAE

rats.

I.t. BIRT-377 reverses PAE induced allodynia at Day 10 post-surgery

Prior reports and the initial studies detailed in the present report demonstrate

robust unilateral allodynia through Day 28 after minor CCI in PAE rats (Sanchez

et al., 2017). To further explore the spinal mechanisms underlying early-

established allodynia following minor injury, adult PAE and Sac rats are

subjected to either sham or minor CCI surgery, and upon established allodynia

observed on Day 10, the effect of i.t. BIRT-377 on allodynia was assessed. As

before (Fig. 1), BL light touch sensory thresholds are similar across all groups

(Fig. 7). While normal sensitivity is maintained near BL values in Sac groups with

sham or minor CCI throughout the time-course, a pronounced level of unilateral

allodynia is observed ipsilateral to sciatic CCI was observed in PAE rats while no

change in contralateral hindpaw sensitivity (Fig. 7a-b). Following BIRT-377 or

vehicle injection in Sac rats, hindpaw thresholds remained stable throughout the

remainder of the 4-day time-course, hovering close to pretreatment BL values.

However, BIRT-377 induces complete reversal of ipsilateral allodynia for the

remainder of the time-course while contralateral hindpaw thresholds continued to

remain stable and non-allodynic (Fig. 7a-b). These data demonstrate that LFA-1

blockade during early established allodynia may alter factors similar to those

driving enduring (Day 28 or longer) allodynia. Candidate factors that lead to PAE

allodynia susceptibility are carefully examined, as detailed below, from these

behaviorally verified rats.

**PAE may induce allodynia by altering proinflammatory factors at the sciatic
nerve**

To further assess how BIRT-377 may change spinal immune environment

resulting in the reversal of allodynia in PAE rats, ipsilateral sciatic nerve (SCN) as

well as ipsilateral and contralateral (as a potential within animal biochemical

control) lumbar spinal cord is collected at Day 4 post-injection at maximal i.t.

BIRT-377 efficacy for protein analysis using the V-plex immunoassay.

Expression levels of IL-10, IL-1β, and TNFα are measured in the SCN and

lumbar spinal cord as well as CXCL1 in the SCN. Results for the SCN

demonstrate that following vehicle injection, minor CCI induces a modest but

significant increase in IL-10 expression in PAE rats compared to Sac rats.

Additionally, allodynic PAE rats with vehicle or BIRT-377 reveal significant

elevations of IL-1β, CXCL1, and TNFα expression compared to Sac/CCI and PAE/sham groups (Fig. 8a). Ipsilateral lumbar spinal cord IL-10 data reveal no significant differences between groups. Similar IL-1β expression is seen in both PAE and Sac rats with minor CCI and vehicle injection despite ongoing allodynia only observed in PAE rats, which may reflect other factors downstream of IL-1β expression are important for controlling allodynia in the Sac rats. While a modest reduction of IL-1β in allodynic PAE rats treated with BIRT-377 is measured, the reduction was not significant. Spinal TNFα is significantly increased in PAE allodynic rats compared to Sac non-allodynic rats with minor CCI. Following BIRT-377 treatment, a strong trend towards reduced levels of TNFα is observed in pain-reversed PAE rats (Fig. 8b). Contralateral lumbar spinal cord did not show any significant differences between rat groups (data not shown) which coincides with the normal sensitivity observed. These data demonstrate that pronounced immune reactivity by peripheral leukocytes around the injured nerve as well as augmented levels of spinal TNFα likely play significant roles in driving allodynia in PAE rats following a minor CCI. Furthermore, BIRT-377 may reverse PAE allodynia through multiple cytokine actions; through the reduction of both IL-1β and TNFα which are known to act synergistically to mediate pathological pain (McGee et al., 1995).

Minor CCI alters CCL2 and CXCL1 in the ipsilateral SCN and DRG

Previous reports demonstrate that following sciatic nerve injury, the chemokines CCL2, CXCL1, CX3CL1, and CXCL10 become upregulated (Lindia et al., 2005;

Akimoto et al., 2013; Zhang et al., 2013; Jiang et al., 2016). Furthermore,

separate studies find that astrocytes may mediate allodynia through the release

of CXCL1 (Chen et al., 2014), CX3CL1, and CXCL10 (Liu et al., 2013).

Interestingly, minor CCI results in the activation of spinal astrocytes but not

microglia (Sanchez et al., 2017). In addition, PAE alters the release of CCL2

(Noor et al., 2017). Together, these reports suggest that susceptibility to

allodynia in PAE rats may result from alterations in chemokine production and

release. Thus, in order to characterize the chemokine profile following minor CCI,

qRT-PCR is used to assess the expression of CCL2, CXCL1, CX3CL1, and

CXCL10 gene expression in the ipsilateral SCN, DRG, and ipsilateral and

contralateral lumbar spinal cord. SCN data show that only following CCI are

significant increases seen in expression of CCL2, CXCL1, and CXCL10 in both

Sac and PAE rats (Fig. 9a). Interestingly, significant differences in CXCL1

expression are seen between SCN of PAE and Sac rats with CCI that received

BIRT-377 (Fig. 9a). Assessment of the DRG demonstrated that CCL2 is

upregulated following CCI in both Sac and PAE rats (Fig. 9b). Only PAE rats with

BIRT-377 display significant increases in CXCL1 and CX3CL1 (Fig. 9b). Overall,

data suggest that minor CCI upregulates pain relevant chemokines within the

periphery that is not solely the result of PAE. Our mRNA analysis reveals that

immune signals known to drive leukocyte trafficking at the SCN and DRG during

chronic neuropathy are similar between rats exposed to Sac or PAE.

I.t. BIRT-377 alters chemokine expression only in PAE rats with minor CCI within the spinal cord

Assessment of mRNA within the ipsilateral and contralateral spinal cord reveals that minor CCI increases CCL2 gene expression in Sac rats compared to sham conditions (Fig. 9c) irrespective of BIRT-377. Interestingly, CCL2 gene expression is blunted in PAE rats with CCI in that no significant differences seen when compared to Sham rats (Fig. 9c). Significant differences in CCL2 and CXCL10 gene expression are only observed in PAE rats with minor CCI that received BIRT-377 (Fig. 9c). It should be noted that these increases are not significantly different when compared to Sac rats with minor CCI and BIRT-377 injection (Fig. 9c). Contralateral data demonstrated no significant differences in CCL2, CXCL1, and CXCL10 gene expression are seen between groups which correspond with normal sensitivity seen in the contralateral hindpaw (Fig. 1c-d and 7b). Interestingly, PAE alone was sufficient to induce increases in CXCL1 gene expression (Fig. 9d).

The lack of changes in chemokines assessed in this report at the lumbar spinal cord may suggest that BIRT-377 may not work primarily by transcriptional regulation of these chemokines.

Discussion

A growing body of evidence has demonstrates that PAE leads to heightened immune reactivity peripherally, as well as in the brain and spinal cord (Topper et al., 2015; Noor et al., 2017; Sanchez et al., 2017). Interestingly, the effects of

PAE are not unmasked until a secondary insult is applied (Noor et al., 2017; Sanchez et al., 2017). Furthermore, PAE alters the ☐2-adhesion molecule LFA-1, which is classically known to facilitate immune cell trafficking in response to CCL2-CCR2 signaling on immune cells followed by migration to regions where tissue damage has occurred. In the present report, we identify a possible novel additional role of LFA-1 activation in that the local milieu is biased toward the proinflammatory cytokine network leading to susceptibility to pathological pain (Noor et al., 2017). These reports demonstrate that a minor injury results in enduring unilateral allodynia up to 28 days post-surgery only in PAE rats. Furthermore, previous work demonstrates that PAE alone alters LFA-1, while separate reports show the negative consequences of LFA-1 on proinflammatory actions are influenced by IL-10 expression. In light of these existing data, we explore whether antagonism of LFA-1 could influence allodynia. i.t. injection of the LFA-1 antagonist BIRT-377, abolishes allodynia with maximum reversal occurring at Day 4 post-injection (Fig. 1). It is important to note this is a small molecule antagonist with high specificity to LFA-1, and is not an antibody that could have unintended off-target effects. The present report additionally demonstrates that spinal and DRG glial activation as well as proinflammatory cytokine expression is reduced (Fig. 2, 3 and 5). Together, these data are the first demonstration that LFA-1 is a potential therapeutic target for a primed neuroimmune response that leads to neuropathic pain susceptibility.

Curiously, prenatal Sac-treated controls demonstrate upregulation of microglial activation and IL-1β expression following a 1-suture nerve injury that is

considered minor and does not produce allodynia (Fig 1 and 2b). Despite this upregulation in both Sac and PAE rats, blocking the actions of IL-1β binding to its receptor demonstrates a transient but robust reversal of allodynia in PAE rats with minor CCI injury , an efficacy time-course observed in prior reports (Fig. 6)(Milligan et al., 2003). This suggests that spinal IL-1β action is necessary to induce allodynia following minor injury, but is not the only final common denominator to generate allodynia in this minor nerve injury model in PAE, because allodynia is not observed in Sac controls with minor injury with elevated spinal IL-1β. However, the actions of IL-10 may indeed be the critical factor in controlling allodynia because IL-10 levels are blunted within the spinal cord and DRG only in PAE rats (Fig. 3 and 5). Thus, the data suggest that PAE induced sensitivity to allodynia may be a result of heightened proinflammatory immune factors *in combination* with blunted anti-inflammatory cytokine expression.

Our data show that although microglia become upregulated following minor injury, astrocytes show greater activation in PAE rats when compared to controls (Fig. 2). Previous studies show that LFA-1 is upregulated on spinal microglia (and possibly macrophages) as a result of PAE alone (Noor et al., 2017), and interestingly, previous reports show that LFA-1 is expressed on microglia whereas its ligand ICAM-1 is expressed on astrocytes (Rozemuller et al., 1989; Akiyama et al., 1993; Lee et al., 2000). In light of these prior reports, it is possible that during pathological conditions, microglia may communicate to astrocytes expressing ICAM-1 resulting in an ICAM-1 to LFA-1 interaction consequently inducing proinflammatory cytokine and chemokines during the

induction of allodynia. Furthermore, in addition to our own data (Fig. 2a), prior reports show that PAE is able to alter astrocytes within the spinal cord following peripheral nerve injury (Noor et al., 2017; Sanchez et al., 2017). Together these data suggest that although spinal microglia are activated similarly between Sac controls and PAE, dysfunctional astrocytes in PAE rats may be sensitized and require only modest stimulation to undergo augmented activation. This alteration would underlie the induction of allodynia following minor injury.

The current study additionally demonstrates that TNFα is upregulated both at the SCN and the spinal cord compared to Sac controls (Fig. 8). Previous studies show that TNFα is upregulated following CCI (George et al., 1999). Additionally, reports demonstrate that TNFα is able to induce allodynia when injected at the sciatic nerve (Wagner and Myers, 1996). Together, these data suggest a critical role for TNFα during the induction of allodynia. Furthermore, previous reports show that TNFα is able to induce the expression of LFA-1 (Hideshima et al., 2001). As noted above , LFA-1 expression impacts the expression of IL-10 (Labuda et al., 1998; Emoto et al., 2003). Thus, TNFα may play a role in the susceptibility to allodynia created by PAE following minor injury by increasing spinal LFA-1 and consequent immune and glial sensitization. Under states of immune and glial sensitization, the expression of IL-10 is diminished, further contributing to enhanced immune reactivity upon a second challenge. Considering that PAE rats reveal altered IL-10 expression (Fig. 3b and 5b), any further dysregulation as a result of TNFα expression may result in susceptibility to developing allodynia.

Interestingly, we show that SGCs within the DRG are upregulated as a result of minor injury only in our PAE rats (Fig. 5a). These cells are supportive by providing sensory neuron cell bodies with essential amino acids as well as clearing toxic substances from the extracellular space (Hanani, 2005; Milligan and Watkins, 2009; Takeda et al., 2009; Wong et al., 2017). During pathological conditions, pain signals from the periphery travel into the DRG and on to the dorsal horn spinal cord (Milligan and Watkins, 2009). In the DRG, SGCs can communicate with neurons through the release of IL-1β and IL-10 (Takeda et al., 2009). Our data demonstrate that following minor injury, IL-1β is significantly upregulated whereas IL-10 expression is blunted within the DRG as a result of PAE alone (Fig. 5), suggesting that pro- and anti-inflammatory SGC responses to minor challenges are dysregulated as a result of PAE. The data demonstrate that one source of heightened IL-1β expression and dysregulated IL-10 expression occurs in the DRG. Ultimately, unchecked IL-1β actions in the DRG due to the lack of IL-10 can contribute to amplified pain signals projecting into the spinal cord during minor CCI.

Curiously, microglial states of activation are not always altered by PAE , particularly under models of moderate PAE (Wong et al., 2017). In support of these prior reports, data from the current study also show that in spinal cords of PAE rats with minor injury, a significant upregulation of the astrocyte activation marker , GFAP is present but no differences in microglial activation was observed in PAE neuropathic and non-neuropathic Sac rats. In fact, levels of Iba1 IR (a potential indicator of heightened microglial activation) was similar

between Sac rats with 1-suture sciatic manipulation (no allodynia) and PAE rats

with 1-suture sciatic manipulation (with allodynia) (Fig. 2). These data suggest

that PAE induced sensitivity to allodynia may be mediated through astrocyte

mechanisms. Interestingly, prior reports show that PAE downregulates the

expression of the astrocyte specific glutamate transporter GLAST that coincided

with a decrease in glutamate uptake (Brolese et al., 2015). In addition, a

separate report demonstrated that only after GLAST function is inhibited in

addition to the other glutamate transporters, GLT-1 (on glia and neurons) and

EAAC1 (solely on neurons), potentiated allodynia is observed (Sung et al., 2003).

Curiously, it is demonstrated that following a standard 4-suture sciatic CCI,

potentiated allodynia is observed in PAE rats (Noor et al., 2017). Together, these

data suggest that PAE may lead to susceptibility to developing allodynia by

altering astrocytes, and in doing so, also alter the functional response of the

astrocyte-specific glutamate transporter GLAST upon minor challenge.

In conclusion, data from the current report support the possibility that PAE

may lead to susceptibility to developing pathological pain through the alteration of

LFA-1 function and expression. By antagonizing the spinal activation of LFA-1, a

switch in the local environment within the spinal cord from proinflammatory to an

anti-inflammatory phenotype occurred, abolishing allodynia. Normal protective

responses of astrocyte glia are altered as a consequence of PAE, which is

unmasked only following a second minor challenge in adulthood; the challenge

being minor peripheral nerve injury. Additionally, these data demonstrate that

PAE suppresses healthy IL-10 expression, which may aid in the induction of a

proinflammatory phenotype following injury and over-reactive astrocytes. Overall,

these data shed light on potential mechanisms underlying PAE's glial and

neuroimmune actions that renders one vulnerable to chronic CNS diseases such

as neuropathic pain.
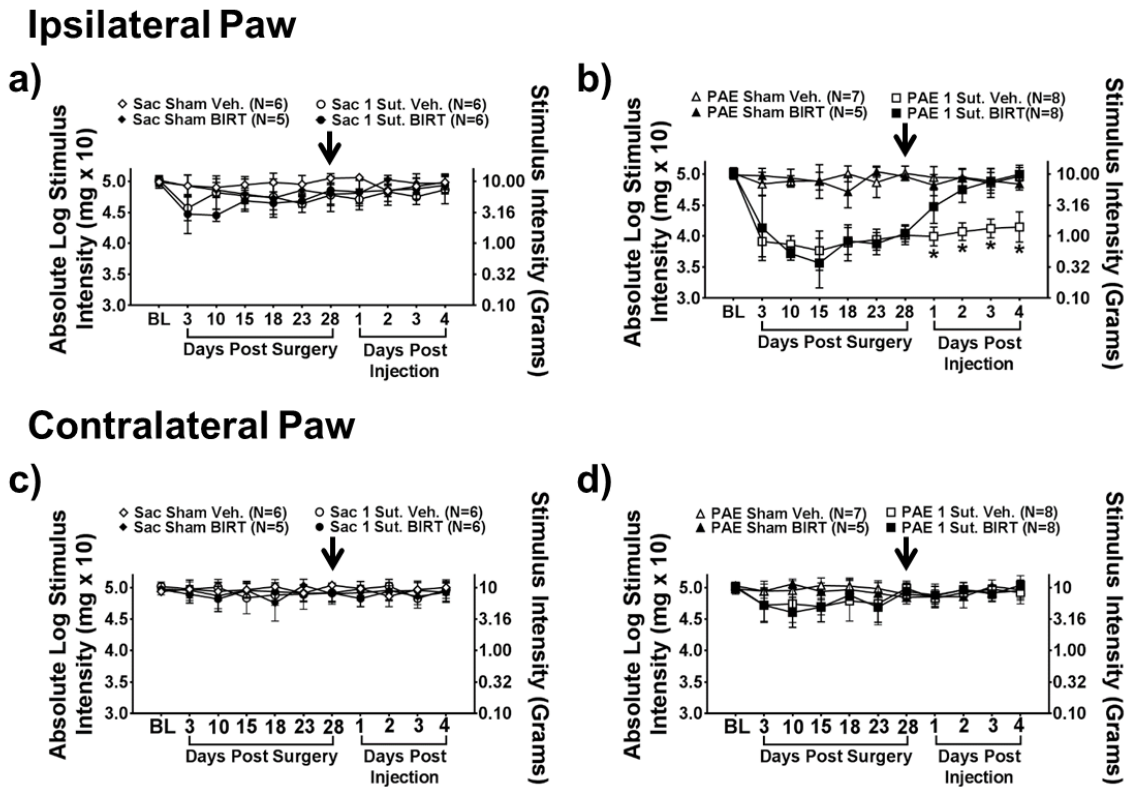
Figure 1. Enduring allodynia from minor injury in PAE rats is controlled by i.t. BIRT-377. Ipsilateral and contralateral hindpaw response thresholds from minor sciatic nerve injury (CCI) in adult PAE and Sac control rats. (**a-b**) At baseline (BL), rats displayed no differences in hindpaw sensitivity (ipsilateral, $F_{1,43} = 1.568$, $p = 0.217$). Following CCI, a main effect of alcohol exposure (ipsilateral, $F_{1,43} = 152.120$, $p < 0.0001$), surgery (ipsilateral, $F_{1,43} = 404.296$, $p < 0.0001$) and an interaction between alcohol exposure and surgery (ipsilateral, $F_{1,43} = 170.740$, $p < 0.0001$) is observed. (**a-b**) Following minor CCI, Sac control rats do not develop increased sensitivity whereas PAE rats develop enduring unilateral allodynia up to Day 28 post-surgery (ipsilateral, $F_{1,43} = 165.47$, $p < 0.0001$). (**c-d**) No changes in contralateral hindpaw sensitivity is observed following sham or CCI in Sac or PAE rats (contralateral, $F_{1,43} = 0.953$, $p = 0.334$). (**a-b**) At Day 28, all animals received either vehicle or BIRT-377 where a significant interaction is seen in the ipsilateral hindpaw between alcohol exposure, surgery, and injection (ipsilateral, $F_{1,43} = 26.280$, $p < 0.0001$;). (**a-b**) Following injection of BIRT-377, Sac rats maintain normal sensitivity. In contrast, allodynic rats with PAE return to normal sensitivity compared to vehicle injected rats. Sensitivity in the contralateral paw remained normal in all rat groups (contralateral, $F_{1,343} = 0.181$, $p = 0.672$). N = 5-8 rats per group. Arrow indicates time of i.t. injection.
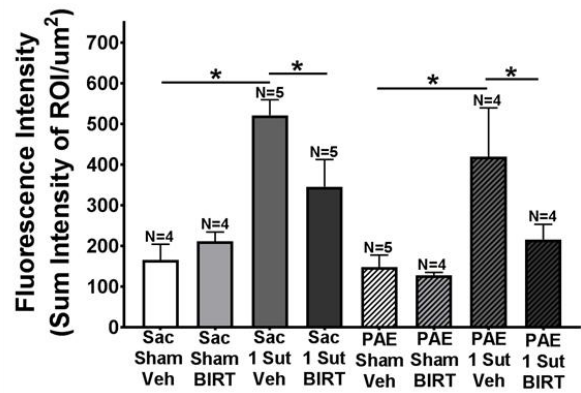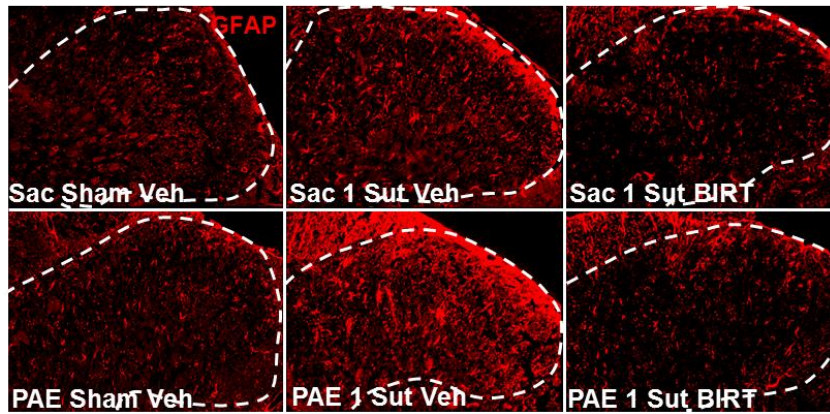
Figure 2

Spinal Cord - Ipsilateral

a) Astrocyte (GFAP)
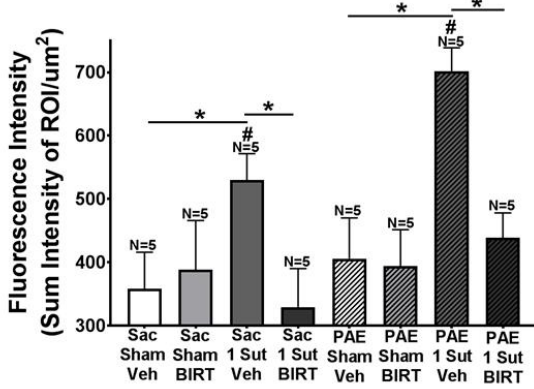
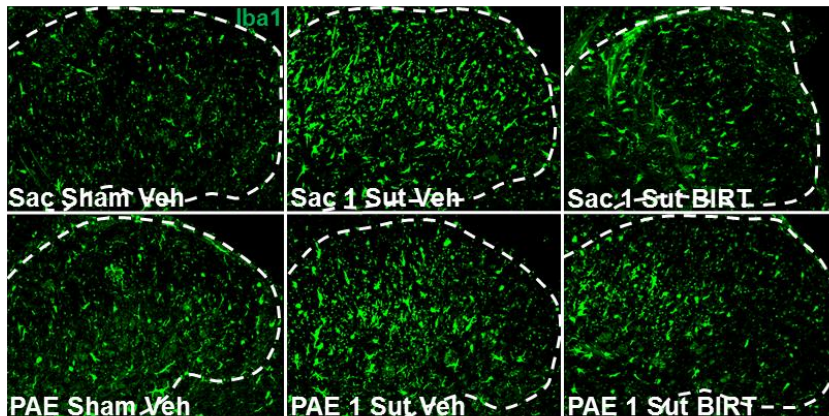### b) Microglia (Iba1)

## c) Astrocyte (GFAP)

d) Microglia (Iba1)

Figure 2. Glial activation is significantly decreased following i.t. BIRT-377 injection in rats with enduring allodynia. (a-d) At Day 4 post-injection spinal

116

cord tissues is harvested for quantification of immunohistochemical (IHC) immunoreactivity (IR) for (**a**) astrocyte activation (GFAP) and (**b**) microglial activation (Iba1) within the ipsilateral dorsal horn of the spinal cord. Fluorescence intensity is defined as the total IR within the dorsal spinal cord [identified as a region of interest (ROI)] divided by the area of the ROI. (**a-b**) A significant interaction is seen between surgery and injection (GFAP, $F_{1,32} = 9.237$, $p = .005$; Iba1, $F_{1,27} = 6.775$, $p = 0.015$). Following minor CCI, both PAE and Sac rats display significant increases in GFAP and Iba1 IR compared to their corresponding sham groups, with spinal cords from PAE/1-sut rats revealing the most robust GFAP increases. BIRT-377 resulted in significant decreases in both GFAP and Iba1 IR in rats with minor CCI. Minor CCI PAE rats reveal elevated GFAP IR compared to Sac rats with minor CCI. Representative images of (**c**) GFAP and (**d**) Iba1 IR used in IHC analysis are shown for Sac/Sham/Veh, Sac/1-Sut/Veh, Sac/1-Sut/BIRT, PAE/ Sham/Veh, PAE/1-Sut/Veh, and PAE/1-Sut/BIRT at 20x. The white dashed line represents a portion of the superficial dorsal horn as is the ROI under examination. N = 4-8 rats per group. "1-sut CCI" is the same as "minor CCI". N = 4-5 rats per group. Asterisks indicate $p < 0.05$. Pound sign indicates significance amongst groups at $p < 0.05$.

Figure 3

Spinal Cord - Ipsilateral

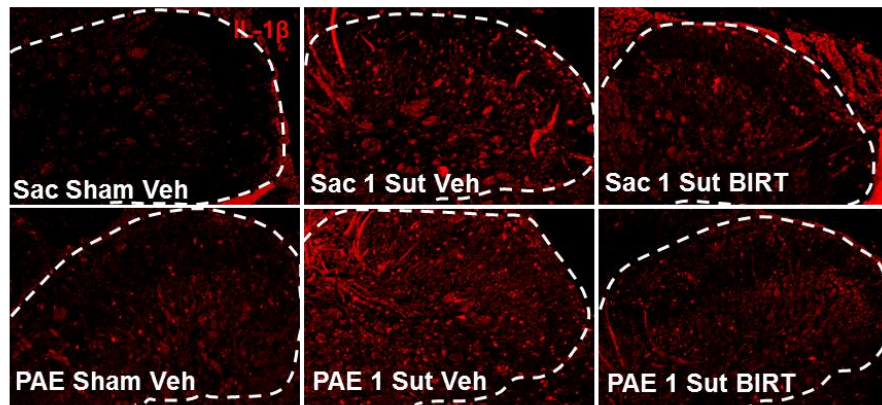### a) IL-1β

b) IL-10

c) IL-1β
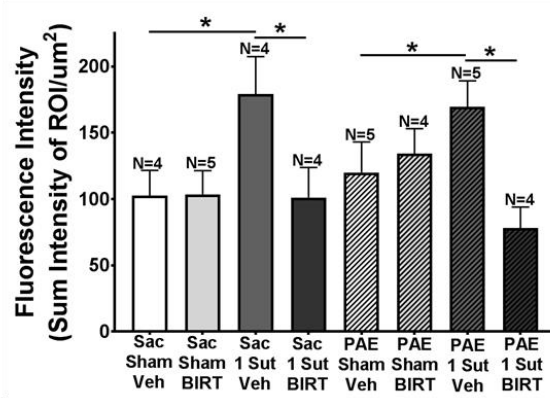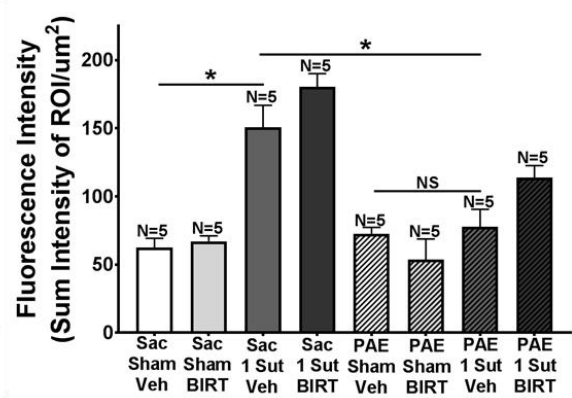
d) IL-10

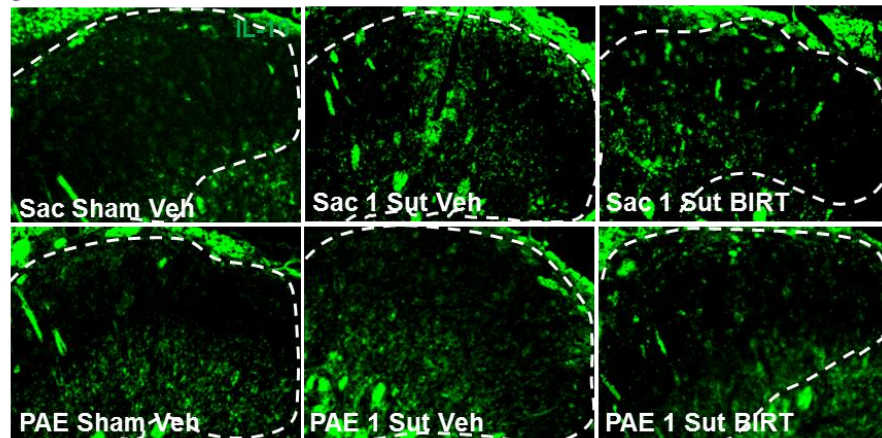**Figure 3. i.t. BIRT-377 injection significantly decreases IL-1β expression. (a-b)** Separate analysis of IL-1β and IL-10 IR within the dorsal horn spinal cord at Day 4 post-injection reveal an interaction between surgery and injection (IL-1β,

$F_{1,27} = 9.559$, $p < 0.001$; IL-10, $F_{1,32} = 7.066$, $p = 0.012$), while no significant differences are observed between Sac and PAE rats with minor CCI and vehicle injection. Following BIRT-377 injection, IL-1β is significantly decreased compared to vehicle injected rats with minor CCI regardless of prenatal exposure. (**b**) Significant differences in IL-10 expression are observed in between Sac-sham rats and Sac-minor CCI rats given vehicle, whereas no differences are observed between all experimental conditions in PAE rats. Sac rats with minor CCI given vehicle reveal elevated IL-10 IR compared to allodynic PAE rats given vehicle. PAE rats lack the compensatory IL-10 elevation to minor injury. Representative images of (**c**) IL-1β and (**d**) IL-10 IR used in IHC analysis are shown for Sac/Sham/Veh, Sac/1-Sut/Veh, Sac/1-Sut/BIRT, PAE/Sham/Veh, PAE/1-Sut/Veh, and PAE/1-Sut/BIRT at either 20x for IL-1β and 40x for IL-10. The white dashed line represents a portion of the superficial dorsal horn as is the ROI under examination. "1-sut CCI" is the same as "minor CCI". N = 4-5 rats per group. Asterisks indicate $p < 0.05$.

Figure 4

Spinal Cord - Ipsilateral

a) LFA-1 (Cd11a)
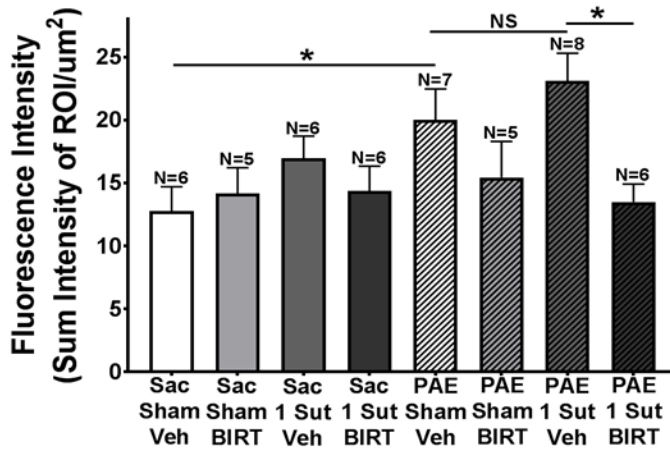
Figure 4. Increased basal levels of LFA-1 expression is present in PAE rats. Quantification of LFA-1 (Cd11a) IR expression reveal elevated expression of Cd11a observed in PAE- sham rats given vehicle compared to Sac-sham given vehicle (p = 0.0188). Additionally, a main effect of BIRT-377 ($F_{1,42}$ = 5.529, p = 0.027) is seen. That is, BIRT-377 injection resulted in significant decreases of Cd11a in PAE minor CCI rats. Additionally, no significant differences are observed between PAE rats given vehicle with sham or minor CCI. "1-sut CCI" is the same as "minor CCI". N = 5-8 rats per group. Asterisks indicate p < 0.05.

Figure 5

Dorsal Root Ganglia - Ipsilateral
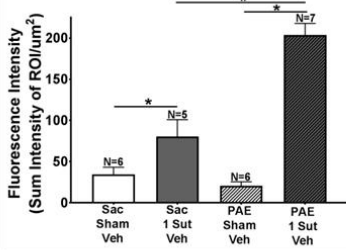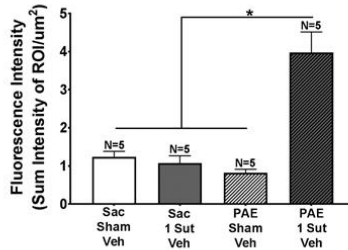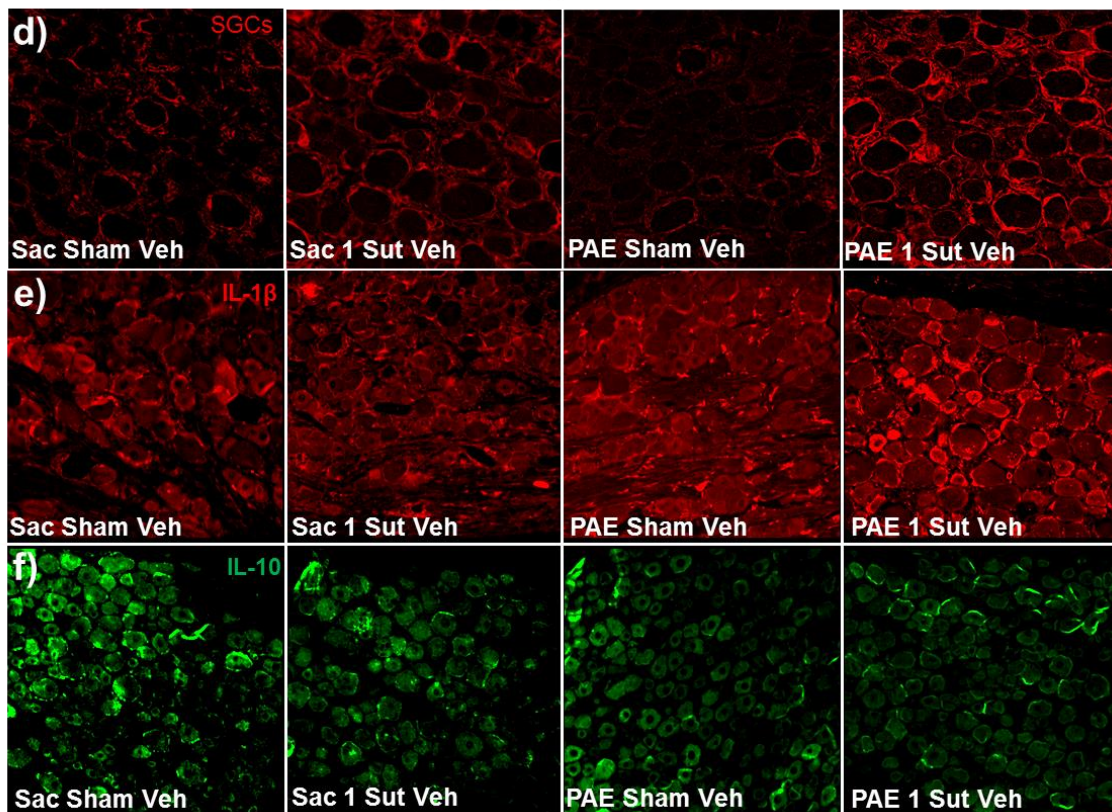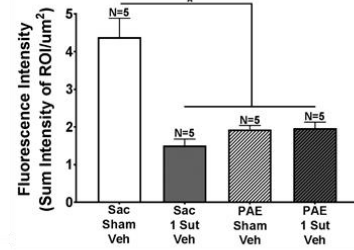
Figure 5. PAE results in elevated SGC activation and cytokine immunoreactivity in the dorsal root ganglia (DRG). IR of (**a**) SGCs (as measured by GFAP IR), (**b**) IL-1β, and (**c**) IL-10 are determined for the ipsilateral L4-L6 DRG of PAE and Sac minor CCI vehicle injected rats at Day 4 post-injection. A main effect of PAE (SGCs, $F_{1,20} = 17.74$, $p = 0.0004$; IL-1β, $F_{1,16} = 17.16$, $p < 0.0008$; IL-10, $F_{1,16} = 12.58$, $p = 0.0027$), surgery (SGCs, $F_{1,20} = 77.53$, $p < 0.0001$; IL-1β, $F_{1,16} = 24.87$, $p < 0.0001$; IL-10, $F_{1,16} = 25.7$, $p = 0.0001$), and an interaction of PAE and surgery is seen (SGCs, $F_{1,20} = 27.81$, $p < 0.0001$; IL-1β, $F_{1,16} = 30.67$, $p < 0.001$; IL-10, $F_{1,16} = 26.81$, $p < 0.001$). (**a**) SGCs activation is significantly upregulated following minor CCI in both Sac and PAE rats.

Additionally, compared to Sac rats, PAE rats have heightened SGCs activation. (**b**) Significant increases are observed following minor CCI in vehicle injected PAE rats compared to Sac rats with sham or minor CCI. (**c**) Sac-sham rats with vehicle display significantly greater IL-10 IR compared to PAE-sham rats with vehicle rats. N = 5 rats per group. Asterisks indicate $p < 0.05$. Representative images of SGCs, IL-1β, and IL-10 IR used in IHC analysis are shown for Sac/Sham/Veh, Sac/1-Sut/Veh, PAE/Sham/Veh, PAE/1-Sut/Veh, at 20x. "1-sut CCI" is the same as "minor CCI". N = 5=7 rats per group. Asterisks indicate $p < 0.05$.

Figure 6
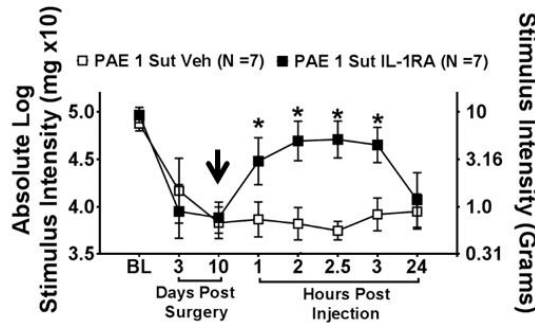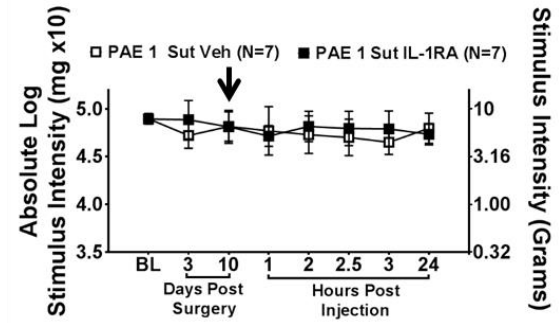
Figure 6. Spinal IL-1β is necessary for PAE induced allodynia following minor CCI. (**a**) PAE rats with minor CCI receive either i.t. IL-1 receptor antagonist (IL-1RA) or vehicle and ipsilateral and contralateral hindpaw responses are assessed. Prior to surgery, no hindpaw response threshold differences ae observed between vehicle and IL-1RA groups (Ipsilateral, $F_{1,12}$ = 4.523, p = 0.055; Contralateral, $F_{1,12}$ = 0.014, p = 0.907). Following minor CCI and prior to injection, similar levels of robust allodynia is observed in both groups (Ipsilateral, $F_{1,12}$ = 0.743, p = 0.406; Contralateral, $F_{1,12}$ = 2.213, p = 0.163). PAE rats receiving IL-1RA reveal reversal from allodynia by 1 hr that persisted throughout the 3h time-course compared to vehicle injected rats (Ipsilateral, $F_{1,12}$ = 139.459, p < 0.001; Contralateral, $F_{1,12}$ = 1.089, p = 0.317). By 24 hours post-injection, all rats demonstrate full allodynia, with no significant differences observed between groups (Ipsilateral, $F_{1,12}$ = 0.887, p = 0.365; Contralateral, $F_{1,12}$ = 0.743, p = 0.406). "1-sut CCI" is the same as "minor CCI". N = 7 rats per group. Asterisks indicate p < 0.05.

123

Figure 7

a) Ipsilateral Paw

b) Contralateral Paw

Figure 7. BIRT-377 reverses PAE induced allodynia following i.t. injection. (**a-b**) At baseline (BL), rats displayed no differences in hindpaw sensitivity (ipsilateral, $F_{1,35} = 0.687$, $p = 0.413$; contralateral, $F_{1,35} = 0.041$, $p = 0.840$). Additionally, sham groups maintain normal sensitivity throughout the time-course demonstrating that repeate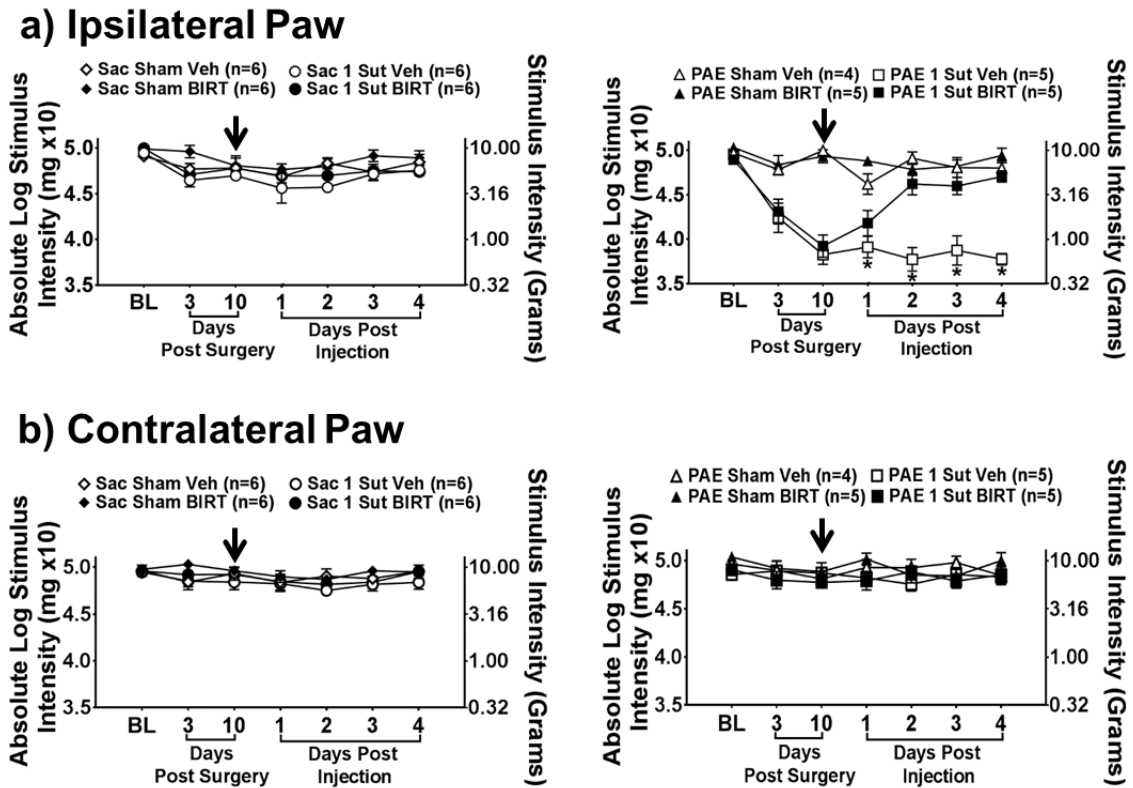d von Frey behavioral testing has no significant effects on touch stimuli. Following CCI, a main effect of alcohol exposure (ipsilateral, $F_{1,35} = 52.497$, $p < 0.0001$; contralateral, $F_{1,35} = 1.929$, $p = 0.174$), surgery (ipsilateral, $F_{1,35} = 148.009$, $p < 0.0001$; contralateral, $F_{1,35} = 3.118$, $p = 0.086$) and an interaction between alcohol exposure and surgery (ipsilateral, $F_{1,35} = 87.448$, $p < 0.0001$; contralateral, $F_{1,35} = 0.387$, $p = 0.538$) is seen only in the ipsilateral hindpaw. Additionally, PAE, but not Sac rats, develop robust unilateral allodynia as measured on Day 28 and Day 10 (ipsilateral, $F_{1,35} = 89.118$, $p < 0.0001$; contralateral, $F_{1,35} = 0.710$, $p = 0.405$). Following injection of BIRT-377, PAE rats return to normal sensitivity through Day 4 post-injection (ipsilateral, $F_{1,35} = 9.808$, $p = 0.003$; contralateral, $F_{1,35} = 0.032$, $p = 0.858$) at which time, the experiment was terminated for tissue collection. "1-sut CCI" is the same as "minor CCI". Arrow indicates when i.t. injection was given. N = 4-6 rats per group. Asterisks indicate $p < 0.05$.

Figure 8
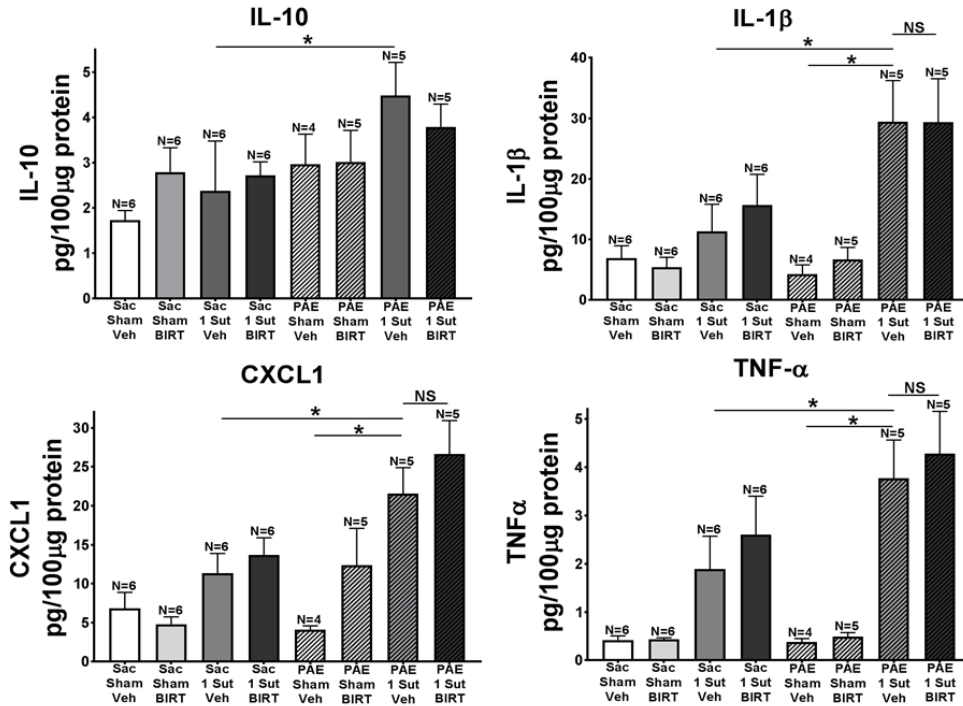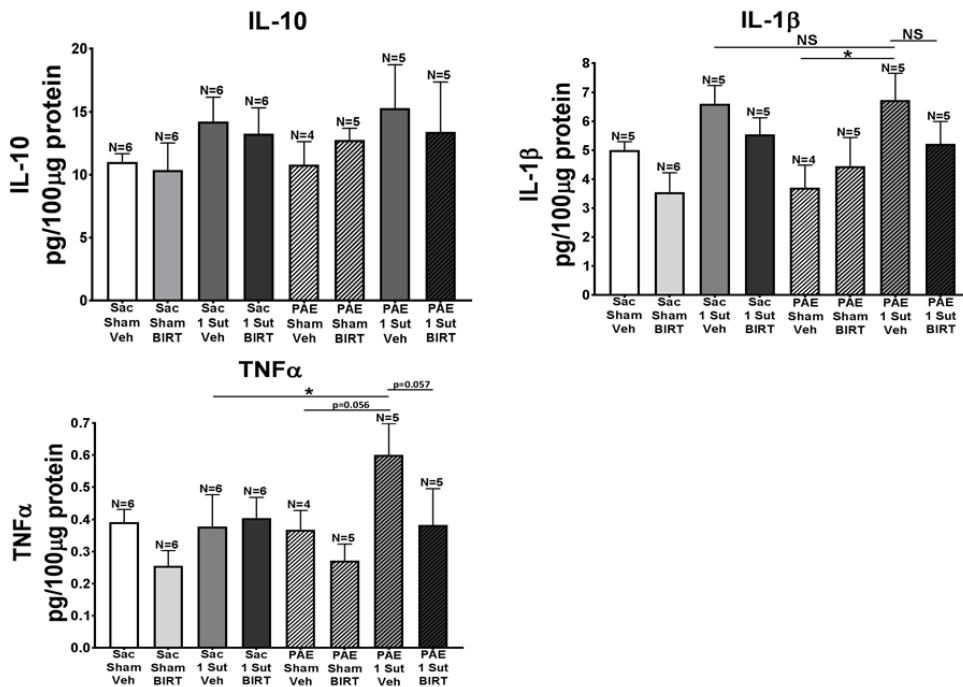
Figure 8. PAE alters cytokine expression in the ipsilateral sciatic nerve and

spinal cord. Ipsilateral sciatic nerve and spinal cord are collected at Day 4 post-injection and examined by multiplex protein analysis for levels of IL-10, IL-1β, TNFα, and CXCL1 (sciatic nerve only). Levels of protein are expressed as picograms of target protein per 100μg of total protein. Data for ipsilateral (**a**) sciatic nerve and (**b**) lumbar spinal cord are represented. (**a**) IL-10 significantly increased in PAE rats with minor CCI given vehicle injection compared to Sac CCI vehicle injected rats ($F_{7,35}$ = 1.672, p = 0.0271). Additionally, compared to Sac/minor CCI vehicle injected rats and PAE sham vehicle rats, PAE minor CCI rats with vehicle injection displayed elevated levels of IL-1β ($F_{7,35}$ = 5.224, Sac minor CCI: p = 0.0060; PAE Sham Veh: p = 0.0008), TNFα ($F_{7,35}$ = 5.224, Sac minor CCI: p = 0.0239; PAE Sham Veh: p = 0.0005) and CXCL1 ($F_{7,35}$ = 5.224, Sac minor CCI: p = 0.0158; PAE Sham Veh: p = 0.0004). No significant differences were seen between PAE minor CCI vehicle groups and PAE minor CCI BIRT groups ($F_{7,35}$ = 5.224, IL-10: p = 0.4716; IL-1β: p = 0.9904, TNFα: p = 0.5436, CXCL1: p = 0.2309). (**b**) IL-10 expression did not change significantly throughout any groups in the ipsilateral lumbar spinal cord. PAE minor CCI vehicle injected rats had significant increases in IL-1β expression compared to PAE sham vehicle rats ($F_{7,32}$ = 5.224, Sac minor CCI: p = 0.0097). Additionally, no significant differences are seen in IL-1β between Sac minor CCI vehicle rats and PAE minor CCI vehicle rats ($F_{7,32}$ = 5.224, Sac minor CCI: p = 0.9070). Significant differences are seen between Sac minor CCI vehicle rats and PAE minor CCI rats ($F_{7,32}$ = 5.224, Sac minor CCI: p = 0.0432). "1-sut CCI" is the same as "minor CCI". N = 4-6 rats per group. Asterisks indicate p < 0.05.

126

Figure 9

a) Sciatic Nerve - Ipsilateral
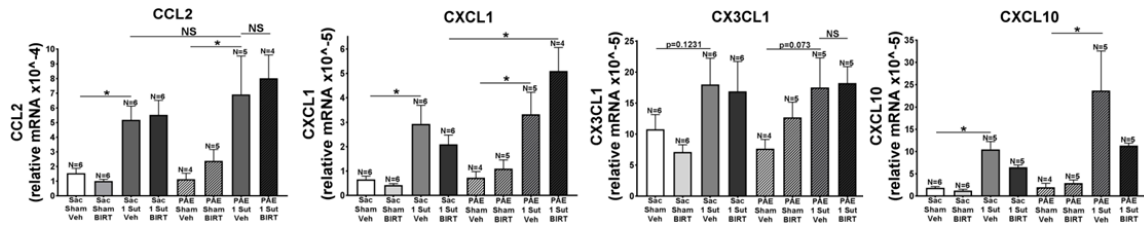
b) DRG - Ipsilateral
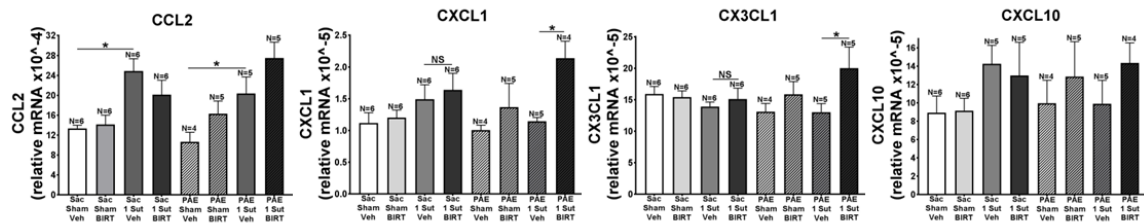
c) Lumbar Spinal Cord - Ipsilateral
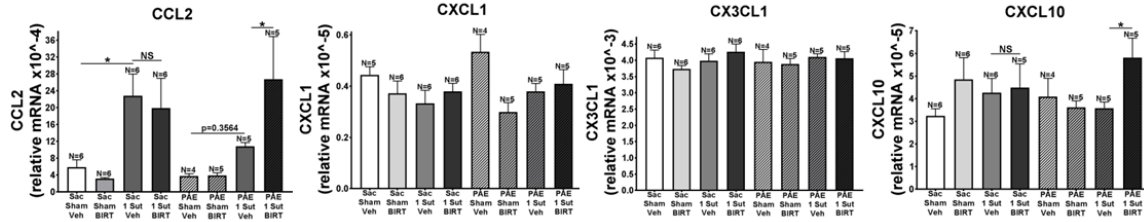
d) Lumbar Spinal Cord - Contralateral
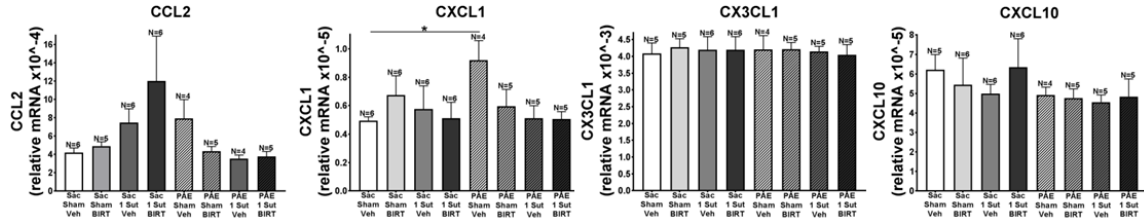
Figure 9. i.t. BIRT-377 alters mRNA expression of specific chemokines only in PAE neuropathic rats. Ipsilateral SCN and DRG as well as ipsilateral and contralateral spinal cord are collected from rats at Day 4 post-injection for qRT-PCR analysis. Messenger RNA expression from ipsilateral (**a**) SCN and (**b**) DRG, as well as (**c**) ipsilateral and (**d**) contralateral lumbar spinal cord are shown. (**a**) CCL2, CXCL1, and CXCL10 expression is significantly increased following minor CCI in both Sac and PAE rats (Sac: CCL2 $F_{7,34}$ = 5.32, p = 0.0242, CXCL1 $F_{7,34}$ = 5.32, p = 0.0033, CXCL10 $F_{7,34}$ = 5.32, p = 0.0117; PAE: CCL2 $F_{7,34}$ = 5.32, p = 0.0027, CXCL1 $F_{7,34}$ = 5.32, p = 0.0038, CXCL10 $F_{7,34}$ = 5.32, p = 0.0133). Interestingly, CXCL1 is significantly increased following minor CCI in PAE rats

compared to Sac rats receiving BIRT-377 ($F_{7,34}$ = 5.32, p = 0.0007). (**b**) Minor CCI significantly increases CCL2 in the DRG in both Sac and PAE rats (Sac: $F_{7,35}$ = 5.26, p = 0.0014; PAE: $F_{7,35}$ = 5.26, p = 0.0168). BIRT-377 significantly increases CXCL1 and CX3CL1 only in PAE rats with Minor CCI (CXCL1: $F_{7,34}$ = 2.377, p = 0.0057; CX3CL1: $F_{7,35}$ = 1.593, p = 0.0079). (**c**) The expression of CCL2 is increased following minor CCI in Sac rats (Sac: $F_{7,35}$ = 3.879, p = 0.0139). Additionally, BIRT-377 increased CCL2 and CXCL10 only in PAE minor CCI rats that reversed from allodynia (CCL2: $F_{7,35}$ = 3.879, p = 0.0321; CXCL10: $F_{7,35}$ = 3.879, p = 0.0373). (**d**) Contralateral dorsal spinal cord revealed significant CXCL1 increases from PAE when compared to Sac rats ($F_{7,35}$ = 1.289, p = 0.0182). "1-sut CCI" is the same as "minor CCI". N = 4-6 rats per group. Asterisks indicate p < 0.05.

Chapter 4 – PAE alters glutamate transporter expression leading to enhanced susceptibility to developing neuropathic pain

Abstract

Background

Prenatal alcohol exposure (PAE) alters immune function rendering children susceptible to infection and other disorders. Animal models with moderate PAE demonstrate susceptibility to developing increased sensitivity to light touch clinically termed allodynia. These studies demonstrate that PAE alters spinal astrocytes, which is apparent only following sciatic nerve injury. Additionally, the astrocyte specific glutamate transporter, glutamate aspartate transporter (GLAST) is dysregulated by PAE. Considering GLAST clears glutamate from the synaptic cleft following sciatic nerve injury, it would stand to reason that PAE may increase susceptibility to developing allodynia through its alteration. Thus, the goals of this study are to determine whether PAE dysregulates GLAST resulting in allodynia following minor sciatic nerve injury.

Methods

Minor chronic constriction injury (CCI) or sham surgery was applied to adult male Long Evans rats that underwent prenatal saccharin (Sac) or alcohol exposure. At Day 10 post-surgery, a GLAST inhibitor (UCPH101) was given intrathecally (i.t.) and behavior was assessed. Spinal cords from a separate group of non-injected behaviorally verified rats were collected to determine gene and protein expression of glutamate transporters using qrt-PCR and immunohistochemistry

(IHC). Additionally, western blot is used to determine the expression of phosphor-GluN2B and total GluN2B following CCI.

Results

Data show that following GLAST inhibition, only PAE rats with sham surgery develop allodynia. When minor CCI is applied and GLAST is inhibited, Sac rats develop allodynia whereas PAE rats display potentiated allodynic responses. Gene and protein expression data show no significant differences in glutamate transporters or in phosphorylated GluN2B. Interestingly, IHC data demonstrate that PAE alone upregulates both GLAST and Glutamate Transporter 1 (GLT-1) expression followed by downregulation when minor CCI is applied.

Conclusion

These studies demonstrate that PAE alters glutamate transporter expression within the dorsal horn spinal cord which may contribute to susceptibility to developing allodynia.

Introduction

Significant modulation of pain signaling occurs within the spinal cord dorsal horn. Following peripheral nerve damage, the release of glutamate and other pain neurotransmitters not only activate their respective receptors on the post-synaptic membrane of pain projection neurons, such as N-methyl-d-aspartate (NMDA) receptor in the spinal dorsal horn, but also peri-synaptic glial cells (astrocytes and microglia). In turn, glia release cytokines IL-1β and TNF-α (Hashizume et al., 2000; Milligan and Watkins, 2009), which bind to and further activate receptors on pain projection neurons as well as on nearby glial cells. This creates positive feedforward excitation of pain signaling. Ultimately, over-excited pain projection neurons relay these amplified signals to the brain (Milligan and Watkins, 2009).

Following peripheral nerve injury, the excitatory pain neurotransmitter glutamate is released in the synaptic terminal within the dorsal horn of the spinal cord (Milligan and Watkins, 2009). Over time persistent release of glutamate amongst other excitatory neurotransmitters results in depolarization of pain projection neurons leading to phosphorylation of the NMDA receptor subunit NR2B at serine 1303 (Ser 1303) (Castany et al., 2018). This phosphorylation results in plasticity changes to the NMDA receptor allowing its depolarization leading to amplifications of the pain signal that is relayed to the brain (Milligan and Watkins, 2009).

Synaptic glutamate concentration is influenced not only by the degree of presynaptic release, but also by glutamate clearance through glutamate

transporters (Danbolt, 2001). Among the glutamate transporters that have been identified, GLAST is found exclusively on astrocytes, GLT-1 is found on neurons and glia, and EAAC1 is found solely on neurons. Normally, these glutamate transporters clear glutamate from the synaptic and perisynaptic cleft (Danbolt, 2001). However, during peripheral nerve injury, an initial excessive release of glutamate causes compensatory responses of the glutamate transporters, GLAST, GLT-1, and EAAC1 to upregulate (Sung et al., 2003). Within a few days, this up-regulation is followed by their downregulation resulting in increased glutamate accumulation thought to generate exaggerated pain signaling (Sung et al., 2003).

Interestingly, prior reports demonstrate potentiated allodynia in PAE rats with standard sciatic nerve damage. This corresponded with elevations in microglial and astrocyte activation (Noor et al., 2017). Additionally, significantly reducing the damage to the sciatic nerve reveals that PAE rats have an increased susceptibility to developing allodynia. These rats in parallel, show spinal astrocyte activation but not microglial activation (Sanchez et al., 2017). This suggests that the increased susceptibility to developing allodynia may be astrocyte mediated. Interestingly, previous reports show that PAE down-regulates the expression of the astrocyte specific glutamate transporter, GLAST within the hippocampus (Brolese et al., 2015). Furthermore, only after inhibiting GLAST expression within the spinal cord do rats develop potentiated allodynia similar to what is seen in PAE rats with a standard CCI (Sung et al., 2003; Noor

et al., 2017). These data support a larger role for astrocyte dysregulation via the astrocyte-specific glutamate transporter GLAST.

The current study explores the mechanisms that PAE alters to increase susceptibility to developing neuropathic pain. Determining the expression pattern of phosphorylated NMDAR may shed light on whether PAE increases neuronal sensitivity to glutamate. Additionally, it is possible that PAE alters spinal glutamate transporter expression results in accumulation of glutamate in the synapse leading to allodynia following minor injury. Thus, the goals of the study are to determine whether PAE increases susceptibility to developing allodynia by changing glutamate mediated functions.

Materials and Methods

Animals and Study Group Strategy

All procedures were approved by the Institutional Animal Care and Use Committee (IACUC) of the University of New Mexico Health Sciences Center and closely adhered to guidelines from the International Association for the Study of Pain for the use of animals in research. Long-Evans rat breeders purchased from Harlan Industries (Indianapolis, IN) were maintained in a breeding colony on a 12:12-hour reverse light/dark schedule (lights on from 2100 to 0900 hours), and fed Harlan Teklad rat chow and water, available *ad libitum*. For all experiments, 5-8-month male prenatal alcohol or saccharin exposed (described below) rat offspring derived from 56 litters are used. Offspring are transferred to a standard light/dark cycle (lights on from 0600 hours to 1800 hours) and allowed to

acclimate to these conditions for at least 30 days before commencing experiments. Additionally, rats are kept in these conditions for the duration of the study. A total of 102 male offspring are used in all experiments. Offspring are predominantly pair-housed with 5 rats single-housed due to incompatibility with a cage mate. Rat offspring are split into three groups. The first group consists of 54 (29 with prenatal saccharin exposure, Sac; and 25 with prenatal alcohol exposure; PAE) rats and are used for examination of behavioral hindpaw sensitivity following intrathecal (i.t.) treatment of UCPH101 and its effects on neuropathy produced by minor peripheral nerve injury. The second and third groups consists of 27 (12 Sac and 15 PAE) and 21 (12 Sac and 9 PAE) behaviorally verified rats and are used for spinal cord immunohistochemical (IHC) analysis (Group 2) or for protein and mRNA analysis (Group 3).

Moderate Prenatal Alcohol Exposure Using the Voluntary Drinking Paradigm

Pregnant female rat dams are given either ethanol or saccharin throughout pregnancy until birth according to the voluntary drinking paradigm previously described (Savage et al., 2010). Briefly, 3 to 4-month pre-pregnant female Long-Evans rat breeders are acclimated for 4 hours per day, from 1000 to 1400 hours (during their active phase), to drinking water containing 0.066% (w/v) saccharin (Sac) that gradually increased in ethanol content from 0% (v/v) on Days 1-2, to 2.5% (v/v) on Days 3-4, to 5% (v/v) on Day 5 and thereafter for two weeks. Regular drinking water is available at all times during housing. Thus, rats

voluntarily choose to drink either saccharin sweetened water containing 5% ethanol or regular water during the 4-h drinking period. At the end of the 2-week pre-pregnancy drinking phase, the mean daily ethanol consumption is determined for each rat and rats that consumed 1 standard deviation above or below the group mean are excluded from the study. Subsequently, female rats are assigned to either a 5% ethanol or Sac control drinking group such that the mean pre-pregnancy ethanol consumption is similar between groups. The females are then placed with proven male rat breeders until pregnant (~2 days). No alcohol is consumed during the breeding period. Beginning on gestational day 1, rat dams were given either 0% (Sac) or 5% (PAE) ethanol in Sac water (4 hours/day, during the active phase). Sac rats are given a volume of 0% ethanol in Sac water that is matched to the mean volume voluntarily consumed by the 5% ethanol group. Total ethanol consumption is recorded for each dam, which averaged 2.04 g of ethanol/kg body weight/day. This level of drinking by rat dams produced a mean peak serum blood alcohol concentration of 0.06 g/dl. No significant differences are observed between prenatal treatment groups in dam weight gain during pregnancy, pup birth weights, or litter size, replicating previous reports (Savage et al., 2010; Noor et al., 2017; Sanchez et al., 2017). Offspring are weaned at 24 days of age and male offspring pair-housed with the exception of five single-housed rats due to incompatibility with a cage mate. For all experiments, 5-8-month prenatal alcohol or saccharin exposed animals are used. A total of 102 male offspring are used in these experiments. Behavioral testing of offspring is performed during the first three hours of the light cycle

(inactive phase) to avoid the influence of elevated hormones under normal circadian rhythms.

Chronic constriction injury (CCI)

In adult male Sac or PAE rats, sham or CCI aseptic surgical procedures are performed as previously described (Bennett and Xie, 1988; Noor et al., 2017; Sanchez et al., 2017) and modified, as described here. Under isoflurane anesthesia (3% volume in oxygen), the sciatic nerve is carefully isolated with sterile glass prongs and snuggly ligated with 1 (minor injury) segment of sterile 4-0 chromic gut suture (Ethicon, Somerville, NJ) without pinching into the nerve. Sterile isotonic saline (0.9%) is applied to the nerve during the procedure to prevent dehydration. Sham surgery involved isolation of the sciatic nerve similar to CCI but without nerve ligation. The nerve is then gently placed back into position and the overlying muscle was sutured closed with two 3–0 sterile silk sutures (Ethicon, Somerville, NJ). Rats fully recovered from anesthesia within approximately 5 minutes and are monitored daily following surgery for any post-operative complications. The number of rats that are excluded from the study due to the presence of hindpaw autotomy was 2 (1.8%).

Behavioral Assessment of Allodynia

Allodynia is assessed using the von Frey fiber test as previously described (Dengler et al., 2014; Sanchez et al., 2017). Briefly, rats are habituated to the testing environment for approximately 45 min/day for 4 sequential days within the

first 3 hours of the light cycle (inactive phase) in a sound- and temperature-controlled dimly lit section of the colony room. Baseline (BL) responses are then assessed using the von Frey behavioral test. A total of 13 calibrated monofilaments were are in these studies. Additionally, these calibrated monofilaments (3.61–5.18 log stimulus intensity) are applied to the plantar surface of the left and right hindpaw for a maximum of 8 seconds per application. Random order between left and right hindpaw assessment is conducted. A metronome placed in the room provided guidance at 1 tick/sec. Lifting, licking, or shaking of the paw is considered a response. In a similar manner to BL evaluation, rats are re-assessed following CCI or sham surgery through Day 10 prior to drug treatment. A second group of rats is assessed through Day 32. The last group of rats is assessed through Day 14. The experimental tester was blind to the prenatal and surgical treatment groups. At Day 10, Group 1 rats are given an intrathecal (i.t.) injection of UCPH101 or vehicle (described below) and behavioral re-assessment occurrs at 1hr, 2hr, 3hr, and 24hrs post injection.

Drug preparation

UCPH101 is a selective non-competitive inhibitor that prevents glutamate uptake of EAAT1 (GLAST) which is expressed solely on astrocytes (Kugler and Schleyer, 2004; Abrahamsen et al., 2013). UCPH101 (Abcam, Cambridge, UK) is initially reconstituted in 100% DMSO as a stock solution at a concentration of 10.56mg/ml, aliquoted into 0.5 ml sterile Eppendorf tubes and stored in a clean sealed container at -20°C for later use. On the day of intrathecal (i.t.) injection,

sterile ddH20 is warmed in a water bath and UCPH101 is added to reach a concentration of either 100nM or 10µM for i.t. injection and vortexed for 2 min. Vehicle consisted of sterile ddH$_2$O. Animals are injected within the hour following drug dilution.

Intrathecal (i.t.) Injection

Drug (UCPH101 or vehicle) is administered using an i.t. catheter on Day 10 post-surgery and is conducted as described previously (Milligan et al., 2005). Briefly, under isoflurane anesthesia (3% volume in oxygen), the beveled needle end of an 18-guage sterile (Bectin Dickson, Franklin Lakes, NJ) needle with the plastic hub removed is inserted between lumbar vertebrae L5-L6. PE-10 tubing (Fisher Scientific, Hampton, NH) is fitted with a 30-guage sterile needle (Bectin Dickson, Franklin Lakes, NJ) containing a Hamilton syringe at one end and labeled with a marking at 7.7 cm at the opposite end. Drug or equivolume vehicle (20µl) is withdrawn from the open side of the PE-10 tubing. The open end of the tubing is then threading into the 18-guage needle until the 7.7 cm marking was reached. This position corresponds to the lower lumbar L4-L5 region of the spinal cord. Correct placement of the PE-10 is determined by twitching of the hindleg and/or tail during catheter advancement, as well as cerebrospinal fluid efflux from the externalized portion of the 18-g needle. Drug is administered over a 25 second interval. Immediately following drug or vehicle administration, tubing is removed followed by removal of the 18-guage needle and rats are allowed to recover

before being placed in home cage. Rats fully recover from anesthesia within 5 minutes and 100% motor recovery is observed following i.t. injection.

Immunohistochemical (IHC) tissue sample preparation

All tissue from behaviorally verified Group 2 rats on Day 32 post-surgery are collected for IHC processing. Tissues were processed as described previously (Noor et al., 2017; Sanchez et al., 2017). Briefly, rats are overdosed with sodium phenobarbital (390 mg/ml Sleepaway, Fort Dodge Animal Health, Fort Dodge, IA) and transcardially perfused with 0.1M phosphate buffered saline (PBS; pH = 7.4), initially at a rate of 28 ml/min, then increased to 32 ml/min (~10 min), followed by 4% paraformaldehyde (PFA; pH = 7.4; 28-34 ml/min, 8 min). Immediately following transcardial perfusion, the spinal vertebral column from C2-L6 with the spinal cord intact within the vertebral column are collected and cut at vertebra T7 into a rostral and caudal half of the spinal vertebral column. All spinal cord sections underwent 48-hour post-fixation in 4% PFA at 4 °C.

Following post-fixation entire spinal cord (T7- L6) are carefully isolated making sure to maintain tissue integrity. The isolated spinal cords subsequently paraffin processed. Paraffin-embedded blocks are subsequently sliced on a microtome with adjacent 7 μm tissue sections mounted onto vectabond-treated slides.

To investigate spinal glutamate transporters, we analyzed the expression of glutamate transporter 1 (GLT-1), Glutamate Aspartate Transporter (GLAST), and Excitatory Amino-acid Carrier 1 (EAAC1). Paraffin-processed tissues undergo deparaffinization followed by rehydration and antigen retrieval procedures in a

rice cooker at 94-96° C allowing for gentle and equal distribution of temperature warming throughout tissue sections. For antigen retrieval, polyclonal GLAST antibody requires a Tris-based buffer at pH 9.5 (BioCare Medical, Concord, CA) and polyclonal GLT-1 and EAAC1 antibody requires a Tris-based buffer at pH 9.0 (Vector, Burlingame, CA). All tissue sections are incubated with 5% normal donkey serum (NDS), PBS pH 7.4 for 2h, followed by overnight primary antibody incubation using rabbit anti-rat polyclonal EAAT1 (GLAST) (1:300; Abcam, Cambridge, UK), EAAT2 (GLT-1) (1:1000; Abcam, Cambridge, UK), or EAAT3 (EAAC1) (1:500; Abcam, Cambridge, UK). All tissues are incubated with donkey-anti rabbit TRITC- conjugated secondary antibody incubation for 2h in a humidity chamber at room temperature and rinsed in 0.1 M PBS. All tissues are then stained with the nuclear stain 4,6-diamidino-2-phenylindole (DAPI) (Vector Labs, Burlingame, CA) separately before cover slipping. These slides are left at room temperature overnight and then placed at 4° C until proceeding with image acquisition and microscopy analysis (Wilkerson et al., 2012a; Sanchez et al., 2017).

Microscope spectral imaging for immunofluorescent quantification

Image acquisition for spectral analysis was preformed using the Nuance spectral imaging system (http://www.cri-inc.com/products/nuancew.asp; Perkin Elmer, Waltham, MA) as described previously (Noor et al., 2017; Sanchez et al., 2017). Briefly, images of dorsal horn spinal cord are obtained using either a 20X or 40x objective with a Zeiss Axioplan2 inverted fluorescence microscope. Flat-field

corrections is applied to correct for uneven illumination (modest vignetting) image acquisition. Image cubes are obtained from multi-labeled tissue containing DAPI, conjugated secondary antibody, as well as autofluorescence. A spectral library is then created using single-labeled slides for each fluorophore (e.g. TRITC) and a label-free (autofluorescence) slide. A computed spectrum (420 nm – 720 nm) was obtained by separating the known spectrum (autofluorescence) from mixed spectrum (single labeled) to produce pure spectrum of each fluorophore. This allowed the separation of spectrum from multi-labeled slides (e.g. DAPI + TRITC) to obtain composite images containing only labels of interest. These composite images are then used for further analysis using Slidebook 6 software (below). For dorsal horn spinal cord sections ipsilateral to sciatic manipulation, sixteen to twenty-eight images per experimental group (4 sections per animal, 4-7 animals per condition) were acquired and analyzed.

SlideBook6 software image analysis

Composite images are analyzed using SlideBook6 software (Intelligent Imaging Innovations, Denver, CO, USA) as described previously (Noor et al., 2017; Sanchez et al., 2017). Briefly, to discriminate signals originating from artifacts, the experimenter determined an acceptable threshold of very low-level emission fluorescent intensity per individual animal (monoclonal GFAP, IL-1β and IL-10 analysis). This was done by closely replicating the on-screen composite computer image with that observed through the microscope eyepiece, as described previously (Noor et al., 2017; Sanchez et al., 2017). In addition, for

spinal cord sections, the dorsal horn (region of interest (ROI)) is outlined for analysis eliminating the surrounding white matter and peri-spinal blank space (intrathecal space). The image is then refined to include the predetermined threshold within the outlined area. The 'Sum Intensity' (the total signal within the outlined area in the dorsal horn) is determined and divided by the 'Area' (total area in micrometers squared (μm^2)) to obtain the 'Fluorescence Intensity'. The average of the adjacent sections from a single slide (representing a single animal) is calculated to determine the value for each animal. Finally, averages for each slide within the same condition are calculated along with the standard deviation and standard error of the mean. Data are analyzed as "Sum Intensity of ROI/μm^2.

Tissue collection and total RNA isolation

Following behavioral assessment on Day 14 post-surgery (Group 3) rats are deeply anesthetized (induction 3% vol. followed by 5% in oxygen) for ≥ 10 minutes. Rats are then transcardially perfused with ice cold 0.1M PBS pH 7.4 for 3 min at a rate of 24 ml per minute. Perfused body is then placed on a frozen gel refrigerant pack (Glacier Ice, Pelton Shepherd Industries, Columbus, OH). Laminectomy and tissue dissection is performed to collect both ipsilateral and contralateral lumber (L4-L6) spinal cord. All samples are placed in DNase/RNAse-free 1.5 ml centrifuge tubes (VWR International, Radnor, PA), flash frozen on dry ice, and stored at -80° C for future analysis.

Flash frozen tissues are transferred to ice and 100µl sterile 1x PBS was added. All tissues are then homogenized using a motorized VWR disposable Pellet

Mixer and motor pestle system (VWR International, Radnor, PA) for about 30 seconds. 60% of the tissue homogenate is then processed for protein analysis (described below). The remaining 40% of the homogenate is added to chilled Qiazol Lysis Reagent (Qiagen, Hilden, Germany) for total RNA isolation (described below).

Tissue lysate preparation and Western Blot Analysis

Flash frozen ipsilateral and contralateral lower lumbar (L4-L6) spinal cord sections are collected from animals as previously described (Jantzie et al., 2013; Jantzie et al., 2014). Briefly, tissues are homogenized using a Fisherbrand Disposable Pestle system (Fisher Scientific, Hampton, NH). Samples are then sonicated in buffer containing protease inhibitors. All samples are then centrifuged at 4200g, at 4° C, for 10 minutes. Lysate is then collected from samples and Braford protein assay (Biorad, Hercules, Ca) is used to determine protein concentrations.

Western blot is used to detect NMDA receptor subunits GluN2B (NR2B) and phosphorylated GluN2B (p-NR2B) (Huang et al., 2018). This was done on ipsilateral spinal cord whole cell fractions from Group 3 rats. Each sample is normalized to 30µg and loaded onto Criterion Precast 4-20% Tris-HCl Precast gels (Bio-Rad, Hercules, CA). For electrophoresis, gels are run at 125V for 1.5 hours. Protein is then transferred to polyvinylidine difluoride (PVDF) membranes, blocked, and are incubated with NMDA receptor subunit antibodies. For anti-NR2B (1:1500, Abcam, Cambridge, MA), 5% milk in Tris Buffered Saline with

Tween 20 (TBS-T) is used to block membrane and dilute antibody. For anti-NR2B (p-Ser1303; 1:3000, Abcam, Cambridge, MA), 1% Bovine Serum Albumin (BSA) (Sigma-Aldrich, St. Louis, MO) in TBS-T is used to block and dilute antibody. Primary antibody incubations are done at 4°C overnight. The next day, a goat anti-rabbit HRP secondary antibody (1:5000; Thermofisher, Waltham, MA) is applied and the membranes are incubated at room temperature for 1 hour. For band detection, ImageQuant LAS 4000 (GE Healthcare Life Sciences, Chicago, IL) is used. GAPDH (1:40,000; Sigma-Aldrich, St. Louis, MO) is used as a loading control.

Total RNA isolation and mRNA analysis by quantitative real-time PCR

Total RNA is extracted from ipsilateral and contralateral spinal cord. Tissue is placed in chilled Qiazol Lysis Reagent (Qiagen, Hilden, Germany) and homogenized for 15 seconds. Total RNA is then extracted using an miRNeasy Micro Kit (qiagen, Hilden, Germany) per manufacturer's instructions. It should be noted that an additional RPE and 80% EtOH wash steps are added to remove any additional salt contaminants added from PBS step. Tissue is centrifuged at 15,000rpm for 1.5 min at 4° C. PBS is aspirated and 35µl of protease inhibitor solution is added and samples are stored in dry ice and later stored at -80° C for future analysis (described below).

RNA concentration and quality is assessed using Nanodrop (Thermofisher Scientific, Walham, MA). RNA samples are then diluted to standardized RNA concentrations of 137ng/µl for ipsilateral and contralateral lumbar spinal cord.

Standardized samples are then transcribed to cDNA at 1438.5ng for ipsilateral and contralateral lumbar spinal cord. Reverse transcription is performed for all tissue types using a Superscript IV VILO cDNA Synthesis Kit (Invitrogen, Carlsbad, CA).

Levels of mRNA expression are measured and analyzed as described previously (Mellios et al., 2014). For assessment of transcripts a dilution factor of 1:2.2 for ipsilateral and contralateral lumbar spinal cord is done. cDNA dilution for assessment of rat 18S rRNA normalizer is 1:200 for all tissue types. Levels of mRNA and "Normalizer" rat 18s rRNA (Rn18s, Taqman Assay ID#: Mm03928990_g1), are assayed in triplicate using quantitative real-time PCR (qRT-PCR) with Taqman Gene Expression Assays (ThermoFisher Scientific, Waltham, MA). Gene expression assays are deemed to be "best coverage" assay by the manufacturer and are analyzed with the formula $C = 2^\wedge CT^{Normalizer}/2^\wedge CT^{Target}$ in order to exclude detection of genomic DNA. Glutamate transporters target include SLC1A3 (EAAT1) (Taqman Assay ID#: Rn00665089_m1), SLC1A1 (EAAT3) (Taqman Assay ID#: Rn00564705_m1), and SLC1A2 (EAAT2) (Taqman Assay ID#: Rn00691548_m1).

Statistical analysis

SPSS (IBM, Chicago, IL, USA) is used for all behavioral analysis. At BL, a 3-way (2 x 2 x 2) analysis of variance (ANOVA) is applied to assess differences between prenatal exposure (Sac versus PAE), surgical treatment (Sham versus minor CCI), and drug injection (vehicle versus UCPH101). Additionally, a 3-way

(2 x 3) repeated measures ANOVA is used for analysis of the between-subject factors of prenatal exposure, surgery, and injection for days post-surgery as well as days post-injection. Data acquired from IHC, western blot, and qRT-PCR are analyzed using GraphPad Prism version 7 software (Graphpad Software Inc., San Diego, CA, USA). Post-hoc examination of IHC IR, western blot, and qRT-PCR is determined prior to experiments and is analyzed using Fisher's LSD test. The threshold for statistical significance is set *a priori* at α = 0.05 for all sets of multiple comparisons. In order to minimize unnecessary duplication, the minimum number of animals possible to make statistically significant conclusions is used, which is based on our previous publications (Wilkerson et al., 2012a; Dengler et al., 2014; Noor et al., 2017; Sanchez et al., 2017; Whitehead et al., 2017). Outliers were removed following Grubbs' Z-test (Grubbs, 1950). In all cases, the data are presented as the mean ± SEM. All figures are created in GraphPad Prism version 7 software (Graphpad Software Inc., San Diego, CA, USA).

Results

Inhibiting GLAST function leads to induction of allodynia only in PAE rats

Prior to either sham (Fig. 1) or minor CCI (Fig. 2) surgery, all rats display basal levels of light touch sensory thresholds in that both ipsilateral and contralateral hindpaw responses occurred at about 10 grams of stimulus intensity (Fig. 1a-d and Fig. 2a-b). These responses remain consistent following sham surgery at Day 3 and 10 post-surgery (Fig. 1a-d). At Day 10 post-surgery all rat groups are

given i.t. 10μM or 100nM UCPH101 or equivolume vehicle and tested at 1hr, 2hr, 3hr, and 24hrs post-injection. Vehicle injected Sac and PAE rats maintained hindpaw responses comparable to pre-injection values (Fig. 1a-d). Additionally, Sac rats receiving only 10μM UCPH101 maintained normal sensitivity through the behavioral time-course (Fig. 1a,c). Interestingly, PAE rats receiving 100nM UCPH101 demonstrate increased sensitivity to light touch. Furthermore, when the dose of UCPH101 is increased to 10μM, sensitivity is increased in both ipsilateral and contralateral hindpaw (Fig. 1b,d). Sensitivity returns to BL levels by 24 hours post-injection. These data indicate that increasing glutamate at the synaptic cleft of the lower lumbar spinal cord is able to induce allodynia only following PAE. Additionally, these data suggest that PAE leads to enhanced reactivity to glutamate either on glia or at the post-synaptic terminal.

Alteration of GLAST function enhances susceptibility to developing allodynia

Following BL assessment, Sac and PAE rats receive minor (1 Sut.) CCI surgery (Fig. 2a-b). Data show that in comparison to Sac rats which maintain sensitivity comparable to baseline at Days 3 and 10, PAE rats develop robust unilateral allodynia (Fig. 2a-b) which has previously been demonstrated (Sanchez et al., 2017). At Day 10 post-surgery rats receive either i.t. 10μM or 100nM UCPH101. Strikingly, Sac rats with minor CCI develop allodynia similar to PAE rats with injury (Fig. 2a). PAE rats with minor CCI do not develop increases in sensitivity following 100nM injection but there are increases in sensitivity following 10μM

injection at 2 hours and 3 hours post-injection (Fig. 2a). Normal sensitivity in Sac

rats returns whereas allodynia comparable to pre-injection values in PAE rats

returns by 24 hours post-injection (Fig. 2a). Interestingly, assessment of

contralateral hindpaw sensitivity demonstrates normal sensitivity at BL and up to

Day 10 post-surgery (Fig. 2b). Following i.t. injection of either 10μM or 100nM

UCPH101 at Day-10 post-surgery, Sac and PAE rats develop slight increases in

sensitivity (Fig. 2b). Furthermore, no changes in sensitivity are seen as a result of

increasing UCPH101 concentration. Considering allodynia is induced in Sac rats

with minor CCI only following GLAST inhibition, this would suggest that PAE may

increase susceptibility to developing allodynia through alteration of GLAST

function.

PAE does not alter gene expression of spinal glutamate transporters

In behaviorally assessed Sac and PAE rats receiving either sham or minor CCI,

dorsal horn spinal cord is collected to determine gene expression of GLAST,

GLT-1, and EAAC1 (Fig. 3). Interestingly, minor CCI or PAE does not

significantly alter the expression of GLAST or EAAC1. Furthermore, although not

significant, slight increases in GLT-1 are seen following minor CCI in both Sac

and PAE rats. Our data indicate that PAE does not alter gene expression of

glutamate transporters. In addition, considering our behavioral data (Fig. 1-2)

suggests a role for GLAST function it is possible that alterations may be seen at

the protein level which is demonstrated by previous reports (Brolese et al., 2015).

Glutamate transporter expression is altered following PAE within the spinal cord

Sac and PAE rats that are behaviorally assessed following sham and minor CCI, IHC is used to determine immunoreactivity (IR) of glutamate transporters within the dorsal horn spinal cord (Fig. 4). Interestingly, compared to Sac rats with sham surgery, PAE rats demonstrate upregulation of both GLAST and GLT-1 (Fig. 3a-b). Furthermore, when minor CCI is applied, Sac rats demonstrate an upregulation of only GLAST expression whereas PAE rats demonstrate a downregulation in both GLAST and GLT-1 (Fig. 3a-b). IR for EAAC1 show no significant changes in expression as a result of prenatal exposure or surgery (Fig. 3c). These data indicate the PAE alone is able to significantly alter the expression of GLAST and GLT-1 resulting in a downregulation following minor CCI. Additionally, no changes are seen in the expression of the neuronal specific glutamate transporter EAAC1. Together our data demonstrate that PAE may alter glutamate transporters which may lead to increased susceptibility to developing allodynia.

PAE or minor CCI do not alter p-NR2B in the dorsal horn spinal cord

Spinal cords from Sac and PAE rats with minor CCI are assessed through western blot to determine the protein expression of phosphorylated GluN2B (p-NR2B) and total GluN2B (NR2B) (Fig. 5). Data are presented as a ratio of p-NR2B divided by total NR2B. No significant differences are seen in the phosphorylated NR2B as a result of PAE or minor CCI. Previous reports

demonstrate that p-NR2B/NR2B is increased following a standard CCI but this is not observed following a minor CCI.

Discussion

An emerging body of literature supports the idea that moderate PAE alters neuroimmune function (Drew and Kane, 2014; Topper et al., 2015) which may lead to heightened susceptibility to developing neuropathic pain as previously shown (Noor et al., 2017; Sanchez et al., 2017). Interestingly, the effects of PAE are not unmasked until a secondary insult such as CCI is applied. Recent reports demonstrate that susceptibility is mediated through alteration of glial cells within the spinal cord, specifically astrocytes (Noor et al., 2017; Sanchez et al., 2017). This suggests that induction of allodynia following minor CCI may be mediated through an astrocyte specific mechanism. In support this notion, reports demonstrate that moderate PAE alters the astrocyte specific glutamate transporter GLAST (Brolese et al., 2015). Thus, the current work sought to determine what effect PAE has on glutamate transporters and whether alteration of GLAST function can induce a PAE behavioral phenotype in healthy Sac controls. Additionally, we sought to determine whether PAE alters the phosphorylation of the NMDA receptor subunit NR2B within the spinal cord.

In the current report, only PAE rats with sham surgery receiving i.t. UCPH101 demonstrate induction of allodynia in a dose dependent manner (Fig. 1b,d). Interestingly, it was not until minor CCI is applied with GLAST inhibition that Sac control rats demonstrate robust unilateral allodynia (Fig. 2a-b). This

induction of allodynia in Sac rats mimicked allodynia seen in PAE rats with minor

CCI suggesting that PAE alters GLAST function. Gene expression analysis for

glutamate transporters within the dorsal horn spinal cord reveal no significant

differences between Sac and PAE groups receiving either sham or minor CCI

(Fig. 3). Interestingly, IHC analysis demonstrates that PAE alone alters GLAST

and GLT-1 but not EAAC1 expression within the dorsal horn spinal cord (Fig. 4).

Our gene and protein expression data suggests that PAE may alter post-

translational modification of glutamate transporters. Furthermore, when minor

CCI is applied, Sac rats demonstrate compensatory upregulation of GLAST and

GLT-1 whereas PAE rats show a downregulation of these transporters (Fig. 4).

This downregulation potentially allows glutamate to accumulate within the

synaptic cleft of the dorsal horn spinal cord leads to induction of allodynia

following minor CCI. This idea is supported considering allodynia was induced in

Sac with minor CCI and GLAST inhibition. Furthermore, our data suggest that

PAE does not alter neuronal reactivity in that no significant differences are

observed in the neuronal specific transporter EAAC1 (Fig. 4c) or changes in p-

NR2B (Fig. 5). Together, our data suggest that PAE alters glutamate transporter

function making them more susceptible to downregulation which ultimately leads

to allodynia following even a minor CCI.

Susceptibility to allodynia is glial mediated rather than neuronal

It has been well characterized that the induction of allodynia is mediated by glial

activation and release of proinflammatory cytokines (Milligan and Watkins, 2009).

Following sciatic nerve damage, the release of glutamate triggers glial activation, resulting in release of proinflammatory cytokines which ultimately result in NMDA receptor depolarization (Milligan and Watkins, 2009). Studies that explore the effects of PAE on glia show that PAE primes glial cells within the brain and spinal cord making them more reactive following a secondary insult (Topper et al., 2015; Noor et al., 2017; Sanchez et al., 2017). In addition to this, proinflammatory cytokine release is heightened in PAE immune cells compared to controls (Topper et al., 2015; Noor et al., 2017; Sanchez et al., 2017). Together the data support the idea that heightened susceptibility to developing allodynia following PAE is glial mediated.

Although this is true, neuronal mediated mechanisms in neuropathic pain cannot be discounted. Considering pain signals from the periphery travel into the spinal cord through primary afferent terminals where they synapse onto pain projection neurons, it is possible that PAE could result in neuronal alterations. Previous reports have demonstrated that PAE alters NMDA receptor subunits within the brain (Brady et al., 2013). This would lead to the idea that neurons may be more sensitive to the release of glutamate within the post-synaptic terminal. Thus, during minor CCI, allodynia may be induced due to the heightened reactivity of NMDA receptors to glutamate. Interestingly, our data argue for a more glial mediated mechanism. Our behavioral data utilizing 100nM and 10μM show a dose dependent response following sham surgery, which is not present following minor CCI. PAE rats with minor CCI do not show concentration dependent increases in allodynia (Fig. 2a). Similarly, contralateral hindpaw

responses are identical regardless of concentration of UCPH101 used (Fig. 2b).

These data show increasing glutamate at the synapse by increasing the dose of

UCPH101 does not result in an increase in sensitivity. There is a threshold that is

reached preventing allodynia from becoming potentiated. In addition to this data,

our gene expression (Fig. 3) and protein (Fig. 4) expression data show no

significant alterations as a result of PAE for the neuronal specific glutamate

transporter EAAC1. In addition, no significant differences are seen in the

phosphorylation of NR2B as a result of PAE (Fig. 5). Taken together, it would

suggest that PAE induced susceptibility to developing allodynia is mediated

primarily through glial activation.

Regulation of glutamate transporter expression

Previous reports characterizing the expression of glutamate transporters within

the spinal cord demosntrate that following nerve injury there is an initial

upregulation of transporters by Day 1 and 4 post-surgery followed by a

downregulation at Days 7 and 14 (Sung et al., 2003). Interestingly, our data show

that PAE results in an upregulation of GLAST and GLT-1 without nerve injury and

leads to downregulation following a minor injury (Fig. 4a-b). In contrast, healthy

controls demonstrate compensatory upregulation which may be preventing the

development of allodynia (Fig. 4a-b). Thus, this begs the question of what

mechanisms may regulate the expression of glutamate transporters and how

PAE may alter these mechanisms.

As mentioned previously, following nerve injury, glial cells release proinflammatory cytokines including IL-1β. Recent reports demonstrate that this release of IL-1β will work through the calcium/Protein kinase C (PKC) pathway to enhance endocytosis of both GLT-1 and GLAST (Yan et al., 2014). A separate report demonstrates that the proinflammatory cytokine TNFα may also regulate both GLAST and GLT-1 (Dumont et al., 2014). Interestingly, previous reports show that although PAE leads to heightened expression of both TNFα and IL-1β following insult, basal levels remain normal. Furthermore, other studies find that PAE downregulates basal expression of the anti-inflammatory IL-10 (Noor et al., 2017). Although speculative, it is possible that this alteration of IL-10 may lead to a more proinflammatory environment within the spinal cord leading to heightened expression of both GLAST and GLT-1. Thus, when insult is applied and additional IL-1β and TNFα are released, it quickly results in downregulation of both glutamate transporters. Further studies are needed to characterize the immune mechanisms that regulate glutamate transporters within the spinal cord.

Effects of PAE on GLAST and GLT-1 function may be region specific
Interestingly, our data show that PAE upregulates the expression of both GLAST and GLT-1 within the spinal cord dorsal horn (Fig. 4a-b). In contrast separate reports within the hippocampus show that PAE leads to downregulation of GLAST and upregulation of GLT-1 (Brolese et al., 2015). Thus, although GLT-1 data are similar to what we are demonstrating, conflicting data are seen in GLAST expression. One possible reason for this difference may be that

154

alterations in glutamate transporter expression following PAE are a result of differences in exposure paradigms. In this study, alcohol exposure occurred throughout gestation which is the human equivalent to the first and second trimesters. In contrast, Brolese and colleagues utilized a paradigm that exposed rat pups to alcohol throughout gestation and following birth until weaning (Brolese et al., 2015). Considering that a lot of critical hippocampal development occurs during the third trimester in rodents (Mohajerani and Cherubini, 2006; Lohmann and Kessels, 2014), it is possible that further alterations in glutamate transporter expression may occur following third trimester exposure. Thus, it is important to note that the method of PAE may play a role in how glutamate transporters are altered and warrants further exploration.

Alteration of glutamate transporters may lead to susceptibility to developing glutamate mediated disorders

Glutamate transporters as well as glutamate excitotoxicity has been shown to be involved in the development of various neurodegenerative disorders such as amyloid lateral sclerosis (ALS) and Alzheimer's disease (AD) (Masliah et al., 1996; Dumont et al., 2014; Takahashi et al., 2015). Additionally, altered glial function and increase in proinflammatory cytokines have been suggested to be involved in both ALS and AD (Kim et al., 2018). Considering our data as well as other reports (Brolese et al., 2015) demonstrate that PAE may alter glutamate transporter function as well as glial function, it is possible that this may render individuals susceptible to neurodegenerative disorders. Unfortunately, since

FASD has only recently been recognized (Jones and Smith, 1973), it is possible

that life-long effects such as neurodegenerative disorders in clinical studies may

only begin to become apparent in the near future. Thus, further examination in

individuals with FASD and in animal models of FASD would need to be done to

explore this notion.

Conclusions

Taken together, our data demonstrate the PAE leads alterations of glutamate

transporters within the spinal cord. In addition, this alteration may result in

increased glutamate at the synaptic cleft which may in turn lead to activation of

primed glial cells. Overall, this could ultimately lead to heightened susceptibility to

developing neuropathic pain following minor CCI.

Figure 1

Ipsilateral Paw
Sham Surgery

a)

b)
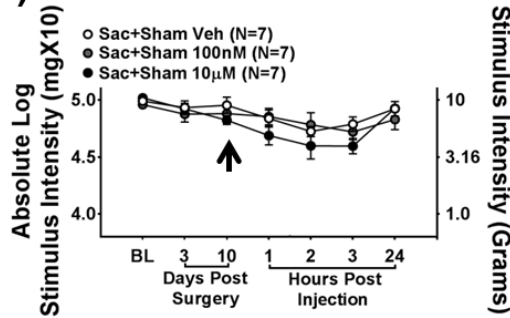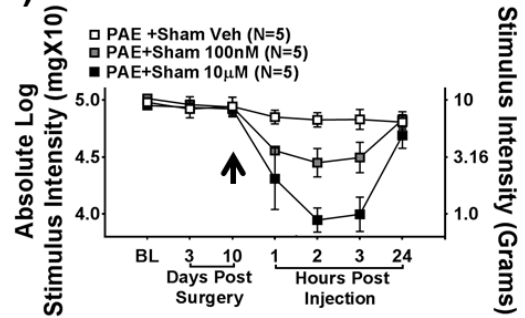
Contralateral Paw
Sham Surgery

c)
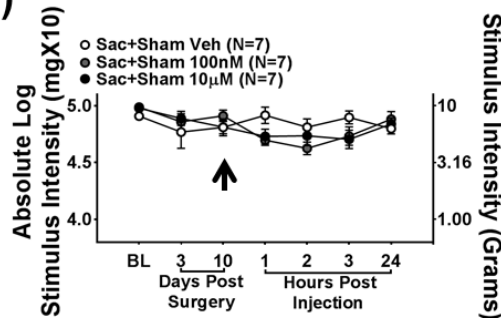
d)
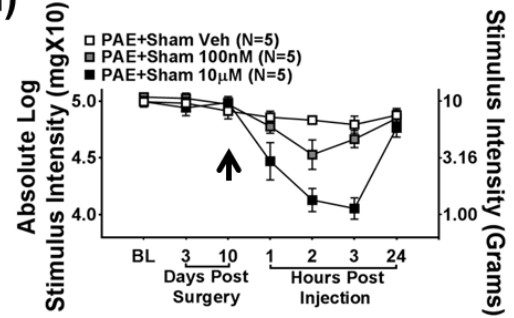
Figure 1 – Inhibition of GLAST function induces allodynia only in PAE rats. Response thresholds from (**a-b**) ipsilateral and (**c-d**) contralateral hindpaw from Sac control and PAE rats with sham surgery. **a-d** Similar hindpaw sensitivity is observed in all Sac and PAE rats prior to surgery (Baseline; BL) [ipsilateral, $F_{1,30}$ =0.143, p = 0.708; contralateral, $F_{1,30}$ = 3.918, p = 0.056]. After sham surgery, normal sensitivity was maintained as no significant differences are observed as a result of exposure in the ipsilateral or contralateral hindpaw [ipsilateral, $F_{1,30}$ =1.137, p = 0.295; contralateral, $F_{1,30}$ = 0.081, p = 0.922]. At Day 10 post-surgery all rats received an i.t. injection of vehicle, 10µM (Sac and PAE rats), or 100nm (only PAE rats) of UCPH101. Interestingly, a main effect of exposure [ipsilateral, $F_{1,30}$ =21.192, p < 0.0001; contralateral, $F_{1,30}$ = 18.519, p < 0.0001], injection [ipsilateral, $F_{1,30}$ =22.208, p < 0.0001; contralateral, $F_{1,30}$ = 23.829, p < 0.0001], and an interaction between exposure and injection [ipsilateral, $F_{1,30}$ =9.362, p = 0.001; contralateral, $F_{1,30}$ = 12.026, p < 0.0001] is observed. All rats return to normal sensitivity by 24 hours post-injection in that no significant differences are seen between groups [ipsilateral, $F_{1,30}$ =1.271, p = 0.295; contralateral, $F_{1,30}$ = 0.758, p = 0.477]. Asterisks indicate p < 0.05. The data are presented as the mean ± SEM. Arrows indicate when i.t. injection was done.

157

Figure 2

Figure 2 – Sac rats develop allodynia following minor CCI following GLAST inhibition. (**a**) Ipsilateral and (**b**) contralateral response thresholds are shown for Sac and PAE rats with minor CCI. At BL similar hindpaw sensitivity is observed between all groups [ipsilateral, $F_{1,16}$ =3.779, p = 0.070; contralateral, $F_{1,16}$ = 1.164, p = 0.222]. Following minor 1-suture CCI PAE rats develop robust allodynia within the ipsilateral paw compared to Sac control rats where a significant effect of exposure is seen [ipsilateral, $F_{1,16}$ =34.332, p < 0.0001; contralateral, $F_{1,16}$ = 0.189, p = 0.670]. Following i.t. injection of either 10µM (Sac and PAE rats) or 100nm (only PAE rats) UCPH101, a main effect of exposure [ipsilateral, $F_{1,15}$ =18.650, p = 0.001; contralateral, $F_{1,15}$ = 4.041, p = 0.063] and injection is demonstrated in the ipsilateral hindpaw [ipsilateral, $F_{1,15}$ =5.085, p = 0.040; contralateral, $F_{1,15}$ = 0.166, p = 0.690]. By 24 hours post-injection the effects of UCPH101 are no longer present as no main effect of injection is seen [ipsilateral, $F_{1,16}$ =0.866, p = 0.367; contralateral, $F_{1,16}$ = 0.520, p = 0.482]. Asterisks indicate p < 0.05. The data are presented as the mean ± SEM. Arrows indicate when i.t. injection was done.

Figure 3

Spinal Cord – Ipsilateral mRNA gene expression
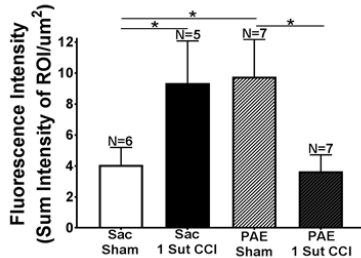
a) EAAT1 (GLAST)   **b) EAAT2 (GLT-1)**   **c) EAAT3 (EAAC1)**

Figure 3. PAE does not alter glutamate transporter gene expression
Gene expression of (**a**) EAAT1, (**b**) EAAT2, and (**c**) EAAT3 within the ipsilateral dorsal horn spinal cord was determined using qRT-PCR. No significant differences are seen between groups in that no main effects of treatment [EAAT1, $F_{3,17}$ =1.104, p = 0.3746; EAAT2, $F_{3,17}$ = 1.241, p = 0.3258; EAAT3, $F_{3,17}$ = 0.5529, p = 0.6531] are observed. No significant increases were observed as a result of PAE. Additionally, no significant differences are seen as a result of minor CCI. The data are presented as the mean ± SEM.

Figure 4

Spinal Cord – Ipsilateral Protein Expression

Figure 4. GLAST and GLT-1 are upregulated as a result of PAE alone. Protein expression of glutamate transporters within the ipsilateral dorsal horn spinal cord was determined through quantification of immunoreactivity (IR) following IHC procedures. IR of (**a**) EAAT1, (**b**) EAAT2, and (**c**) EAAT3 is represented by fluorescence intensity which is defined as the total sum intensity within the dorsal horn spinal cord (identified as a region of interest (ROI)) divided by the area of the ROI. An interaction between surgery and exposure is seen for both EAAT1 and EAAT2 but not EAAT3 [EAAT1, $F_{1,21}$ =8.788, p = 0.0074; EAAT2, $F_{1,18}$ = 5.058, p = 0.0373; EAAT3, $F_{1,19}$ = 0.3217, p = 0.5772]. Sac control rats demonstrate an increase in EAAT1 but not EAAT2 expression following minor CCI. Interestingly, PAE alone upregulates both EAAT1 and EAAT2 expression compared to Sac rats. Applying minor CCI to PAE rats downregulates expression of EAAT1 and EAAT2. No significant differences are seen in EAAT3 expression. Asterisks indicate p < 0.05. The data are presented as the mean ± SEM.

160

Figure 5

Spinal Cord – Ipsilateral Protein Expression

a) p-NR2B/NR2B
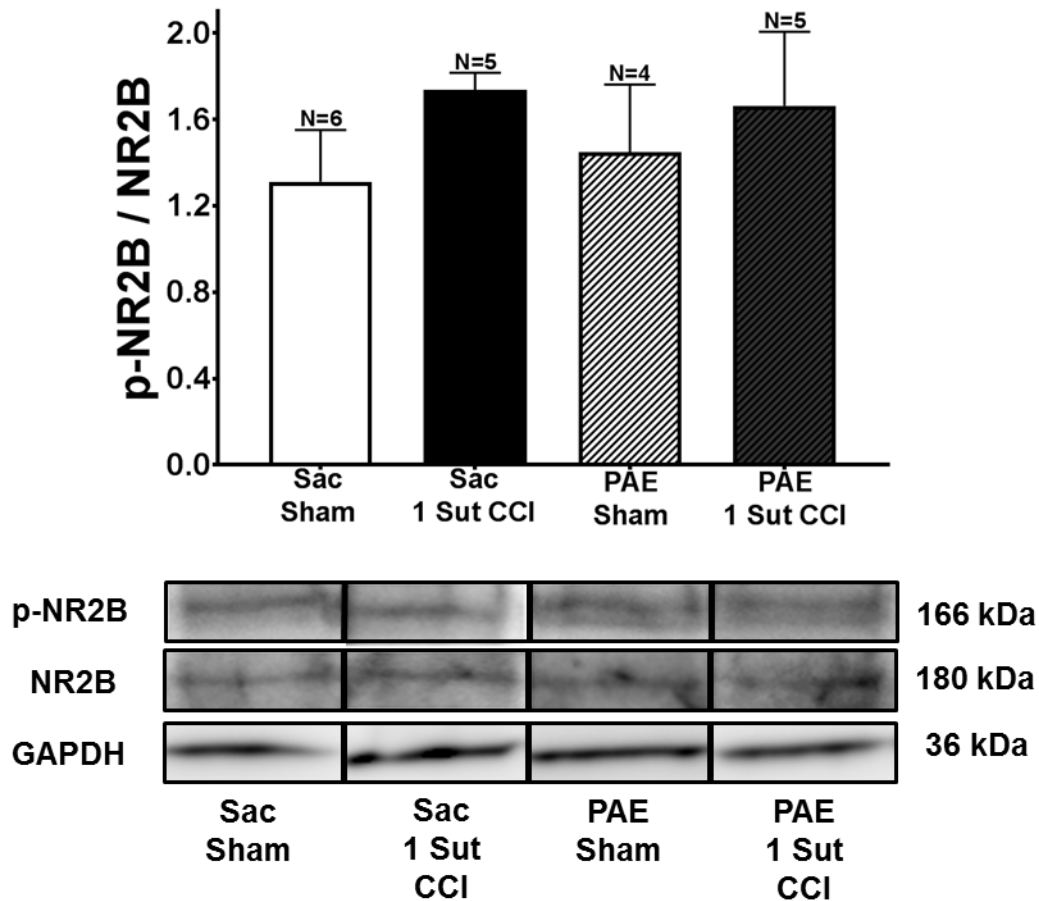
Figure 5. PAE does not alter the phosphorylation of NR2B. The ratio of protein expression of phosphorylated NR2B by total NR2B within the ipsilateral dorsal horn spinal cord was determined using western blot. No significant differences are seen between groups in that no main effects of treatment [EAAT1, $F_{1,16} = 0.1602$, $p = 0.6944$] are observed. No significant increases were observed as a result of PAE. Additionally, no significant differences are seen as a result of minor CCI. The data are presented as the mean ± SEM.

161

Chapter 5 – Discussion

Specific Aim 1: Determine whether PAE generates life-long spinal glial and peripheral immune dysregulation resulting in susceptibility to allodynia

Prior reports demonstrate that PAE results in altered neuroimmune function (Kane et al., 2011; Topper et al., 2015; Noor et al., 2017). More specifcally, glial function is altered within the brain which coincides with increased expression of IL-1β (Topper et al., 2015). Furthermore, peripheral immune responses show heightened reactivit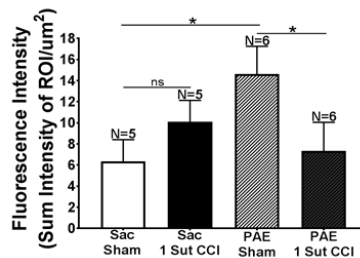y (Noor et al., 2017). Similarly, PAE increased severity and duration of infection as well as increased vulnerability to developing autoimmune disorders (Chiapelli and Taylor, 1995; McGill et al., 2009).

Conditions that are exacerbated by PAE suggests that other chronic CNS diseases with an underlying neuroinflammatory mechanism could also be worsened. Therefore, we used a model of CCI in middle aged rats that have moderate PAE. Applying a standard 4-suture CCI demonstrated potentiated allodynia compared to healthy Sac controls, which coincided with heigthened spinal glial responses. Additionally, peripheral immune responses were amplified, suggesting that PAE primes the immune system resulting in increased reactivity following secondary insult. This led me to hypothesize that PAE may increase susceptibility to allodynia by priming spinal and peripheral immune responses

162

such that significantly reduced damage to the sciatic nerve, a minor 1-suture CCI, would unmask the deleterious effects of PAE on pain processing. *Thus, Aim 1 tested the hypothesis that applying a minor sciatic nerve injury results in allodynia and glial activation only in PAE rats.*

The major findings of this aim include: 1) the effects of PAE are life-long; 2) significantly reducing the damage to the sciatic nerve from a standard 4-suture CCI to a minor 1-suture CCI induces allodynia; 3) minor CCI induces only spinal astrocyte activation but not microglial activation; 4) surgically naïve peripheral immune NK cells of PAE rats are altered within the lymph node and peritoneal exodate; 4) PAE alters myeloid cells within the spleen and lymph node; and 6) stimulation by PMA/io or LPS reveals heigthened expression of both TNF and IL-1β in peripheral leukocytes of PAE rats compared to Sac rats. Collectively, these data demonstrate that PAE heigthens the susceptibility to developing pathological pain. The data suggest that increased suscpetibility is a result of hieghtened immune *reactivity* within spinal astrocytes as well as peripheral immune cells. Furhtermore, the effects of PAE were life-long in that a standard CCI resulted in potentiated allodynia which coincided with heightened glial immune respones. This data supports findings from a prior report where moderate PAE generated increased allodynia (Noor et al., 2017). Overall, the data show that PAE alters both peripheral and spinal immune responses that lead to life-long susceptibility to developing pathological neuropathic pain.

<u>Specific Aim 2</u>: Determine whether susceptibility to allodynia from PAE is mediated by spinal and peripheral immune cytokine dysregulation

Findings from Aim 1 demonstrate that reducing the damage to the sciatic nerve unmasked the effects of PAE, where astrocyte activation is altered and stimulation of immune cells revealed heightened reactivity as measured by proinflammatory cytokine production, IL-1β and TNF-α. Consequently, I investigated whether utilizing a minor 1-suture CCI (referred to as a minor sciatic nerve damage) would reveal specific PAE immune cell responses not only in the damaged sciatic nerve, but also in the sensory ganglia (DRG) and the dorsal horn of the spinal cord.

Recent studies have demonstrate that PAE alone is able to increase the expression of both the chemokine CCL2 as well as the β-2 integrin LFA-1. Interestingly, CCL2 alters the surface receptor ICAM-1 which is the ligand for LFA-1 expressed on peripheral immune cells (Dustin and Springer, 1988). This ultimately aids in the migration of peripheral leukocytes into the spinal cord which aid in the induction of allodynia (Sweitzer et al., 2002). Interestingly, LFA-1 alters the expression of IL-10 (Labuda et al., 1998; Emoto et al., 2003). In support of this, a separate study used a macrophage cell line (RAW 267 cells) and demonstrated that incubating these cells with an LFA-1 antagonist prior to LPS stimulation resulted in heightened IL-10 responses and decreased proinflammatory cytokine expression (Lam et al., 2014). Curiously, rebound IL-10

expression was blunted both at the sciatic nerve and the DRG only in PAE rats following CCI (Noor et al., 2017). Taken together the data suggest that PAE may heighten susceptibility to allodynia by altering the spinal immune profile potentially through the actions of LFA-1 expression. *Thus, Aim 2 tested the hypothesis that PAE alters proinflammatory immune reactivity leading to increased susceptibility to developing pathological pain.*

The major findings of this aim include: 1) induced allodynia in PAE rats with minor CCI is enduring at least until Day 28; 2) the LFA-1 antagonist, BIRT-377, reverses allodynia where peak drug efficacy is seen at Day 4 post i.t. injection; 3) glial activation and IL-1β expression is decreased as a result of LFA-1 antagonism; 4) within the DRG, minor CCI heightens SGCs and IL-1β expression, although PAE alone blunts normal IL-10 responses; 5) PAE alone alters LFA-1 expression; 6) IL-1β is necessary in the induction of allodynia following minor CCI; 7) LFA-1 antagonism may work through TNFα expression *in vivo*; *8*) CXCL1 mRNA is significantly upregulated in PAE rats with minor CCI compared to Sac rats within the ipsilateral sciatic nerve and DRG; 9) and LFA-1 antagonism alters CCL2 expression. Together these data support the idea that PAE increases LFA-1 and antagonizing its activation results in reversal of PAE induced sensitivity to allodynia. Furthermore, the data demonstrate the induction of allodynia following minor CCI in PAE rats could be a result of heightened expression of IL-1β in addition to a blunted IL-10 response. This report also establishes specific chemokines that may be altered as a result of PAE. Specifically, CXCL1 and CCL2 are significantly altered. This could point toward a

role for peripheral leukocytes in the induction of allodynia. Interestingly, this work sheds light on the contribution that the DRG may have in the induction of PAE susceptibility to allodynia. More specifically, the mechanisms may be via the actions of proinflammatory cytokines. For example, IL-1β expression was significantly upregulated whereas normal IL-10 responses were blunted in PAE rats. In addition, SGCs in PAE rats showed significant activation compared to healthy Sac rats following minor CCI. Overall, the data demonstrate that PAE may induce susceptibility to allodynia by altering specific immune factors such as glial cells, SGCs, LFA-1, IL-1β or IL-10both peripherally and in the spinal cord.

Specific Aim 3: **Determine whether PAE-induced susceptibility to allodynia is due to altered astrocyte glutamate transporter function**

The data from Aim 1 as well as Aim 2 demonstrate a significant alteration in the activation of astrocytes. This may explain how PAE induces allodynia following minor challenges such as CCI. As mentioned previously, three glutamate transporters are responsible for clearing glutamate that is released during CCI, and are responsible for minimizing neuronal hyperexcitabilty (inclusive of pain projection neurons). These transporters include GLT-1, EAAC1, and the astrocyte specific transporter GLAST (Furuta et al., 1997). Prior studies show that following CCI, an initial upregulation followed by a downregulation in glutamate transporter expression below basal levels, occurs by Day 7 post-

surgery (Sung et al., 2003). This study also inhibited the function of these transporters. Interestingly, by inhibiting the function of GLT-1 and EAAC1, only a slight increase in allodynia compared to controls is observed. Strikingly, not until GLAST is also inhibited that potentiated allodynia is seen (Sung et al., 2003). This potentiation is similar to what is seen in PAE rats with a standard CCI (**Ch. 1 Fig. 1 and 3**), suggesting that susceptibility to allodynia may be a result of altered astrocyte responses to increased extracellular glutamate, as GLAST is exclusively expressed on astrocytes. In support of GLAST dysfunction in this model of neuropathy, prior reports have shown that PAE alone is able to downregulate the expression of GLAST resulting in decreased uptake of glutamate within the hippocampal slices (Brolese et al., 2015). *Thus, Aim 3 tested the hypothesis that PAE alters glutamate transporters resulting in heightened susceptibility to developing neuropathic pain.*

The major findings of this aim are: 1) inhibition of GLAST function in PAE rats with sham surgery (i.e. rats lacking neuropathy) results in allodynia; 2) no allodynia is induced in Sac rats with sham surgery; 3) applying a minor injury to PAE rats and inhibiting GLAST results in potentiated allodynia similar to that observed in PAE rats with greater CCI; 4) Sac rats with minor injury and GLAST inhibition results in the induction of allodynia; 5) PAE does not alter mRNA expression of glutamate transporters; 6) non-neuronal GLT-1 and GLAST but not the neuronal specific transporter EAAC1 are upregulated as a result of PAE alone; 7) PAE does not alter phosphorylation of the NR2B (not expressed on glia) within the spinal cord. This data sheds light on the potential effects that PAE may

exert on the clearance of glutamate from the synapse. More specifically, the data demonstrate increased susceptibility to allodynia is due to a combination of several discrete factors. For example, if glial and not neuronal glutamate transporter function is altered due to PAE, it may result in large accumulations of glutamate within and around the synapse in the spinal cord region responsible for relaying pain signals. Glutamate accumulation may lead to exaggerated responses of primed glial cells that is disproportionately greater than the initiating stimulation (e.g. minor injury). Activation of primed glial cells results in heightened release of the classic pro-nociceptive cytokine, IL-1β as well as other proinflammatory factors such as TNFα. Considering PAE alone alters LFA-1 shown to influence IL-10 responses, these animals may not be able to mount a healthy anti-inflammatory response. As a result, induction of allodynia following minor injury may be due to a global dysregulation of IL-10 responses. Thus, future studies need to focus on neuronal vs. glial glutamate release and consequent changes in LFA-1 expression alongside astrocyte activation to identify novel targets of adverse neuroinflammatory processes in FASD adults and children.

Discussion

How does PAE lead to enhanced susceptibility to allodynia?

Figure 1.

Figure 1. Dorsal horn spinal cord under healthy non-pathological conditions. Under basal conditions both microglia and astrocytes are not reactive. Proinflammatory cytokines such as IL-1β and TNFα remain as inactive precursors within glial cells. In addition to this, any glutamate that is released into the synapse is cleared using the glutamate transporters GLT-1, EAAC1, and GLAST. Glutamate receptors AMPA, Kainate, and NMDA remain silent. Furthermore, magnesium remains bound to NMDA receptors preventing depolarization. This homeostasis is maintained until a peripheral nerve injury occurs.

During healthy non-pathological conditions where peripheral nerve damage *is not* present, microglia and astrocytes are non-reactive. Both of these glia continue to survey the environment and proinflammatory cytokines such as

IL-1β and TNFα and the anti-inflammatory IL-10 remain in their inactive forms. If glutamate is released from the pre-synaptic afferent terminal, glutamate transporters such as GLT-1, EAAC1, and GLAST will clear glutamate from the synapse. This prevents glia from becoming activated and depolarization of AMPA and Kainate receptors does not occur (**Ch. 5 Fig. 1**). Ultimately, glutamate is not continuously present and the immune response does not occur thus, painful stimuli are not felt.

Data show (**Ch. 2 Fig. 1, Ch. 3 Fig. 1, and Ch3. Fig. 7**) that normal sensitivity is maintained in healthy Sac rats with minor 1-suture CCI. When incoming noxious stimuli comes from the periphery, glutamate is released in the synapse. This results in activation of microglia and astrocytes which then release IL-1β and TNFα within the spinal cord (**Ch. 2 Fig. 2, Ch. 3 Fig. 2, and Ch. 3 Fig. 3**). Furthermore, glutamate binds AMPA receptors resulting in activation and depolarization of the post-synaptic membrane of pain projection neurons via sodium ions entering the cell. Compensatory upregulation of IL-10 as well as GLT-1 and GLAST occurs (**Ch. 4 Fig. 3**). This inhibits the actions of IL-1β and TNFα and it results in clearance of glutamate from the synapse stopping AMPA receptor depolarization. These mechanisms prevent NMDA receptors from becoming phosphorylated and magnesium is maintained keeping these receptors silent. This ultimately maintains normal sensitivity in Sac control rats (**Ch. 5 Fig. 2**).

In contrast, when minor 1-suture CCI is applied to PAE rats robust allodynia is induced (**Ch. 2 Fig. 1, Ch. 3 Fig. 1, and Ch. 3 Fig.** 7). Additionally, data show
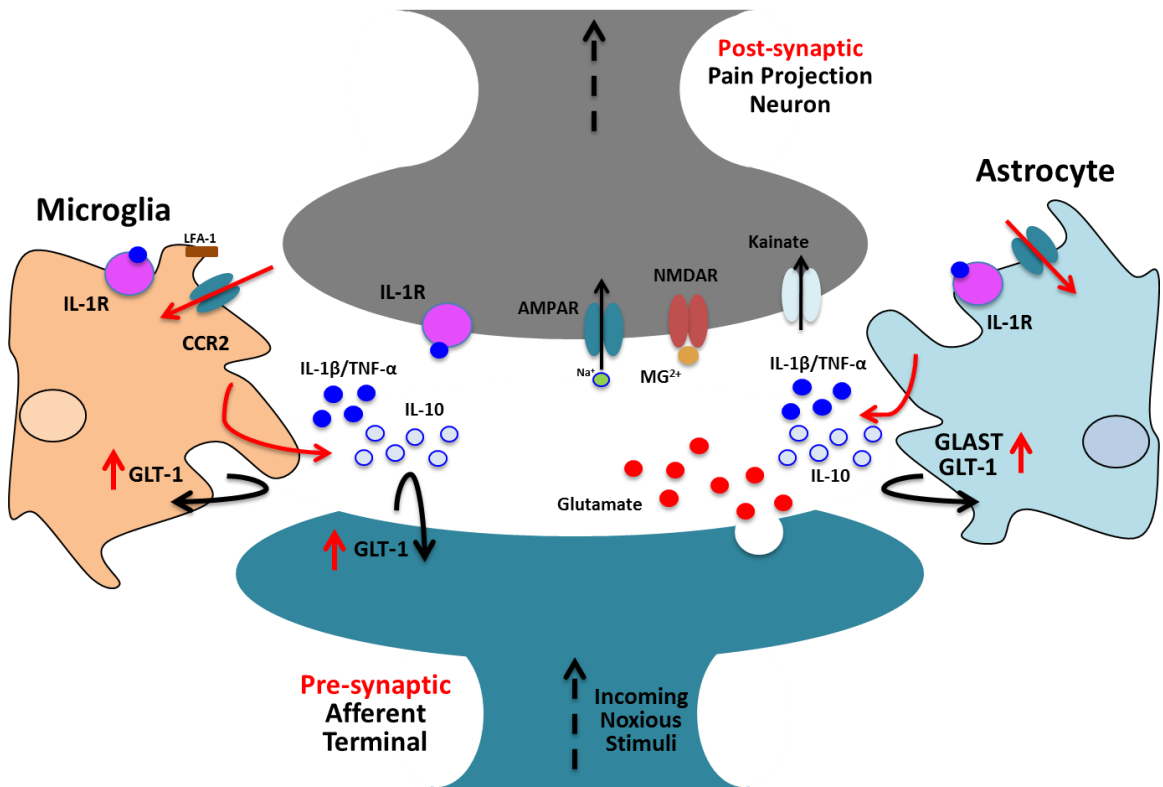
Figure 2. Compensatory mechanisms prevent the induction of allodynia following minor CCI in Sac controls rats. Applying a minor injury to healthy Sac control rats results in release of glutamate from the pre-synaptic afferent terminal. Glutamate binds AMPA and Kainate receptors on the post-synaptic pain projection neuron. Additionally, glutamate activates microglia and astrocytes resulting in the release of IL-1β and TNFα. These cytokines will bind their receptors on pain projection neurons and other nearby glia. To compensate for this response, glia will release the anti-inflammatory IL-10. Additionally, glutamate transporter expression is upregulated. IL-10 inhibits the proinflammatory response and glutamate is cleared from the synapse by glutamate transporters. These compensatory mechanisms prevent the magnesium block on NMDA receptors from coming off, which ultimately prevents the induction of allodynia.

that PAE primes astrocytes (**Ch. 2 Fig. 2 and Ch. 3 Fig. 2**), suppresses healthy

IL-10 responses (**Ch. 3 Fig. 3**), upregulates LFA-1 expression (**Ch. 3 Fig. 4**), as

well as glutamate transporters (**Ch. 4 Fig. 3**) within the spinal cord. Thus, it is possible that when minor CCI is applied, glutamate binds AMPA and Kainate receptors. AMPA receptor expression is increased with the activation and depolarization of the cell membrane on pain projection neurons (Henley and Wilkinson, 2013). Activation of both microglia and primed astrocytes occurs resulting in the release of IL-1β and TNFα. In addition to this, upregulated LFA-1 expression amplifies the release of proinflammatory cytokines potentially through the Src family of kinases. The compensatory IL-10 response is severely blunted in PAE rats which allows for the proinflammatory environment to persist long after the injury occurs. These cytokines will then activate other nearby glia and bind their receptors on post-synaptic pain projection neurons. In addition to this, dysregulated glutamate transporters are quickly downregulated as a result of proinflammatory cytokine release leading to accumulation of glutamate in the synapse. IL-1β binding its receptor on pain projection neurons leads to phosphorylation of NMDA receptor subunits through the Src family kinases leading to a decreased affinity for magnesium (Zhou et al., 2011). Finally, influx of sodium through AMPA receptors leads to strong depolarization of the pain projection neuron cell membrane leading to the release of magnesium (Zhou et al., 2011). Ultimately strong depolarization of glutamate receptors in addition to AMPA receptors occur leading to the induction of allodynia in PAE rats with minor CCI (**Ch. 5 Fig. 3**).

Figure 3.
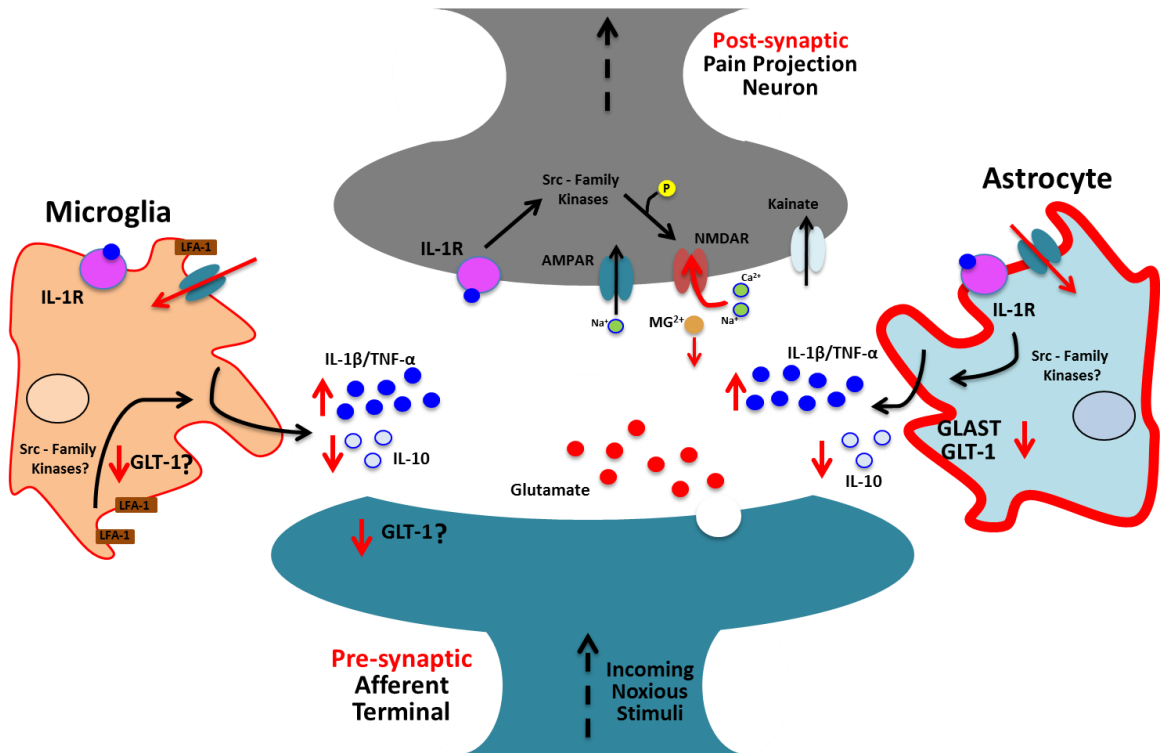
Figure 4. PAE results in alteration of glial mechanisms leading to susceptibility to developing allodynia. PAE results in priming of astrocytes and upregulation of glutamate transporters and LFA-1 expression. Thus, when a minor injury is applied, glutamate is released into the synapse where it binds AMPA and Kainate receptors and activates glial cells. Microglia and astrocytes will release IL-1β and TNFα. LFA-1 upregulation leads to a heightened proinflammatory environment by further increasing the release of IL-1β and TNFα. In addition to this, the normal compensatory upregulation of IL-10 is suppressed potentially through LFA-1 mediated mechanisms. These events result in glutamate transporters to downregulate their expression leading to accumulation of glutamate into the synapse. This leads to further activation of glia cells as well as phosphorylation of NMDA receptor subunits. Additionally, AMPA receptor expression is increased leading to strong depolarization of the pain projection neuron cell membrane. These events lead to magnesium to be released from NMDA receptors. Ultimately, strong depolarization from through AMPA and NMDA receptors occurs resulting in the induction of allodynia.

173

PAE blunts normal IL-10 responses

My data demonstrate that PAE results in blunting normal IL-10 responses in both the spinal cord (**Ch. 3 Fig. 3d and 5c**). It is possible that a combination of increased proinflammatory cytokines with blunted IL-10 may be responsible for induction of allodynia in PAE rats (**Ch. 3 Fig. 1 and Fig. 7**). This raises questions as to what alterations does PAE have leading to blunted IL-10. Previous reports demonstrate mechanisms by which IL-10 is upregulated. Although speculative it is possible that PAE could alter one or all of these mechanisms. For example, IL-10 has been shown to be produced through stimulation of toll like receptor (TLR) 2 as well as the pattern recognition receptor (PRR), dectin (Saraiva and O'garra, 2010). Although no data have demonstrated the effects of PAE on these specific receptors, previous reports do show significant alteration of the TLR4 leading to upregulation of proinflammatory factors (Pascual et al., 2017). This would suggest that PAE could potentially alter both TLR2 and dectin.

In addition to this, upregulation of LFA in PAE rats (**Ch. 3 Fig. 4**) could also potentially influence IL-10 responses. Previous reports show that LFA-1 knockout animals demonstrate changes in their expression of IL-10 (Emoto et al., 2003). Furthermore, a separate study shows that stimulation of the ICAM1, the ligand for LFA-1, suppressed the IL-10 responses (Labuda et al., 1998). In support, of these studies our lab utilized an *in vitro* study to demonstrate the antagonizing LFA-1 results in decreased proinflammatory factors in combination with increases in IL-10 expression following LPS stimulation (data not shown).

These data provide evidence for LFA-1 mediated mechanisms involved in IL-10 expression.

Previous reports suggest that PAE alters the transcription factors (Ogony et al., 2013). Thus, PAE could potentially change IL-10 expression levels through alteration of various transcription factors. More specifically, specific protein 1 (SP1) (Brightbill et al., 2000), CCAAT/enhancer binding protein – β(Brenner et al., 2003), IFN- regulatory factor 1 (IRF1) and STAT3 (Ziegler-Heitbrock et al., 2003) all control IL-10 production. Thus, PAE may blunt normal IL-10 responses by affecting the function of any of these transcription factors.

Interestingly, PAE can disturb micro RNA (miR) function (Wang et al., 2008). Previous reports demonstrate that IL-10 expression is influenced by miR-466l (Ma et al., 2010) which works through the TLR pathway. Thus, it is possible that PAE could alter miR in order to influence IL-10 expression. Overall, the data present intriguing evidence as to potential mechanisms that PAE alters in order to influence IL-10 which leads to susceptibility to developing allodynia.

PAE rats do not display increased sensitivity at BL or following sham surgery

Interestingly, prior reports discuss sensitivity to light touch in children with FASD (O'Malley, 2007). In support of this, a separate study demonstrates that alcohol alone is able to alter sensitivity to light touch in primate models of FASD (Schneider et al., 2008). Curiously, in our PAE rats, no significant differences are demonstrated at BL or after sham surgery. Based on the literature, we would

hypothesize that rats may demonstrate initial sensitivity as a result of PAE. It is not until a second insult is applied that the effects of PAE are unmasked. This leads to the question of why neuroimmune differences as a result of PAE alone are not observed.

Clinically, children with PAE demonstrate altered immune function (Johnson et al., 1981). More specifically, lymphocyte formation is altered in children with FASD. Studies using animal models of FASD without a secondary insult also show immune alteration (Noor et al., 2017). My data demonstrate that in PAE rats with sham surgery display blunted expression of IL-10 within the DRG. As mentioned previously, during the induction of allodynia, glial cells become activated and the expression of IL-1β is increased. This increase in proinflammatory factors is not observed following sham surgery. Thus, although PAE does alter certain factors of the immune system, the critical factors such as astrocytes, microglia, and IL-1β involved in the disruption of sensory processing are not affected. This potentially explains the reason why no sensitivity is seen in our rats that are moderately exposed to alcohol.

In addition to this, many clinical studies of FASD primarily focus on children that have fetal alcohol syndrome (FAS). These children are commonly exposed to high levels of alcohol where women are drinking daily and/or binge drinking multiple times during pregnancy (Jones and Smith, 1973). This would lead one to believe that the amount of alcohol exposure may also result in increased sensitivity to touch in children with severe FAS. Additionally, it is possible that the high levels of alcohol could serve as a secondary insult to an

FAS child which elicits the effects of PAE. In support of this, previous studies utilizing binge alcohol exposure during the third trimester demonstrate glial and proinflammatory cytokine responses only during withdrawal periods (Topper et al., 2015). Thus, it is possible that even though no sensitivity is seen following a moderate PAE, sensitivity would be demonstrated in a binge ethanol exposure during withdrawal periods. This model may more accurately depict what is seen in the clinic using children with FAS.

Does PAE lead to long-lasting allodynia following minor CCI

Results show that PAE causes an increased severity and duration of influenza infection (McGill et al., 2009). This may be a result of the heightened reactivity seen within glial cells as well as peripheral immune cells in PAE, as supported by animal studies (Noor et al., 2017; Sanchez et al., 2017). These studies demonstrate that PAE leads to potentiated allodynia when a standard CCI is applied (**Ch. 1 Fig. 1**), but do not characterize the entire allodynic timecourse. These studies only assessed behavior until Day 28 (**Ch. 1 Fig. 3**). Taken together, this may suggest that PAE could potentially result in long-lasting allodynia in comparison to healthy controls.

Previous studies from our lab characterizing the time-course following standard CCI in healthy rats demonstrate that allodynia can persist up to about 90 days (data not shown) which may coincide with the absorption rate of chromic gut sutures used in CCI (ethicon.com). In addition to this, astrocytes mediate the

maintenance of allodynia (Gao et al., 2010a). Considering my data demonstrates that PAE may work primarily through alteration of astrocytes (**Ch. 1 Fig. 2 and Ch. 2 Fig. 1**), PAE may lead to long-lasting allodynia following both a standard and minor CCI. Future studies should fully characterize the duration of allodynia following both a standard and minor CCI.

Potential sex differences in PAE and neuropathic pain

Interestingly, previous reports demonstrate sex differences in both neuropathic pain processing and in PAE. Clinically, observations demonstrate that women tend to be more at risk for chronic pain (Rosen et al., 2017). Additionally, women tend to experience pain differently than men in that they rate their pain higher and also have lower pain tolerance (Mogil et al., 1993). These reports suggest that mechanisms underlying sex differences may involve neuroimmune processes during chronic neuropathic pain conditions.

Previous reports that investigate the role of peripheral immune cells in the induction of allodynia found that a combination of glia in the spinal cord as well as T-cells facilitate the induction of allodynia (Sweitzer et al., 2002; Milligan and Watkins, 2009). Additionally, when T-cell deficient mice were used, allodynia was reduced (Cao and DeLeo, 2008; Costigan et al., 2009b). Despite these observations, female mice do not require microglia for allodynia to develop (Sorge et al., 2015). Furthermore, neuropathic females reveal peripheral

leukocytes such as T-lymphocytes (T-cells) tend to play a greater role in neuroimmune interactions during the induction of allodynia (Sorge et al., 2015). Thus, sex differences likely exist in neuropathic pain processing, and importantly, results found in males may not apply to females. This is an important consideration because drugs developed to target chronic neuropathic pain have almost exclusively been studied in preclinical male models.

In addition to these findings, sex differences are demonstrated in PAE. Generally, sex differences are observed in social recognition memory (Kelly et al., 2009). Additionally, differences are observed in long-term potentiation in the hippocampus of males and females (Sickmann et al., 2014). Furthermore, differences are seen in reversal learning in FASD males compared to females (O'Leary-Moore et al., 2006). With regard to immune modulation, some studies show sex differences following PAE. More specifically, females show increased neuroinflammation in that they demonstrate heightened expression of CCL2, and in macrophage inflammatory protein-1α (MIP-1α) (Pascual et al., 2017). Taken together, these data suggest that PAE does result in global sex differences that include immune function. In addition, it is possible that sex differences may be observed in my work which combines both PAE and neuropathic pain processing.

As mentioned previously, PAE males have T-cell mediated deficits. Considering that a lack of T-cells has been shown to reduce allodynia, one would hypothesize that PAE males might demonstrate reduced allodynia following CCI. Interestingly, my data do not support this hypothesis (**Ch. 1 Fig. 1**). It is possible that the heightened glial response within both the sciatic nerve and within the

spinal cord is sufficient to prevent this reduction in allodynia. In contrast, one might predict heightened allodynia in PAE females. Considering PAE females show heightened expression of the chemotactic cytokine CCL2, one might predict that there is heightened infiltration of peripheral leukocytes into the spinal cord. Interestingly, no change in allodynia is observed following a standard CCI (**Ch. 5 Fig. 1**). Furthermore, when a minor injury is applied to PAE and Sac females and behavioral responses are assessed up to Day-28 post-surgery, no significant increases are observed in female PAE rats compared to males (**Ch. 1 Fig. 3 and Ch. 5 Fig. 1**). I hypothesize that allodynia is not elevated in females with CCI because neuroimmune mechanisms in females are primarily due to the actions of peripheral leukocytes and not on spinal glial activation. Thus, a heightened peripheral leukocyte response may be sufficient to induce normal allodynic responses.

Considering Aim 2 focused solely on male PAE rats to examine the effects of an i.t. LFA-1 antagonist on allodynic responses and proinflammatory and anti-inflammatory cytokine network, it may be possible that differences in the effects of the LFA-1 antagonist, BIRT377, might be observed in PAE female rats with CCI. In order to investigate this, I did an i.t. injection of BIRT-377 in female PAE and Sac rats at Day 28 post minor CCI surgery (**Ch. 5 Fig. 1a-b**). Strikingly, PAE females did _not return_ to normal sensitivity like the PAE male rats (**Ch. 3 Fig. 1**). This data suggests that inducing an anti-inflammatory environment in the spinal cord by inhibiting LFA-1 activation on microglia is not sufficient to attenuate allodynia in females. Furthermore, peripheral leukocyte infiltration into the spinal

Figure 4
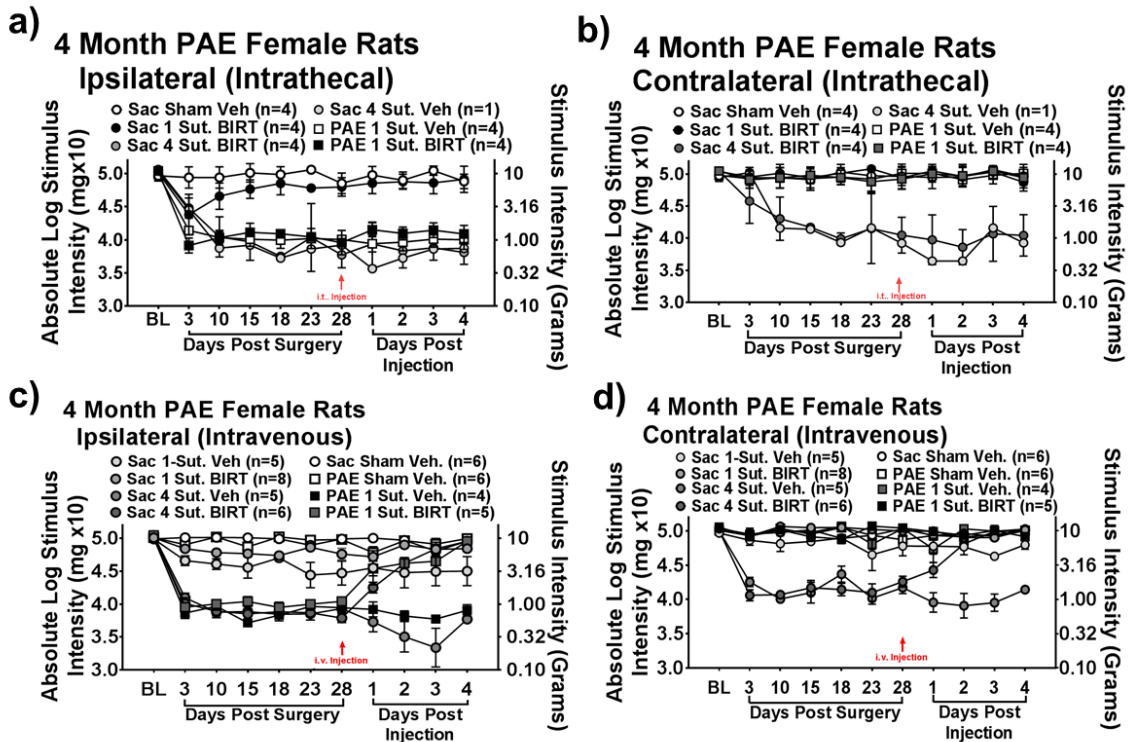
Figure 4. Allodynic female rats return to normal sensitivity only following i.v. injection of BIRT-377. Behavioral responses for both ipsilateral and contralateral hindpaw for i.t. injection (**a-b**) and i.v. injection (**c-d**) of BIRT-377. (**a**)At baseline (BL), behavioral responses were similar amongst all Sac and PAE groups (ipsilateral, $F_{1,18}$ = 0.001, P = 0.975, contralateral, $F_{1,18}$ = 0.032, P = 0.860). Following CCI surgery, Sac rats with standard CCI develop robust bilateral allodynia where a main effect of surgery (ipsilateral, $F_{1,6}$ = 100.131, P < 0.0001, contralateral, $F_{1,6}$ = 50.070, P < 0.0001) is seen. PAE rats with minor CCI develop sensitivity only in the ipsilateral hindpaw comparable to Sac standard CCI rats in that no significant differences are seen between groups (ipsilateral, $F_{1,10}$ = 0.143, P = 0.713, contralateral, $F_{1,9}$ = 69.905, P < 0.0001). Following i.t. injection, allodynic PAE rats do not return to normal sensitivity in that no significant differences are seen between vehicle and BIRT-377 injected groups (ipsilateral, $F_{1,6}$ = 5.826, P = 0.052, contralateral, $F_{1,6}$ = 0.062, P = 0.812). Similarly Sac rats with standard CCI do not return to normal sensitivity as no significant differences were observed when compared to PAE rats with BIRT-377 in the ipsilateral hindpaw (ipsilateral, $F_{1,6}$ = 5.124, P = 0.064, contralateral, $F_{1,36}$ = 49.759, P < 0.0001).(**b**) A separate group of PAE and Sac rats were assessed prior to surgery and show no significant differences at baseline (ipsilateral, $F_{1,36}$ = 0.018, P = 0.895, contralateral, $F_{1,36}$ = 0.562, P = 0.458). Following surgery, a main effect of exposure in the ipsilateral hindpaw was observed (ipsilateral, $F_{1,36}$ = 308.383, P < 0.0001, contralateral, $F_{1,36}$ = 0.153, P = 0.698), a bilateral effect of

surgery (ipsilateral, $F_{1,36} = 651.198$, $P < 0.0001$, contralateral, $F_{1,36} = 464.695$, $P < 0.0001$), and a bilateral interaction between exposure and surgery (ipsilateral, $F_{1,36} = 98.005$, $P < 0.0001$, contralateral, $F_{1,36} = 6.345$, $P = 0.016$) is seen. PAE minor CCI rats develop unilateral allodynia whereas Sac standard CCI rats develop bilateral allodynia up to day 28 post-surgery (ipsilateral, $F_{1,36} = 103.967$, $P < 0.0001$, contralateral, $F_{1,36} = 5.942$, $P = 0.020$). Following i.v. injection, PAE minor CCI and Sac Standard CCI rats return to normal sensitivity up to day 4 post-injection (ipsilateral, $F_{1,36} = 58.633$, $P < 0.0001$, contralateral, $F_{1,36} = 54.229$, $P < 0.0001$).

cord might not be altered as a result of LFA-1 antagonism within the spinal cord. One can consider that the leukocytes primarily involved in inducing allodynia in females, which despite inhibiting LFA-1 in the spinal cord, are producing sufficient expression of proinflammatory factors; leukocytes that have already migrated to the spinal cord and are responsible for generating allodynia. This is supported through prior studies showing that compared to males, females have a two-fold higher T-cell population (Scotland et al., 2011; Sorge et al., 2015). Thus, rather than altering glial cell activation, it may be possible to reverse allodynia by inhibiting infiltration of peripheral leukocytes.

This hypothesis was explored in a separate group of female rats. At Day 28 after minor CCI surgery, females received an intravenous (i.v.) injection of BIRT-377 and behavior was assessed up to Day 4 post injection based on previous male studies (**Ch. 3 Fig. 1 and Ch. 5 Fig. 1**). Interestingly, following i.v. injection, female PAE rats reveal reversal of allodynia similar to male rats where max reversal was seen at Day 4 post-injection (**Ch. 5 Fig. 1c-d**).

Two potential explanations for the reversal of allodynia exist. As is observed with the males, it is possible that injecting an LFA-1 antagonist results in peripheral leukocytes to take on a greater anti-inflammatory phenotype (anti-

inflammatory bias) where these cells expressed more IL-10 than IL-1β amongst other factors. Additionally, it is possible that the migration of peripheral leukocytes is significantly decreased as a result of inhibiting the activation of LFA-1. Considering LFA-1 is not the only adhesion molecule involved in peripheral leukocyte migration, the former hypothesis might be more feasible. Overall, these data as well as previous reports support the idea of sex differences in both PAE and neuropathic pain and warrant further explanation.

A role for adverse *in utero* conditions and increased suscpetibility to neuropathic pain

Studies have focused on the effects of prenatal events and their relation to increasing risk for problems later in life (Gluckman et al., 2008). For example, premature birth has been shown to increase risk for developing diabetes (Hofman et al., 2004) where premature birth can occur as a result of adverse *in utero* conditions such as infection in the mother during pregnancy, stress, or even smoking (Gravett et al., 2010). Additionally, animals subjected to hypoxia are more susceptible to infarction during ischemia (Li et al., 2003). Interestingly, immune system deficits are demonstrated following adverse *in utero* conditions.

Recent studies demonstrate that immune system reactivity is altered following insult during gestation. Reports using an animal model of chorioamnionitis, which is inflammation of the fetal membrane, show heightened reactivty of both astrocytes and microglia (Jantzie et al., 2014). This would suggest that adverse *in utero* conditions such as chorioamnionitis might render

one susceptible to immune mediated pathological issues later in life. In support of this notion, my data demonstrates that PAE rats have an increased susceptibility to developing neuropathic pain (**Ch. 2 Fig. 1**). In addition, my data demonstrate that the effects are not only present in young adult PAE rats (**Fig. 1**) but also in middle aged rats (**Ch. 2 Fig. 1**), suggesting that the effects of PAE are life-long. Additionally, glial activation is significantly increased compared to controls in both young adult and middle aged rats following a standard CCI. Together, these data suggest that adverse *in utero* conditions can render one more susceptible to developing pathological disorders later in life.

Utilizing transgenic animals to explore the effects of PAE on neuroimmune processing

Many studies presented in this dissertation focus solely on the effects of PAE on adult rats but not mice, limiting my ability to use transgenics to explore the effects of PAE on neuroimmune function. The current focus of the lab has shifted towards replicating allodynia following a minor injury in PAE mice. If this effort proves sucessful, knockout (KO) mice could be used to explore how knocking out certain immune factors could result in PAE induced sensitivity to light touch. For example, my data demonstrates the PAE results in blunted IL-10 expression within the DRG and the spinal cord (**Ch3. Fig 3 and 5**). Thus, the question of whether loss of normal IL-10 expression could be explored utilizing IL-10 KO mice with a minor injury. Comparison of PAE IL-10 KO, healthy IL-10 KO, as well as wild type (WT) controls would shed light on whether IL-10 is a

major player in allodynia folling minor CCI. Additionally, IL-1β KO mice could further support whether IL-1β is necessary to induce allodynia in PAE animals. Furthermore, the question of whether LFA-1 could be used as a potential therapeutic can be explored throgh LFA-1 KO mice. These studies would limit the question of whether off target effects of using drugs to inhibit factors such as IL-1β or LFA-1 activation could be causing an effect on the results that I have demonstrated. Thus, the use of transgenic animals could prove to be a powerful tool to fully explore how PAE renders one susceptible to developing neuropathic pain as well as other disorders.

Does PAE induce susceptibility to neuropathic pain through alteration neuronal mediated mechanisms

During neuropathic pain conditions, glutamate is released from the presynaptic terminal. This gluamate can bind the ionotropic receptors α-amino-3-hydroxy-5-methyl-isoxazole propionic acid (AMPA), Kainate, and N-methyl-D-aspartate (NMDA) receptors. As mentioned previously, NMDA receptors do not depolarize because they are kept inactive to cation influx by a magnesium plug (Latremoliere and Woolf, 2009). It is not until central senzitization occurs that magnesium comes off and the induction of allodynia occurs (Milligan and Watkins, 2009). Studies on NMDA receptors demonstrate a role for the subunit NR2B induction of allodynia (Huang et al., 2018). They showed that phosphorylation of NR2B is increased folllowing CCI (Huang et al., 2018). Additionally, Huang and colleagues demonstrate that antagonizing NR2B

attentuated neuropathic pain. These studies demonstrate a critical role for the activation of NMDA receptor subunits in the induction of neuropathic pain.

In addition, glutamate can also bind metabotropic glutamate receptors (mGluRs) which are G-protein-coupled receptors (Masu et al., 1991). These receptors regulate cell excitability and synaptic transmission (Montana and Gereau, 2011). Three groups of mGluRs have been implicated in pain processing (Montana and Gereau, 2011). These receptors are expressed within the dorsal horn spinal cord where they communicate with sensory neurons projecting from the periphery (Montana and Gereau, 2011). Furthermore, these receptors are expressed on DRG cell bodies in rats (Carlton and Hargett, 2007). The ERK signaling pathway, which is necessary for allodynia, is activated by Group 1 mGluRs (Carrasquillo and Gereau, 2007). Additionally, upregulation of Group 2 mGluRs induces sensitivity (Chiechio et al., 2002). Although Group 3 mGluRs play a role in pain, their exact function is still unclear (Montana and Gereau, 2011). Thus, it is possible that increased susceptibility to developing pathological pain could be a result of PAE altering the expression or function of either ionotropic or metabotropic glutamate receptors. It is important to point out that these are expressed on neurons and are ciritical for pain sensitization.

Studies that have explored the effects of PAE on NMDA receptors find significant decreases in the expression of NR2B within the dentate gyrus (Brady et al., 2013). A separate report demonstrates that the altered expression of NR2B in PAE rats seems to be region specific within the brain (Bird et al., 2015). Interestingly, this study found that excitatory post synaptic currents (EPSCs) are

reduced in PAE rats compared to controls (Bird et al., 2015). Furthermore, this study demonstrated no significant differences in expression of mGluR5 expression (Bird et al., 2015). In contrast, a separate study demonstrates that PAE reduced the expression and function of mGluR5 within the dentate gyrus (Galindo et al., 2004). Thus, it is possible that the effects of PAE on mGluR may be region specific. Unfortunately, the effects of PAE on mGluR and NR2B expression within the spinal cord have not been charactered. This makes it difficult to predict whether PAE alters expression of these two factors, which may aid in the induction of allodynia. While speculative, a decrease in NR2B as a result of PAE may lead to decreased allodynia following CCI. The fact that less NR2Bs are present could mean that less NMDA receptors become depolarized leading to decreased pain signals that are relayed to spinal pain projection neurons. Interestingly, changes in NR2B is not observed in my data (**Ch. 1 Fig. 1, Ch. 2 Fig. 1, and Ch.3 Fig. 1**), arguing that NR2B is not affected in the spinal cord of PAE rats. Similarly, a decrease in mGluR expression would argue for decreases in allodynia in PAE rats. This effect is not seen within our behavioral data. Although this is true, it is possible that both NR2B and mGluRs could be either located on or aiding in communication with glial cells resulting in their activation.

Previous studies link neuronal NR2B subunits on NMDA receptors to astrocyte activation (Kato et al., 2006). This study demonstrates that when calcium influx into NMDA receptors was inhibited by NR2B subunit containing NMDA receptor antagonist that the expression of the astrocyte activation marker

187

GFAP was decreased (Kato et al., 2006). This led the researchers to conclude that a potential neuron-to-astrocyte signaling pathway exists that is mediated by NMDA receptors containing the NR2B subunit . Furthermore, a separate study found that only following insult do the NMDA receptor subunits NR2B and NR1colocalize with GFAP expression (Krebs et al., 2003). Interestingly, both these subunits are involved in the induction of neuropathic pain (Ultenius et al., 2006; Huang et al., 2018). Thus, in combination with our astrocyte data (**Ch. 1 Fig. 2a**), it is possible that following minor CCI, significant increases in signaling occurs between astrocytes and NMDA receptors which may potentially explain PAE induced sensitivity to light touch.

In addition to this, mGluRs are expressed by astrocytes and microglia (Drouin‑Ouellet et al., 2011). The results of this study demonstrate that utilizing an NMDA receptor agonist resulted in heightened activation of astrocytes and microglia, but in addition, they measured increases in mGluR5 expression (Drouin‑Ouellet et al., 2011). This is further supported in a separate study that demonstrates disease states result in upregulation of mGluRs as well as increased glial proliferation and heightened astrocyte activation (Anneser et al., 2004), suggesting that PAE could potentially alter mGluR expression specifically on astrocytes. If true, altered mGluR expression may mediate the heightened reactivity observed following a minor CCI (**Ch. 2 Fig. 1 and Ch. 3 Fig. 1**). Further exploration of the effects of PAE in the dorsal horn spinal cord for mGluRs and NMDA receptor subunits would need to be persued to determine the exact involvement of these factors during the induction of allodynia.

Does PAE alter dopamine receptors leading to allodynia following minor CCI

Dopamine is primarily involved in cognition and reward (Potvin et al., 2009). Interestingly, reports suggest that dopamine is also involved in pain processing. More specifically, in patients with Parkinson's disease (PD), when dopaminaergic neurons in the substantia nigra are depleted, patients display a range of pain symptoms (Giuffrida et al., 2005; Tinazzi et al., 2008). Furthermore, Schizophrenia patients, which display dopaminergic hyperactivity, display hypoalgesic responses to mechanical stimuli (Blumensohn et al., 2002; Singh et al., 2006; Potvin et al., 2009). These findings suggest that dopamine and their receptors may play a considerable role in the induction of neuropathic pain. In support, clinical studies have utilized dopamine agonists and found that these drugs reduce hyperalgesia (Altier and Stewart, 1999). A study utilizing dopamine D5 receptor knockout animals found a reduction in hyperalegic responses (Megat et al., 2018). It should be noted that much of these studies focus on hyperalgesia and not allodynia, and therefore, the role of dopamine may not be similar between the two pathological states. Overall, these data do present evidence to consider the actions of dopamine underlying spinal neuropathic pain.

Interestingly, recent studies find that astrocytes express D1 dopamine receptors (Nagatomo et al., 2017). Additionally, this study find that this expression may be region specific in that stronger co-localization of GFAP and D1 dopamine receptors is present within the brain (Nagatomo et al., 2017).

Considering, dopamine receptors, specifically D1 and D2, are expressed within the dorsal horn spinal cord (Millan, 2002), it is possible that dopamine receptor expression may only be upregulated following insult, such as after CCI and augmented following PAE.

Studies that explore the effects of PAE on dopamine receptor expression are limited. A recent study using a binge prenatal alcohol exposure found that D2 receptor expression is decreased within the pituitary (Gangisetty et al., 2015). A separate study utilized a moderate PAE and looked at the effects of D1 dopamine receptor expression. This study found the D1 dopamine receptor binding was increased as a result of PAE whereas this observation is not seen in females (Converse et al., 2014). Unforunately, few studies explore the effects of other dopamine receptor subtypes in the spinal cord following prenatal alcohol exposure.

While limited, data exploring the effects dopamine on PAE and neuropathic pain are enticing. Clinical observations provide support for a role of dopamine receptors in neuropathic pain processing. Additionally, studies suggest that dopamine receptors may be expressed by astrocytes within the spinal cord. Considering the literature is not conclusive regarding the effects of PAE on dopamine receptors in the brain, and much less so in the spinal cord, further exploration is warrented. While speculative, considering I show an alteration of astrocyte activation following PAE, and literature shows alterations in DA receptor expression, I hypothesize PAE influences the expression of dopamine receptors on astrocytic cells. PAE could have direct effects on receptor

expression and/or function. Overall, this change could potentially make astrocytic cells more suscpetible to activation following insult such as CCI, whether that be through dopamine binding or through heightened activation of astrocytes.

Interestingly, studies show that PAE could potentially increase dopamine binding to its receptor (Converse et al., 2014). Under peripheral neuropathic conditions, it is possible dopamine receptors on spinal astocytes activate more readily facilitating heightened astrocyte activation. This would support my data that shows PAE altering astrocyte activation which is displayed only following injury. Overall, this provides a compelling rationale to further explore the effects of spinal dopamine in neuropathic pain processing in animal models of PAE.

PAE as a risk factor for development of neurodegenerative diseases

Reports demonstrate a role for the immune system during the development of neurodegenerative diseases. For example, much evidence has been published showing the involvement of T-cells during the induction of Multiple Sclerosis (MS). Using an animal model of MS called experimental autoimmune encephalomyeltisis (EAE), researchers are able to determine how the inflammatory process occurs through the development of MS. More specifically, T-helper cell 17 (Th17) as a result of IL-23 expression has a significant role in MS induction (Langrish et al., 2005). Additionally, both T-helper cell 1 as well as IL-17 aids in the induction of MS (Gocke et al., 2007; Abromson-Leeman et al., 2009).

PAE significantly alters peripheral leukocyte reactivity as well as chemokines involved in their migration (Noor et al., 2017; Sanchez et al., 2017). Additionally, PAE increases the expression of IL-17 (Pascual et al., 2017). Together, the data suggest that PAE may be a risk factor for developing MS due to the increase in expression and reactivity of T cells involved in MS.

In addition to MS, the immune system plays a major role in Alzheimer's Disease (AD). AD is thought to be a result of accumulation of both amyloid beta (Aβ) and neurofibrillary tau tangles (tau) (Hardy and Selkoe, 2002; Schöll et al., 2016). An increase in these factors correlates with cognitive decline (Brier et al., 2016; Schöll et al., 2016). Thus, much research in AD has focused on increasing clearance of Aβ and tau, but unfortunately, many of these attempts have failed.

Recent literature has focused on the role of the immune system in the development of AD. Interestingly, studies show that the complement immune pathway, which is a pathway initially involved in mediating an innate immune response, is upregulated in AD (Rogers et al., 1992). Many of the factors released from the complement pathway come from astrocytes and neurons (Levi-Strauss and Mallat, 1987). Additionally, the complement pathway factor C1q aids in neuronal atrophy through the actions of microglia (Hong et al., 2016). In addition to the complement pathway, release of IL-1β and TNFα by both astrocytes and microglia play a role in AD (Fakhoury, 2018). As discussed previously and shown in my own data, PAE primes glia resulting in heightened activation as well as increased expression of IL-1β and TNF-α. Thus, it would stand to reason that in individuals with PAE, the accumulation of Aβ and Tau

could trigger heigthened glial responses, rendering one more susceptibilty to developing AD and a more rapid and potentially more severe the progression of the disease.

Conclusions

The aim of this dissertation was to determine the effects of PAE on neuropathic pain processing. I first investigated whether the effects of PAE were lifelong. In addition, I investigated whether I could unmask the effects of PAE by significantly reducing the damage to the sciatic nerve. Interestingly, my hypothesis was supported in that only PAE rats developed allodynia following a minor CCI which coincided with astrocyte but not microglial activation. In addition to this, peripheral leukocytes from PAE rats demonstrated heigthened reactivity and expressed increased levels of IL-1β and TNFα. Together, this data demonstrated that the effects of PAE were lifelong and that immune alterations are a global effect. Consequently, I conclude that PAE increases suscpetibility to developing allodynia potentially through alterations in astrocyte mediated mechanisms.

I next evaluated whether PAE alters the proinflammatory/anti-inflammatory immune profile in order to induce suscpetibility to allodynia. Considering previous data had demonstrated that PAE alone alters LFA-1 expression, which has been shown to alter cytokine expression, I administered an LFA-1 atagonist to explore the effects on PAE induced sensitivity to light touch. Interestingly, I found that following minor CCI, increases in microglial activation, IL-1β, and CCL2 are observed in the dorsal horn spinal cord. Furthermore, TNFα was significantly

increased in PAE rats with minor CCI compared to Sac rats with minor CCI. This would suggest a potentially larger role for TNFα and should be explored further. Interestingly, when the LFA-1 antagonist, BIRT377, was adminstered i.t. allodynia was abolished and proinflammatory factors were all significantly downregulated. Curiously, clear effects between PAE and Sac rats with minor CCI were observed within the L4-L6 DRGs. Significant increases were seen in SGC activation, IL-1β expression, and blunted IL-10 expression. Interestingly, dysregulated IL-10 expression was also observed within the spinal cord. Overall, these data suggest that PAE may heighten susceptibility to developing allodynia through alteration of normal IL-10 responses in addition to enhancing proinflammatory cytokine expression within the spinal cord and DRG.

Lastly, I explored the effects of PAE on glutamate transporter function. Considering my data demonstrates astrocyte dysfunction in addition to previous data showing downregulation of GLAST expression, I examined how PAE may lead to allodynia by preventing the normal function of this transporter to occur. Strikingly, the PAE allodynic phenotype was replicated when a GLAST inhibitor was administered within the spinal cord of Sac rats with minor CCI. Additionally, PAE rats with minor CCI receiving a GLAST inhibitor demonstrated <u>potentiated</u> allodynia. While no significant differences were mesured in gene expression of glutamate transporters, increased protein levels of GLT-1 and GLAST expression in spinal cords from PAE without nerve damage was onserved. In support of GLAST dysregulation, in PAE rats with minor injury, a robust decreases in GLAST and GLT-1 protein was measured, supporting the hypothesis that

astrocytes are not capable of maintianing the demands of consistent glutamate uptake upon increased glutmate accumulation from minor peripheral nerve damage. Additionally, no significant differences as a result of PAE were seen in the neuronal specific glutamate transporter EAAC1 nor in the phosphorylation of the NMDA receptor subunit NR2B.

Overall, this data supports that in addition to the altering proinflammatory and anti-inflammatory cytokine expression, glutamate transporter function may also be altered further enhancing susceptibility to developing allodynia.

Clinical Significance

Clinical studies demonstrate that FASD children have significant immune alterations as well as increased risk for infection and susceptibility to develop autoimmune disorders (Church and Gerkin, 1988; Chiapelli and Taylor, 1995; McGill et al., 2009; Gauthier and Brown, 2017). Furthermore, FASD children (NOFAS.org) and animal models of FASD (Schneider et al., 2005) display increased sensitivity to light touch. In neuropathic pain patients, increased sensitivity to light touch, termed allodynia, is mediated through neuroimmune processing. Together, these data suggest that underlying mechanisms in FASD children may be mediated through immune alterations as a function of PAE. Therefore, investigation into the specific immune processes that occur as a consequence of PAE are important to determine . Through these studies, we have demonstrate that PAE results in life-long alterations to the immune system that are not apparent until a second insult takes place. Furthermore, we

demonstrate that specific immune factors, such as LFA-1, are altered which may result in changes in the proinflammatory/anti-inflammatory cytokine network leading to increased risk for developing neuropathological conditions. More generally, the findings from this investigation demonstrate the adverse *in utero* conditions may render one more suscueptible to developing neuropathic pain. Overall, these findings represent a novel step toward devleoping potential therapeutics for children and adults with FASD.

Future Directions

Although this investigation umasked specific effects that PAE exerts on neuroimmune functioning, and also demonstrate reversal of allodynia following LFA-1 inhibition, several questions remain regarding PAE. The specific role of the DRG in the induction of allodynia following minor CCI in PAE needs to be investigated. Whereas spinal cord data demonstrate elevated IL-1β and TNFα, the DRG presented striking differences in SGC activation, and IL-1β and IL-10 expression. Thus, it is possible that heigthened reactivity at the level of the spinal cord is mediated through amplfication of signals arriving from the DRG. I would speculate that although this may be true, astrocytes and microglia remain sensitized as a result of PAE and are key in the neuroimmune amplification of pain. Considering that SGCs are similar to astrocytes, it is possible that PAE alters both cells similarly. Furthermore, it has been demonstrated in other studies that PAE does in fact alter glial cell reactivity within the brain. Thus, it would stand to reason the glial cells within the spinal cord should demonstrate

heigthened reactivity as a result of PAE as our data demonstrate. Further exploration of this possiblity would need to done to make further conclusions.

In addition to this, IL-10 levels in response to injury are blunted both at the DRG and the spinal cord, suggesting that PAE may work primarily through decreased anti-inflammatory responses. It is also possible that a combination of increased proinflammatory responses and blunted anti-inflammatory responses could be resulting in allodynia following minor CCI. Furthermore, i.t. IL-1RA resulted in full reversal from allodynia in PAE rats, supporting the hypothesis that IL-1β is necessary for allodynia in PAE rats with CCI. Interestingly, the biggest difference was seen in the IL-10 response between Sac and PAE. It would be worth exploring whether applying a minor CCI in an IL-10 KO animals would induce allodynia similar to PAE rats, as discussed earlier. The mechanisms involved in PAE alteration of IL-10 responses needs to be further explored.

The third component of this work demonstrated a potential role for glutamate transporter in PAE induced sensitivity to light touch. Astrocyte alterations were seen in PAE rats with minor CCI, which may be a result of dysregulated GLAST expression previously demonstrated in PAE (Brolese et al., 2015). This alteration also results in increased glutamate at and around the synapse as a aconsequence of PAE, which Brolese and colleagues demonstrated (Brolese et al., 2015). Thus, it is possible that induction of allodynia following minor CCI could be a result of increased sensitivity to glutamate or exaggerated release of glutamate at the synaptic terminal. As discussed previously, the role of glutamate receptors need further investigation to

determine the potential impact that PAE exerts on glutamate release and their respective receptors following a second injury or challenge (i.e. minor CCI conditions).

Appendix A – Abbrevations and Acronyms

Aβ – amyloid beta
AMPA – α-amino-3-hydroxy-5-methyl-4-isoxazolepropionic acid receptor
ANOVA – analysis of variance
BAC – blood alcohol concentration
CCI – chronic constriction injury
CXCL – (C-X-C motif) chemokine ligand 1
CX3CL – (C-X3-C motif) chemokine ligand 1
CCL2 – (C-C motif) chemokine ligand
CCR – chemokine receptor type
CNS - central nervous system
DRG – dorsal root ganglia
EAAC1 – excitatory amino-acid carrier 1
EAAT – excitatory amino acid transporter
FAS – fetal alcohol syndrome
FASD – Fetal alcohol spectrum disorder
GFAP – glial fibrillary acific protein
GLAST – glutamate aspartate transporter
GLT-1 – glutamate transporter
Iba1 – ionized calcium-binding adaptor molecule 1
IHC – immunohistochemistry
i.v. – intravenous
i.t. – intrathecal
IL – interleukin
KO – knockout
LFA-1 – lymphocyte function associated protein 1
LPS – lipopolysaccharide
mGluR – metabotropic glutamate receptors
NMDA – N-methyl-D-aspartate receptor
NR2B – N-methyl D-aspartate receptor substype 2B
PAE – prenatal alcohol exposure
pFAS – partial fetal alcohol syndrome
SCN – sciatic nerve
SGCs - sattelite glial cells
T-cells – T-lymphocytes
TH – Thelper
TNFα – tumor necrosis factor α
WT – wild type
Qrt-PCR – reverse transcription polymerase chain reaction

References

Abrahamsen B, Schneider N, Erichsen MN, Huynh TH, Fahlke C, Bunch L, Jensen AA (2013) Allosteric modulation of an excitatory amino acid transporter: the subtype-selective inhibitor UCPH-101 exerts sustained inhibition of EAAT1 through an intramonomeric site in the trimerization domain. Journal of Neuroscience 33:1068-1087.

Abromson-Leeman S, Bronson RT, Dorf ME (2009) Encephalitogenic T cells that stably express both T-bet and RORγt consistently produce IFNγ but have a spectrum of IL-17 profiles. Journal of neuroimmunology 215:10-24.

Ahluwalia B, Wesley B, Adeyiga O, Smith DM, Da-Silva A, Rajguru S (2000) Alcohol modulates cytokine secretion and synthesis in human fetus: an in vivo and in vitro study. Alcohol 21:207-213.

Akers KG, Martinez-Canabal A, Restivo L, Yiu AP, De Cristofaro A, Hsiang H-LL, Wheeler AL, Guskjolen A, Niibori Y, Shoji H (2014) Hippocampal neurogenesis regulates forgetting during adulthood and infancy. Science 344:598-602.

Akimoto N, Honda K, Uta D, Beppu K, Ushijima Y, Matsuzaki Y, Nakashima S, Kido M, Imoto K, Takano Y (2013) CCL-1 in the spinal cord contributes to neuropathic pain induced by nerve injury. Cell death & disease 4:e679.

Akiyama H, Kawamata T, Yamada T, Tooyama I, Ishii T, McGeer PL (1993) Expression of intercellular adhesion molecule (ICAM)-1 by a subset of astrocytes in Alzheimer disease and some other degenerative neurological disorders. Acta neuropathologica 85:628-634.

Alfonso-Loeches S, Guerri C (2011) Molecular and behavioral aspects of the actions of alcohol on the adult and developing brain. Critical reviews in clinical laboratory sciences 48:19-47.

Altier N, Stewart J (1999) The role of dopamine in the nucleus accumbens in analgesia. Life sciences 65:2269-2287.

Anneser JM, Chahli C, Ince PG, Borasio GD, Shaw PJ (2004) Glial proliferation and metabotropic glutamate receptor expression in amyotrophic lateral sclerosis. Journal of Neuropathology & Experimental Neurology 63:831-840.

Arjona A, Boyadjieva N, Kuhn P, Sarkar DK (2006) Fetal Ethanol Exposure Disrupts the Daily Rhythms of Splenic Granzyme B, IFN-γ, and NK Cell Cytotoxicity in Adulthood. Alcoholism: Clinical and Experimental Research 30:1039-1044.

Astley SJ, Magnuson SI, Omnell LM, Clarren SK (1999) Fetal alcohol syndrome: changes in craniofacial form with age, cognition, and timing of ethanol exposure in the macaque. Teratology 59:163-172.

Bailey BN, Delaney-Black V, Covington CY, Ager J, Janisse J, Hannigan JH, Sokol RJ (2004) Prenatal exposure to binge drinking and cognitive and behavioral outcomes at age 7 years. American journal of obstetrics and gynecology 191:1037-1043.

Barteneva NS, Fasler-Kan E, Vorobjev IA (2012) Imaging flow cytometry: coping with heterogeneity in biological systems. Journal of Histochemistry & Cytochemistry 60:723-733.

Basham KB, Whitmore SP, Adcock AF, Basta PV (1998) Chronic and acute prenatal and postnatal ethanol exposure on lymphocyte subsets from offspring thymic, splenic, and intestinal intraepithelial sources. Alcoholism: Clinical and Experimental Research 22:1501-1508.

Bennett GJ, Xie Y-K (1988) A peripheral mononeuropathy in rat that produces disorders of pain sensation like those seen in man. Pain 33:87-107.

Bennett ML, Bennett FC, Liddelow SA, Ajami B, Zamanian JL, Fernhoff NB, Mulinyawe SB, Bohlen CJ, Adil A, Tucker A (2016) New tools for studying microglia in the mouse and human CNS. Proceedings of the National Academy of Sciences 113:E1738-E1746.

Bird CW, Candelaria-Cook FT, Magcalas CM, Davies S, Valenzuela CF, Savage DD, Hamilton DA (2015) Moderate prenatal alcohol exposure enhances GluN2B containing NMDA receptor binding and ifenprodil sensitivity in rat agranular insular cortex. PloS one 10:e0118721.

Blumensohn R, Ringler D, Eli I (2002) Pain perception in patients with schizophrenia. The Journal of nervous and mental disease 190:481-483.

Bodnar TS, Hill LA, Weinberg J (2016) Evidence for an immune signature of prenatal alcohol exposure in female rats. Brain, behavior, and immunity 58:130-141.

Boschen K, Klintsova A (2017) Chapter Nine-Neurotrophins in the Brain: Interaction With Alcohol Exposure During Development. Vitamins and Hormones 104:197-242.

Brady ML, Allan AM, Caldwell KK (2012) A limited access mouse model of prenatal alcohol exposure that produces long-lasting deficits in hippocampal-dependent learning and memory. Alcoholism: Clinical and Experimental Research 36:457-466.

Brady ML, Diaz MR, Iuso A, Everett JC, Valenzuela CF, Caldwell KK (2013) Moderate prenatal alcohol exposure reduces plasticity and alters NMDA receptor subunit composition in the dentate gyrus. Journal of Neuroscience 33:1062-1067.

Braz J, Solorzano C, Wang X, Basbaum AI (2014) Transmitting pain and itch messages: a contemporary view of the spinal cord circuits that generate gate control. Neuron 82:522-536.

Brier MR, Gordon B, Friedrichsen K, McCarthy J, Stern A, Christensen J, Owen C, Aldea P, Su Y, Hassenstab J (2016) Tau and Aβ imaging, CSF measures, and cognition in Alzheimer's disease. Science translational medicine 8:338ra366-338ra366.

Brolese G, Lunardi P, de Souza DF, Lopes FM, Leite MC, Gonçalves C-A (2015) Pre-and postnatal exposure to moderate levels of ethanol can have long-lasting effects on hippocampal glutamate uptake in adolescent offspring. PLoS One 10:e0127845.

Burd L, Blair J, Dropps K (2012) Prenatal alcohol exposure, blood alcohol concentrations and alcohol elimination rates for the mother, fetus and newborn. Journal of Perinatology 32:652.

Calvo M, Dawes JM, Bennett DL (2012) The role of the immune system in the generation of neuropathic pain. The lancet neurology 11:629-642.

Cao L, DeLeo JA (2008) CNS-infiltrating CD4+ T lymphocytes contribute to murine spinal nerve transection-induced neuropathic pain. European journal of immunology 38:448-458.

Carlton SM, Hargett GL (2007) Colocalization of metabotropic glutamate receptors in rat dorsal root ganglion cells. Journal of Comparative Neurology 501:780-789.

Carrasquillo Y, Gereau RW (2007) Activation of the extracellular signal-regulated kinase in the amygdala modulates pain perception. Journal of Neuroscience 27:1543-1551.

Carvajal AG, Gazeau P, Hillion S, Daïen CI, Cornec DY (2017) Could Lymphocyte Profiling be Useful to Diagnose Systemic Autoimmune Diseases? Clinical reviews in allergy & immunology.

Castany S, Gris G, Vela JM, Verdú E, Boadas-Vaello P (2018) Critical role of sigma-1 receptors in central neuropathic pain-related behaviours after mild spinal cord injury in mice. Scientific reports 8:3873.

Chasnoff IJ, Wells AM, King L (2015) Misdiagnosis and missed diagnoses in foster and adopted children with prenatal alcohol exposure. Pediatrics:peds. 2014-2171.

Chen G, Park C-K, Xie R-G, Berta T, Nedergaard M, Ji R-R (2014) Connexin-43 induces chemokine release from spinal cord astrocytes to maintain late-phase neuropathic pain in mice. Brain 137:2193-2209.

Chiapelli F, Taylor AN (1995) The fetal alcohol syndrome and fetal alcohol effects on immune competence. Alcohol and Alcoholism 30:259-263.

Chiechio S, Caricasole A, Barletta E, Storto M, Catania M, Copani A, Vertechy M, Nicolai R, Calvani M, Melchiorri D (2002) L-Acetylcarnitine induces analgesia by selectively up-regulating mGlu2 metabotropic glutamate receptors. Molecular pharmacology 61:989-996.

Choi IY, Allan AM, Cunningham LA (2005) Moderate fetal alcohol exposure impairs the neurogenic response to an enriched environment in adult mice. Alcoholism: Clinical and Experimental Research 29:2053-2062.

Church M, Gerkin K (1988) Hearing disorders in children with fetal alcohol syndrome: findings from case reports. Pediatrics 82:147-154.

Converse AK, Moore CF, Holden JE, Ahlers EO, Moirano JM, Larson JA, Resch LM, DeJesus OT, Barnhart TE, Nickles RJ (2014) Moderate-Level Prenatal Alcohol Exposure Induces Sex Differences in Dopamine D1 Receptor Binding in Adult Rhesus Monkeys. Alcoholism: Clinical and Experimental Research 38:2934-2943.

Costa FAL, Moreira Neto FL (2015) Satellite glial cells in sensory ganglia: its role in pain. Revista brasileira de anestesiologia 65:73-81.

Costigan M, Scholz J, Woolf CJ (2009a) Neuropathic pain: a maladaptive response of the nervous system to damage. Annual review of neuroscience 32:1-32.

Costigan M, Moss A, Latremoliere A, Johnston C, Verma-Gandhu M, Herbert TA, Barrett L, Brenner GJ, Vardeh D, Woolf CJ (2009b) T-cell infiltration and signaling in the adult dorsal spinal cord is a major contributor to neuropathic pain-like hypersensitivity. Journal of Neuroscience 29:14415-14422.

D'mello R, Dickenson A (2008) Spinal cord mechanisms of pain. British journal of anaesthesia 101:8-16.

Danbolt NC (2001) Glutamate uptake. Progress in neurobiology 65:1-105.

Dengler EC, Alberti LA, Bowman BN, Kerwin AA, Wilkerson JL, Moezzi DR, Limanovich E, Wallace JA, Milligan ED (2014) Improvement of spinal non-viral IL-10 gene delivery by D-mannose as a transgene adjuvant to control chronic neuropathic pain. Journal of neuroinflammation 11:92.

DeVito WJ, Stone S (2001) Prenatal exposure to ethanol alters the neuroimmune response to a central nervous system wound in the adult rat. Alcohol 25:39-47.

Drew PD, Kane CJ (2014) Fetal alcohol spectrum disorders and neuroimmune changes. International review of neurobiology 118:41.

Drouin-Ouellet J, Brownell AL, Saint-Pierre M, Fasano C, Emond V, Trudeau LE, Lévesque D, Cicchetti F (2011) Neuroinflammation is associated with changes in glial mGluR5 expression and the development of neonatal excitotoxic lesions. Glia 59:188-199.

Dumont AO, Goursaud S, Desmet N, Hermans E (2014) Differential regulation of glutamate transporter subtypes by pro-inflammatory cytokine TNF-α in cortical astrocytes from a rat model of amyotrophic lateral sclerosis. PLoS One 9:e97649.

Dustin ML, Springer TA (1988) Lymphocyte function-associated antigen-1 (LFA-1) interaction with intercellular adhesion molecule-1 (ICAM-1) is one of at least three mechanisms for lymphocyte adhesion to cultured endothelial cells. The Journal of Cell Biology 107:321-331.

Dworkin RH, Backonja M, Rowbotham MC, Allen RR, Argoff CR, Bennett GJ, Bushnell MC, Farrar JT, Galer BS, Haythornthwaite JA (2003) Advances in neuropathic pain: diagnosis, mechanisms, and treatment recommendations. Archives of neurology 60:1524-1534.

Emoto M, Emoto Y, Brinkmann V, Miyamoto M, Yoshizawa I, Stäber M, van Rooijen N, Hamann A, Kaufmann SH (2003) Increased resistance of LFA-1-deficient mice to lipopolysaccharide-induced shock/liver injury in the presence of TNF-α and IL-12 is mediated by IL-10: a novel role for LFA-1 in the regulation of the proinflammatory and anti-inflammatory cytokine balance. The Journal of Immunology 171:584-593.

Evans BJ, McDowall A, Taylor PC, Hogg N, Haskard DO, Landis RC (2006) Shedding of lymphocyte function–associated antigen-1 (LFA-1) in a human inflammatory response. Blood 107:3593-3599.

Fakhoury M (2018) Microglia and Astrocytes in Alzheimer's Disease: Implications for Therapy. Current neuropharmacology 16:508-518.

Falgreen Eriksen HL, Mortensen EL, Kilburn T, Underbjerg M, Bertrand J, Støvring H, Wimberley T, Grove J, Kesmodel US (2012) The effects of low to moderate prenatal alcohol exposure in early pregnancy on IQ in 5-year-old children. BJOG: An International Journal of Obstetrics & Gynaecology 119:1191-1200.

Fehniger TA, Cooper MA, Nuovo GJ, Cella M, Facchetti F, Colonna M, Caligiuri MA (2003) CD56 bright natural killer cells are present in human lymph nodes and are activated by T cell–derived IL-2: a potential new link between adaptive and innate immunity. Blood 101:3052-3057.

Franke H, Verkhratsky A, Burnstock G, Illes P (2012) Pathophysiology of astroglial purinergic signalling. Purinergic signalling 8:629-657.

Franklin L, Deitz J, Jirikowic T, Astley S (2008) Children with fetal alcohol spectrum disorders: problem behaviors and sensory processing. American Journal of Occupational Therapy 62:265-273.

Furuta A, Rothstein JD, Martin LJ (1997) Glutamate transporter protein subtypes are expressed differentially during rat CNS development. Journal of Neuroscience 17:8363-8375.

Galindo R, Frausto S, Wolff C, Caldwell KK, Perrone-Bizzozero NI, Savage DD (2004) Prenatal ethanol exposure reduces mGluR5 receptor number and function in the dentate gyrus of adult offspring. Alcoholism: Clinical and Experimental Research 28:1587-1597.

Gallo A, Leerink M, Michot B, Ahmed E, Forget P, Mouraux A, Hermans E, Deumens R (2017) Bilateral tactile hypersensitivity and neuroimmune responses after spared nerve injury in mice lacking vasoactive intestinal peptide. Experimental Neurology 293:62-73.

Gangisetty O, Wynne O, Jabbar S, Nasello C, Sarkar DK (2015) Fetal alcohol exposure reduces dopamine receptor D2 and increases pituitary weight and prolactin production via epigenetic mechanisms. PloS one 10:e0140699.

Gao Y-J, Xu Z-Z, Liu Y-C, Wen Y-R, Decosterd I, Ji R-R (2010a) The c-Jun N-terminal kinase 1 (JNK1) in spinal astrocytes is required for the maintenance of bilateral mechanical allodynia under a persistent inflammatory pain condition. Pain 148:309-319.

Gao YJ, Zhang L, Ji RR (2010b) Spinal injection of TNF-α-activated astrocytes produces persistent pain symptom mechanical allodynia by releasing monocyte chemoattractant protein-1. Glia 58:1871-1880.

Gaudet AD, Popovich PG, Ramer MS (2011) Wallerian degeneration: gaining perspective on inflammatory events after peripheral nerve injury. Journal of neuroinflammation 8:110.

Gauthier TW, Brown LAS (2017) In utero alcohol effects on foetal, neonatal and childhood lung disease. Paediatric respiratory reviews 21:34-37.

George A, Schmidt C, Weishaupt A, Toyka KV, Sommer C (1999) Serial determination of tumor necrosis factor-alpha content in rat sciatic nerve after chronic constriction injury. Experimental neurology 160:124-132.

Ghasemlou N, Chiu IM, Julien J-P, Woolf CJ (2015) CD11b+ Ly6G− myeloid cells mediate mechanical inflammatory pain hypersensitivity. Proceedings of the National Academy of Sciences 112:E6808-E6817.

Giuffrida R, Vingerhoets F, Bogousslavsky J, Ghika J (2005) Pain in Parkinson's disease. Revue neurologique 161:407-418.

Gluckman PD, Hanson MA, Cooper C, Thornburg KL (2008) Effect of in utero and early-life conditions on adult health and disease. New England Journal of Medicine 359:61-73.

Gocke AR, Cravens PD, Ben L-H, Hussain RZ, Northrop SC, Racke MK, Lovett-Racke AE (2007) T-bet regulates the fate of Th1 and Th17 lymphocytes in autoimmunity. The Journal of Immunology 178:1341-1348.

Grace PM, Hutchinson MR, Maier SF, Watkins LR (2014) Pathological pain and the neuroimmune interface. Nature Reviews Immunology 14:217-231.

Gravett MG, Rubens CE, Nunes TM (2010) Global report on preterm birth and stillbirth (2 of 7): discovery science. BMC pregnancy and childbirth 10:S2.

Grubbs FE (1950) Sample criteria for testing outlying observations. The Annals of Mathematical Statistics:27-58.

Hailer NP, Bechmann I, Heizmann S, Nitsch R (1997) Adhesion molecule expression on phagocytic microglial cells following anterograde degeneration of perforant path axons. Hippocampus 7:341-349.

Hanani M (2005) Satellite glial cells in sensory ganglia: from form to function. Brain research reviews 48:457-476.

Hardy J, Selkoe DJ (2002) The amyloid hypothesis of Alzheimer's disease: progress and problems on the road to therapeutics. science 297:353-356.

Harrell MI, Iritani BM, Ruddell A (2008) Lymph node mapping in the mouse. Journal of immunological methods 332:170-174.

Hashizume H, DeLeo JA, Colburn RW, Weinstein JN (2000) Spinal glial activation and cytokine expression after lumbar root injury in the rat. Spine 25:1206-1217.

Hideshima T, Chauhan D, Schlossman R, Richardson P, Anderson KC (2001) The role of tumor necrosis factor α in the pathophysiology of human multiple myeloma: therapeutic applications. Oncogene 20:4519.

Hofman PL, Regan F, Jackson WE, Jefferies C, Knight DB, Robinson EM, Cutfield WS (2004) Premature birth and later insulin resistance. New England Journal of Medicine 351:2179-2186.

Hong S, Beja-Glasser VF, Nfonoyim BM, Frouin A, Li S, Ramakrishnan S, Merry KM, Shi Q, Rosenthal A, Barres BA (2016) Complement and microglia mediate early synapse loss in Alzheimer mouse models. Science 352:712-716.

Hoyme HE, Kalberg WO, Elliott AJ, Blankenship J, Buckley D, Marais A-S, Manning MA, Robinson LK, Adam MP, Abdul-Rahman O (2016) Updated clinical guidelines for diagnosing fetal alcohol spectrum disorders. Pediatrics:e20154256.

Huang L-E, Guo S-H, Thitiseranee L, Yang Y, Zhou Y-F, Yao Y-X (2018) N-methyl D-aspartate receptor subtype 2B antagonist, Ro 25-6981,

attenuates neuropathic pain by inhibiting postsynaptic density 95 expression. Scientific reports 8:7848.

Hucho T, Levine JD (2007) Signaling pathways in sensitization: toward a nociceptor cell biology. Neuron 55:365-376.

Ito D, Tanaka K, Suzuki S, Dembo T, Fukuuchi Y (2001) Enhanced expression of Iba1, ionized calcium-binding adapter molecule 1, after transient focal cerebral ischemia in rat brain. Stroke 32:1208-1215.

Jäger A, Kuchroo VK (2010) Effector and Regulatory T-cell Subsets in Autoimmunity and Tissue Inflammation. Scandinavian journal of immunology 72:173-184.

Janeway CA, Travers P, Walport M, Shlomchik M (2017) Immunobiology: the immune system in health and disease. 2005. New York: Garland Science 6.

Jantzie LL, Corbett CJ, Berglass J, Firl DJ, Flores J, Mannix R, Robinson S (2014) Complex pattern of interaction between in utero hypoxia-ischemia and intra-amniotic inflammation disrupts brain development and motor function. Journal of neuroinflammation 11:131.

Jantzie LL, Talos DM, Jackson MC, Park H-K, Graham DA, Lechpammer M, Folkerth RD, Volpe JJ, Jensen FE (2013) Developmental expression of N-methyl-D-aspartate (NMDA) receptor subunits in human white and gray matter: potential mechanism of increased vulnerability in the immature brain. Cerebral cortex 25:482-495.

Jatana S, Palmer BC, Phelan SJ, Gelein R, DeLouise LA (2017) In vivo quantification of quantum dot systemic transport in C57BL/6 hairless mice following skin application post-ultraviolet radiation. Particle and fibre toxicology 14:12.

Jerrells TR, Weinberg J (1998) Influence of ethanol consumption on immune competence of adult animals exposed to ethanol in utero. Alcoholism: Clinical and Experimental Research 22:391-400.

Ji X-T, Qian N-S, Zhang T, Li J-M, Li X-K, Wang P, Zhao D-S, Huang G, Zhang L, Fei Z (2013) Spinal astrocytic activation contributes to mechanical allodynia in a rat chemotherapy-induced neuropathic pain model. PLoS One 8:e60733.

Jiang B-C, He L-N, Wu X-B, Shi H, Zhang W-W, Zhang Z-J, Cao D-L, Li C-H, Gu J, Gao Y-J (2016) Promoted interaction of C/EBPα with demethylated Cxcr3 gene promoter contributes to neuropathic pain in mice. Journal of Neuroscience:2262-2216.

Jirikowic T, Olson HC, Kartin D (2008) Sensory processing, school performance, and adaptive behavior of young school-age children with fetal alcohol spectrum disorders. Physical & occupational therapy in pediatrics 28:117-136.

Johnson S, Knight R, Marmer DJ, Steele RW (1981) Immune deficiency in fetal alcohol syndrome. Pediatric research 15:908-911.

Jones K, Smith D (1973) Recognition of the fetal alcohol syndrome in early infancy. The Lancet 302:999-1001.

Kane CJ, Phelan KD, Han L, Smith RR, Xie J, Douglas JC, Drew PD (2011) Protection of neurons and microglia against ethanol in a mouse model of fetal alcohol spectrum disorders by peroxisome proliferator-activated receptor-γ agonists. Brain, behavior, and immunity 25:S137-S145.

Kato H, Narita M, Miyatake M, Yajima Y, Suzuki T (2006) Role of neuronal NR2B subunit-containing NMDA receptor-mediated Ca2+ influx and astrocytic activation in cultured mouse cortical neurons and astrocytes. Synapse 59:10-17.

Kelly SJ, Leggett DC, Cronise K (2009) Sexually dimorphic effects of alcohol exposure during development on the processing of social cues. Alcohol & Alcoholism 44:555-560.

Kelly YJ, Sacker A, Gray R, Kelly J, Wolke D, Head J, Quigley MA (2010) Light drinking during pregnancy: still no increased risk for socioemotional difficulties or cognitive deficits at 5 years of age? Journal of Epidemiology & Community Health:jech. 2009.103002.

Kettenmann H, Hanisch U-K, Noda M, Verkhratsky A (2011) Physiology of microglia. Physiological reviews 91:461-553.

Khan J, Ramadan K, Korczeniewska O, Anwer MM, Benoliel R, Eliav E (2015) Interleukin-10 levels in rat models of nerve damage and neuropathic pain. Neuroscience letters 592:99-106.

Kim YS, Jung HM, Yoon B-E (2018) Exploring glia to better understand Alzheimer's disease. Animal Cells and Systems 22:213-218.

Korn T, Oukka M, Kuchroo V, Bettelli E (2007) Th17 cells: effector T cells with inflammatory properties. In: Seminars in immunology, pp 362-371: Elsevier.

Krebs C, Fernandes HB, Sheldon C, Raymond LA, Baimbridge KG (2003) Functional NMDA receptor subtype 2B is expressed in astrocytes after ischemia in vivo and anoxia in vitro. Journal of Neuroscience 23:3364-3372.

Kugler P, Schleyer V (2004) Developmental expression of glutamate transporters and glutamate dehydrogenase in astrocytes of the postnatal rat hippocampus. Hippocampus 14:975-985.

Labuda T, Wendt J, Hedlund G, Dohlsten M (1998) ICAM-1 costimulation induces IL-2 but inhibits IL-10 production in superantigen-activated human CD4+ T cells. Immunology 94:496.

Lam NCK, Ornatowski W, Alberti LB, Wilkerson JL, Moezzi D, Tuffli K, Sun MS, Contri SD, Bowman BN, Wallace JA, Anderson T, Norenberg JP, Hoppin J, Milligan ED (2014) The role of leukocyte accumulation and diminshed spinal IL-10 expression in chronic neuropathy. In.

Lange S, Rehm J, Bekmuradov D, Mihic A, Popova S (2012) RISK OF INCARCERATION FOR INDIVIDUALS WITH PRENATAL ALCOHOL EXPOSURE. In: American Journal of Epidemiology, pp 80-80: OXFORD UNIV PRESS INC JOURNALS DEPT, 2001 EVANS RD, CARY, NC 27513 USA.

Langrish CL, Chen Y, Blumenschein WM, Mattson J, Basham B, Sedgwick JD, McClanahan T, Kastelein RA, Cua DJ (2005) IL-23 drives a pathogenic T

cell population that induces autoimmune inflammation. Journal of Experimental Medicine 201:233-240.

Larkby CA, Goldschmidt L, Hanusa BH, Day NL (2011) Prenatal alcohol exposure is associated with conduct disorder in adolescence: findings from a birth cohort. Journal of the American Academy of Child & Adolescent Psychiatry 50:262-271.

Latremoliere A, Woolf CJ (2009) Central sensitization: a generator of pain hypersensitivity by central neural plasticity. The journal of pain 10:895-926.

Lee SJ, Drabik K, Van Wagoner NJ, Lee S, Choi C, Dong Y, Benveniste EN (2000) ICAM-1-induced expression of proinflammatory cytokines in astrocytes: involvement of extracellular signal-regulated kinase and p38 mitogen-activated protein kinase pathways. The Journal of Immunology 165:4658-4666.

Levi-Strauss M, Mallat M (1987) Primary cultures of murine astrocytes produce C3 and factor B, two components of the alternative pathway of complement activation. The Journal of Immunology 139:2361-2366.

Li G, Xiao Y, Estrella JL, Ducsay CA, Gilbert RD, Zhang L (2003) Effect of fetal hypoxia on heart susceptibility to ischemia and reperfusion injury in the adult rat. Journal of the Society for Gynecologic Investigation 10:265-274.

Lindborg JA, Niemi JP, Howarth MA, Liu KW, Moore CZ, Mahajan D, Zigmond RE (2018) Molecular and cellular identification of the immune response in peripheral ganglia following nerve injury. Journal of neuroinflammation 15:192.

Lindia JA, McGowan E, Jochnowitz N, Abbadie C (2005) Induction of CX3CL1 expression in astrocytes and CX3CR1 in microglia in the spinal cord of a rat model of neuropathic pain. The Journal of Pain 6:434-438.

Liu X, Tian Y, Lu N, Gin T, Cheng CH, Chan MT (2013) Stat3 inhibition attenuates mechanical allodynia through transcriptional regulation of chemokine expression in spinal astrocytes. PLoS One 8:e75804.

Livak KJ, Schmittgen TD (2001) Analysis of relative gene expression data using real-time quantitative PCR and the $2^{-\Delta\Delta CT}$ method. methods 25:402-408.

Lohmann C, Kessels HW (2014) The developmental stages of synaptic plasticity. The Journal of physiology 592:13-31.

Mamluk L, Edwards HB, Savović J, Leach V, Jones T, Moore TH, Ijaz S, Lewis SJ, Donovan JL, Lawlor D (2017) Low alcohol consumption and pregnancy and childhood outcomes: time to change guidelines indicating apparently 'safe'levels of alcohol during pregnancy? A systematic review and meta-analyses. BMJ open 7:e015410.

Marin I, Kipnis J (2013) Learning and memory… and the immune system. Learning & memory 20:601-606.

Marlin SD, Springer TA (1987) Purified intercellular adhesion molecule-1 (ICAM-1) is a ligand for lymphocyte function-associated antigen 1 (LFA-1). Cell 51:813-819.

Martín-Fontecha A, Lanzavecchia A, Sallusto F (2009) Dendritic cell migration to peripheral lymph nodes. In: Dendritic Cells, pp 31-49: Springer.

Martín-Fontecha A, Thomsen LL, Brett S, Gerard C, Lipp M, Lanzavecchia A, Sallusto F (2004) Induced recruitment of NK cells to lymph nodes provides IFN-γ for TH1 priming. Nature immunology 5:1260-1265.

Masliah E, Hansen L, Alford M, Deteresa R, Mallory M (1996) Deficient glutamate tranport is associated with neurodegeneration in Alzheimer's disease. Annals of Neurology: Official Journal of the American Neurological Association and the Child Neurology Society 40:759-766.

Masu M, Tanabe Y, Tsuchida K, Shigemoto R, Nakanishi S (1991) Sequence and expression of a metabotropic glutamate receptor. Nature 349:760.

Mattson SN, Riley EP, Gramling L, Delis DC, Jones KL (1998) Neuropsychological comparison of alcohol-exposed children with or without physical features of fetal alcohol syndrome. Neuropsychology 12:146.

Maxwell JR, Denson JL, Joste NE, Robinson S, Jantzie LL (2015) Combined in utero hypoxia-ischemia and lipopolysaccharide administration in rats induces chorioamnionitis and a fetal inflammatory response syndrome. Placenta 36:1378-1384.

May PA, Baete A, Russo J, Elliott AJ, Blankenship J, Kalberg WO, Buckley D, Brooks M, Hasken J, Abdul-Rahman O (2014) Prevalence and characteristics of fetal alcohol spectrum disorders. Pediatrics:peds. 2013-3319.

McFarlin BK, Gary MA (2017) Flow cytometry what you see matters: Enhanced clinical detection using image-based flow cytometry. Methods 112:1-8.

McGee D, Bamberg T, Vitkus S, McGhee J (1995) A synergistic relationship between TNF-alpha, IL-1 beta, and TGF-beta 1 on IL-6 secretion by the IEC-6 intestinal epithelial cell line. Immunology 86:6.

McGill J, Meyerholz DK, Edsen-Moore M, Young B, Coleman RA, Schlueter AJ, Waldschmidt TJ, Cook RT, Legge KL (2009) Fetal exposure to ethanol has long-term effects on the severity of influenza virus infections. The Journal of Immunology 182:7803-7808.

Megat S, Shiers S, Moy JK, Barragan-Iglesias P, Pradhan G, Seal RP, Dussor G, Price TJ (2018) A critical role for dopamine D5 receptors in pain chronicity in male mice. Journal of Neuroscience 38:379-397.

Mellios N, Woodson J, Garcia RI, Crawford B, Sharma J, Sheridan SD, Haggarty SJ, Sur M (2014) β2-Adrenergic receptor agonist ameliorates phenotypes and corrects microRNA-mediated IGF1 deficits in a mouse model of Rett syndrome. Proceedings of the National Academy of Sciences:201309426.

Millan MJ (2002) Descending control of pain. Progress in neurobiology 66:355-474.

Milligan ED, Watkins LR (2009) Pathological and protective roles of glia in chronic pain. Nature reviews neuroscience 10:23-36.

Milligan ED, Twining C, Chacur M, Biedenkapp J, O'Connor K, Poole S, Tracey K, Martin D, Maier SF, Watkins LR (2003) Spinal glia and proinflammatory cytokines mediate mirror-image neuropathic pain in rats. Journal of Neuroscience 23:1026-1040.

Milligan ED, Langer SJ, Sloane EM, He L, Wieseler-Frank J, O'connor K, Martin D, Forsayeth JR, Maier SF, Johnson K (2005) Controlling pathological pain by adenovirally driven spinal production of the anti-inflammatory cytokine, interleukin-10. European Journal of Neuroscience 21:2136-2148.

Mogil JS, Sternberg WF, Kest B, Marek P, Liebeskind JC (1993) Sex differences in the antagonism of swim stress-induced analgesia: effects of gonadectomy and estrogen replacement. Pain 53:17-25.

Mohajerani MH, Cherubini E (2006) Role of giant depolarizing potentials in shaping synaptic currents in the developing hippocampus. Critical Reviews™ in Neurobiology 18.

Montana M, Gereau R (2011) Metabotropic glutamate receptors as targets for analgesia: antagonism, activation, and allosteric modulation. Current pharmaceutical biotechnology 12:1681-1688.

Morse BA, Cermak SA (1994) Sensory processing in children with Fetal Alcohol Syndrome. Alcoholism: Clinical and Experimental Research 18.

Moscatello K, Biber K, Jennings S, Chervenak R, Wolcott R (1999) Effects ofin UteroAlcohol Exposure on B Cell Development in Neonatal Spleen and Bone Marrow. Cellular immunology 191:124-130.

Muggli E, Matthews H, Penington A, Claes P, O'leary C, Forster D, Donath S, Anderson PJ, Lewis S, Nagle C (2017) Association between prenatal alcohol exposure and craniofacial shape of children at 12 months of age. JAMA pediatrics 171:771-780.

Murray J, Burgess S, Zuccolo L, Hickman M, Gray R, Lewis SJ (2016) Moderate alcohol drinking in pregnancy increases risk for children's persistent conduct problems: causal effects in a Mendelian randomisation study. Journal of child psychology and psychiatry 57:575-584.

Nagatomo K, Suga S, Saitoh M, Kogawa M, Kobayashi K, Yamamoto Y, Yamada K (2017) Dopamine D1 receptor immunoreactivity on fine processes of GFAP-positive astrocytes in the substantia nigra pars reticulata of adult mouse. Frontiers in neuroanatomy 11:3.

Nascimento DSM, Castro-Lopes JM, Neto FLM (2014) Satellite glial cells surrounding primary afferent neurons are activated and proliferate during monoarthritis in rats: is there a role for ATF3? PloS one 9:e108152.

Noor S, Milligan ED (2018) Life-long Impacts of Moderate Prenatal Alcohol Exposure (PAE) on Neuro-immune Function. Frontiers in immunology 9:1107.

Noor S, Sanchez JJ, Vanderwall AG, Sun MS, Maxwell JR, Davies S, Jantzie LL, Petersen TR, Savage DD, Milligan ED (2017) Prenatal alcohol exposure potentiates chronic neuropathic pain, spinal glial and immune cell activation and alters sciatic nerve and DRG cytokine levels. Brain, Behavior, and Immunity 61:80-95.

Norman DC, Chang MP, Wong CM, Branch BJ, Castle S, Taylor AN (1991) Changes with age in the proliferative response of splenic T cells from rats exposed to ethanol in utero. Alcoholism: Clinical and Experimental Research 15:428-432.

O'Callaghan FV, O'Callaghan M, Najman JM, Williams GM, Bor W (2007) Prenatal alcohol exposure and attention, learning and intellectual ability at 14 years: a prospective longitudinal study. Early human development 83:115-123.

O'Leary-Moore SK, McMechan AP, Mathison SN, Berman RF, Hannigan JH (2006) Reversal learning after prenatal or early postnatal alcohol exposure in juvenile and adult rats. Alcohol 38:99-110.

O'Malley KD (2007) ADHD and fetal alcohol spectrum disorders (FASD): Nova Publishers.

Okuse K (2007) Pain signalling pathways: from cytokines to ion channels. The international journal of biochemistry & cell biology 39:490-496.

Ostermann G, Weber KS, Zernecke A, Schröder A, Weber C (2002) JAM-1 is a ligand of the β 2 integrin LFA-1 involved in transendothelial migration of leukocytes. Nature immunology 3:151.

Pascual M, Montesinos J, Montagud-Romero S, Forteza J, Rodríguez-Arias M, Miñarro J, Guerri C (2017) TLR4 response mediates ethanol-induced neurodevelopment alterations in a model of fetal alcohol spectrum disorders. Journal of neuroinflammation 14:145.

Perry VH, Teeling J (2013) Microglia and macrophages of the central nervous system: the contribution of microglia priming and systemic inflammation to chronic neurodegeneration. In: Seminars in immunopathology, pp 601-612: Springer.

Popova S, Lange S, Probst C, Gmel G, Rehm J (2017) Estimation of national, regional, and global prevalence of alcohol use during pregnancy and fetal alcohol syndrome: a systematic review and meta-analysis. The Lancet Global Health 5:e290-e299.

Potvin S, Grignon S, Marchand S (2009) Human evidence of a supra-spinal modulating role of dopamine on pain perception. Synapse 63:390-402.

Prasad S, Hu S, Sheng WS, Chauhan P, Singh A, Lokensgard JR (2017) The PD-1: PD-L1 pathway promotes development of brain-resident memory T cells following acute viral encephalitis. Journal of neuroinflammation 14:82.

Prinz M, Priller J (2017) The role of peripheral immune cells in the CNS in steady state and disease. Nature neuroscience 20:136.

Prochazka A, Mushahwar V (2001) Spinal Cord Function and Rehabilitation-an Overview. The Journal of physiology 533:3-4.

Reid N, Dawe S, Shelton D, Harnett P, Warner J, Armstrong E, LeGros K, O'callaghan F (2015) Systematic review of fetal alcohol spectrum disorder interventions across the life span. Alcoholism: Clinical and Experimental Research 39:2283-2295.

Riley EP, Infante MA, Warren KR (2011) Fetal alcohol spectrum disorders: an overview. Neuropsychology review 21:73.

Roberson R, Kuddo T, Benassou I, Abebe D, Spong C (2011) Neuroprotective fractalkine in fetal alcohol syndrome. American journal of obstetrics and gynecology 204:400. e401-400. e403.

Robinson M, Oddy W, McLean N, Jacoby P, Pennell C, De Klerk N, Zubrick S, Stanley F, Newnham J (2010) Low–moderate prenatal alcohol exposure

and risk to child behavioural development: a prospective cohort study. BJOG: An International Journal of Obstetrics & Gynaecology 117:1139-1152.

Robinson S, Berglass JB, Denson JL, Berkner J, Anstine CV, Winer JL, Maxwell JR, Qiu J, Yang Y, Sillerud LO (2017) Microstructural and microglial changes after repetitive mild traumatic brain injury in mice. Journal of neuroscience research 95:1025-1035.

Rogers J, Cooper NR, Webster S, Schultz J, McGeer PL, Styren SD, Civin WH, Brachova L, Bradt B, Ward P (1992) Complement activation by beta-amyloid in Alzheimer disease. Proceedings of the National Academy of Sciences 89:10016-10020.

Rosen S, Ham B, Mogil JS (2017) Sex differences in neuroimmunity and pain. Journal of neuroscience research 95:500-508.

Rozemuller J, Eikelenboom P, Pals S, Stam F (1989) Microglial cells around amyloid plaques in Alzheimer's disease express leucocyte adhesion molecules of the LFA-1 family. Neuroscience Letters 101:288-292.

Ryan JC, Niemi EC, Nakamura MC, Seaman WE (1995) NKR-P1A is a target-specific receptor that activates natural killer cell cytotoxicity. Journal of Experimental Medicine 181:1911-1916.

Sanchez JJ, Noor S, Davies S, Savage D, Milligan ED (2017) Prenatal alcohol exposure is a risk factor for adult neuropathic pain via aberrant neuroimmune function. Journal of neuroinflammation 14:254.

Satoh Ji, Kino Y, Asahina N, Takitani M, Miyoshi J, Ishida T, Saito Y (2016) TMEM119 marks a subset of microglia in the human brain. Neuropathology 36:39-49.

Savage DD, Becher M, de la Torre AJ, Sutherland RJ (2002) Dose-dependent effects of prenatal ethanol exposure on synaptic plasticity and learning in mature offspring. Alcoholism: Clinical and Experimental Research 26:1752-1758.

Savage DD, Rosenberg MJ, Wolff CR, Akers KG, El-Emawy A, Staples MC, Varaschin RK, Wright CA, Seidel JL, Caldwell KK (2010) Effects of a Novel Cognition-Enhancing Agent on Fetal Ethanol-Induced Learning Deficits. Alcoholism: Clinical and Experimental Research 34:1793-1802.

Schäfers M, Svensson CI, Sommer C, Sorkin LS (2003) Tumor necrosis factor-α induces mechanical allodynia after spinal nerve ligation by activation of p38 MAPK in primary sensory neurons. Journal of Neuroscience 23:2517-2521.

Schmittgen TD, Livak KJ (2008) Analyzing real-time PCR data by the comparative C T method. Nature protocols 3:1101.

Schneider ML, Moore CF, Gajewski LL, Larson JA, Roberts AD, Converse AK, DeJesus OT (2008) Sensory processing disorder in a primate model: evidence from a longitudinal study of prenatal alcohol and prenatal stress effects. Child development 79:100-113.

Schneider ML, Moore CF, Barnhart TE, Larson JA, DeJesus OT, Mukherjee J, Nickles RJ, Converse AK, Roberts AD, Kraemer GW (2005) Moderate-Level Prenatal Alcohol Exposure Alters Striatal Dopamine System

Function in Rhesus Monkeys. Alcoholism: Clinical and Experimental Research 29:1685-1697.

Schöll M, Lockhart SN, Schonhaut DR, O'Neil JP, Janabi M, Ossenkoppele R, Baker SL, Vogel JW, Faria J, Schwimmer HD (2016) PET imaging of tau deposition in the aging human brain. Neuron 89:971-982.

Scotland RS, Stables MJ, Madalli S, Watson P, Gilroy DW (2011) Sex-differences in resident immune cell phenotype underlies more efficient acute inflammatory responses in female mice. Blood:blood-2011-2003-340281.

Sickmann H, Patten A, Morch K, Sawchuk S, Zhang C, Parton R, Szlavik L, Christie B (2014) Prenatal ethanol exposure has sex-specific effects on hippocampal long-term potentiation. Hippocampus 24:54-64.

Sims KD, Robinson MB (1999) Expression patterns and regulation of glutamate transporters in the developing and adult nervous system. Critical Reviews™ in Neurobiology 13.

Singh MK, Giles LL, Nasrallah HA (2006) Pain insensitivity in schizophrenia: trait or state marker? Journal of Psychiatric Practice® 12:90-102.

Sofroniew MV, Vinters HV (2010) Astrocytes: biology and pathology. Acta neuropathologica 119:7-35.

Sood B, Delaney-Black V, Covington C, Nordstrom-Klee B, Ager J, Templin T, Janisse J, Martier S, Sokol RJ (2001) Prenatal alcohol exposure and childhood behavior at age 6 to 7 years: I. dose-response effect. Pediatrics 108:e34-e34.

Sorge RE, Mapplebeck JC, Rosen S, Beggs S, Taves S, Alexander JK, Martin LJ, Austin J-S, Sotocinal SG, Chen D (2015) Different immune cells mediate mechanical pain hypersensitivity in male and female mice. Nature neuroscience 18:1081.

Spataro LE, Sloane EM, Milligan ED, Wieseler-Frank J, Schoeniger D, Jekich BM, Barrientos RM, Maier SF, Watkins LR (2004) Spinal gap junctions: potential involvement in pain facilitation. The Journal of Pain 5:392-405.

Stevens SA, Major D, Rovet J, Koren G, Fantus E, Nulman I, Desrocher M (2012) Social problem solving in children with fetal alcohol spectrum disorders. Journal of Population Therapeutics and Clinical Pharmacology 19:e99-e110.

Sung B, Lim G, Mao J (2003) Altered expression and uptake activity of spinal glutamate transporters after nerve injury contribute to the pathogenesis of neuropathic pain in rats. Journal of Neuroscience 23:2899-2910.

Sweitzer SM, Hickey WF, Rutkowski MD, Pahl JL, DeLeo JA (2002) Focal peripheral nerve injury induces leukocyte trafficking into the central nervous system: potential relationship to neuropathic pain. Pain 100:163-170.

Takahashi K, Kong Q, Lin Y, Stouffer N, Schulte DA, Lai L, Liu Q, Chang L-C, Dominguez S, Xing X (2015) Restored glial glutamate transporter EAAT2 function as a potential therapeutic approach for Alzheimer's disease. Journal of Experimental Medicine 212:319-332.

Takeda M, Takahashi M, Matsumoto S (2009) Contribution of the activation of satellite glia in sensory ganglia to pathological pain. Neuroscience & Biobehavioral Reviews 33:784-792.

Terasaki LS, Schwarz JM (2016a) Effects of Moderate Prenatal Alcohol Exposure during Early Gestation in Rats on Inflammation across the Maternal-Fetal-Immune Interface and Later-Life Immune Function in the Offspring. Journal of neuroimmune pharmacology: the official journal of the Society on NeuroImmune Pharmacology 11:680-692.

Terasaki LS, Schwarz JM (2016b) Effects of moderate prenatal alcohol exposure during early gestation in rats on inflammation across the maternal-fetal-immune interface and later-life immune function in the offspring. Journal of Neuroimmune Pharmacology 11:680-692.

Tinazzi M, Del Vesco C, Defazio G, Fincati E, Smania N, Moretto G, Fiaschi A, Le Pera D, Valeriani M (2008) Abnormal processing of the nociceptive input in Parkinson's disease: a study with CO2 laser evoked potentials. Pain 136:117-124.

Tiwari V, Chopra K (2011) Resveratrol prevents alcohol-induced cognitive deficits and brain damage by blocking inflammatory signaling and cell death cascade in neonatal rat brain. Journal of neurochemistry 117:678-690.

Topper LA, Baculis BC, Valenzuela CF (2015) Exposure of neonatal rats to alcohol has differential effects on neuroinflammation and neuronal survival in the cerebellum and hippocampus. Journal of neuroinflammation 12:160.

Uban KA, Sliwowska JH, Lieblich S, Ellis LA, Wayne KY, Weinberg J, Galea LA (2010) Prenatal alcohol exposure reduces the proportion of newly produced neurons and glia in the dentate gyrus of the hippocampus in female rats. Hormones and behavior 58:835-843.

Ultenius C, Linderoth B, Meyerson BA, Wallin J (2006) Spinal NMDA receptor phosphorylation correlates with the presence of neuropathic signs following peripheral nerve injury in the rat. Neuroscience letters 399:85-90.

Valenzuela CF, Morton RA, Diaz MR, Topper L (2012) Does moderate drinking harm the fetal brain? Insights from animal models. Trends in neurosciences 35:284-292.

Van den Broeck W, Derore A, Simoens P (2006) Anatomy and nomenclature of murine lymph nodes: Descriptive study and nomenclatory standardization in BALB/cAnNCrl mice. Journal of immunological methods 312:12-19.

Verderio C, Matteoli M (2011) ATP in neuron–glia bidirectional signalling. Brain research reviews 66:106-114.

Vorderstrasse BA, Dearstyne EA, Kerkvliet NI (2003) Influence of 2, 3, 7, 8-tetrachlorodibenzo-p-dioxin on the antigen-presenting activity of dendritic cells. Toxicological Sciences 72:103-112.

Wagner R, Myers RR (1996) Endoneurial injection of TNF-alpha produces neuropathic pain behaviors. Neuroreport 7:2897-2901.

Warren HS, Smyth MJ (1999) NK cells and apoptosis. Immunology and cell biology 77:64-75.

Whitehead RA, Lam NL, Sun MS, Sanchez J, Noor S, Vanderwall AG, Petersen TR, Martin HB, Milligan ED (2017) Chronic sciatic neuropathy in rat

reduces voluntary wheel-running activity with concurrent chronic mechanical allodynia. Anesthesia & Analgesia 124:346-355.

Wilkerson JL, Gentry KR, Dengler EC, Wallace JA, Kerwin AA, Kuhn MN, Zvonok AM, Thakur GA, Makriyannis A, Milligan ED (2012a) Immunofluorescent spectral analysis reveals the intrathecal cannabinoid agonist, AM1241, produces spinal anti-inflammatory cytokine responses in neuropathic rats exhibiting relief from allodynia. Brain and behavior 2:155-177.

Wilkerson JL, Gentry KR, Dengler EC, Wallace JA, Kerwin AA, Armijo LM, Kuhn MN, Thakur GA, Makriyannis A, Milligan ED (2012b) Intrathecal cannabilactone CB 2 R agonist, AM1710, controls pathological pain and restores basal cytokine levels. PAIN® 153:1091-1106.

Wong EL, Lutz NM, Hogan VA, Lamantia CE, McMurray HR, Myers JR, Ashton JM, Majewska AK (2017) Developmental alcohol exposure impairs synaptic plasticity without overtly altering microglial function in mouse visual cortex. Brain, Behavior, and Immunity.

Yan X, Yadav R, Gao M, Weng HR (2014) Interleukin-1 beta enhances endocytosis of glial glutamate transporters in the spinal dorsal horn through activating protein kinase C. Glia 62:1093-1109.

Zamanian JL, Xu L, Foo LC, Nouri N, Zhou L, Giffard RG, Barres BA (2012) Genomic analysis of reactive astrogliosis. Journal of neuroscience 32:6391-6410.

Zhang X, Lan N, Bach P, Nordstokke D, Yu W, Ellis L, Meadows GG, Weinberg J (2012) Prenatal alcohol exposure alters the course and severity of adjuvant-induced arthritis in female rats. Brain, behavior, and immunity 26:439-450.

Zhang Z-J, Cao D-L, Zhang X, Ji R-R, Gao Y-J (2013) Chemokine contribution to neuropathic pain: respective induction of CXCL1 and CXCR2 in spinal cord astrocytes and neurons. PAIN® 154:2185-2197.

Zhuang Z-Y, Gerner P, Woolf CJ, Ji R-R (2005) ERK is sequentially activated in neurons, microglia, and astrocytes by spinal nerve ligation and contributes to mechanical allodynia in this neuropathic pain model. Pain 114:149-159.

Zhuang Z-Y, Kawasaki Y, Tan P-H, Wen Y-R, Huang J, Ji R-R (2007) Role of the CX3CR1/p38 MAPK pathway in spinal microglia for the development of neuropathic pain following nerve injury-induced cleavage of fractalkine. Brain, behavior, and immunity 21:642-651.

Brenner S, Prösch S, Schenke-Layland K, Riese U, Gausmann U, Platzer C (2003) cAMP-induced interleukin-10 promoter activation depends on CCAAT/enhancer-binding protein expression and monocytic differentiation. Journal of Biological Chemistry 278:5597-5604.

Brightbill HD, Plevy SE, Modlin RL, Smale ST (2000) A prominent role for Sp1 during lipopolysaccharide-mediated induction of the IL-10 promoter in macrophages. The Journal of Immunology 164:1940-1951.

Emoto M, Emoto Y, Brinkmann V, Miyamoto M, Yoshizawa I, Stäber M, van Rooijen N, Hamann A, Kaufmann SH (2003) Increased resistance of LFA-1-deficient mice to lipopolysaccharide-induced shock/liver injury in the presence of TNF-α and IL-12 is mediated by IL-10: a novel role for LFA-1 in the regulation of the proinflammatory and anti-inflammatory cytokine balance. The Journal of Immunology 171:584-593.

Labuda T, Wendt J, Hedlund G, Dohlsten M (1998) ICAM-1 costimulation induces IL-2 but inhibits IL-10 production in superantigen-activated human CD4+ T cells. Immunology 94:496.

Ma F, Liu X, Li D, Wang P, Li N, Lu L, Cao X (2010) MicroRNA-466l upregulates IL-10 expression in TLR-triggered macrophages by antagonizing RNA-binding protein tristetraprolin-mediated IL-10 mRNA degradation. The Journal of Immunology:ji_0902308.

Ogony JW, Malahias E, Vadigepalli R, Anni H (2013) Ethanol alters the balance of Sox2, Oct4, and Nanog expression in distinct subpopulations during differentiation of embryonic stem cells. Stem cells and development 22:2196-2210.

Pascual M, Montesinos J, Montagud-Romero S, Forteza J, Rodríguez-Arias M, Miñarro J, Guerri C (2017) TLR4 response mediates ethanol-induced neurodevelopment alterations in a model of fetal alcohol spectrum disorders. Journal of neuroinflammation 14:145.

Saraiva M, O'garra A (2010) The regulation of IL-10 production by immune cells. Nature reviews immunology 10:170.

Wang G, Wang X, Wang Y, Yang JY, Li L, Nephew KP, Edenberg HJ, Zhou FC, Liu Y (2008) Identification of transcription factor and microRNA binding sites in responsible to fetal alcohol syndrome. BMC genomics 9:S19.

Zhou H-Y, Chen S-R, Pan H-L (2011) Targeting N-methyl-D-aspartate receptors for treatment of neuropathic pain. Expert review of clinical pharmacology 4:379-388.

Ziegler-Heitbrock L, Lötzerich M, Schaefer A, Werner T, Frankenberger M, Benkhart E (2003) IFN-α induces the human IL-10 gene by recruiting both IFN regulatory factor 1 and Stat3. The Journal of Immunology 171:285-290.